ISTANBUL TECHNICAL UNIVERSITY ★ INSTITUTE OF SCIENCE AND TECHNOLOGY

OIL PRODUCTION BY WATERFLOODING

M.Sc. Thesis by
Nurbol ZHARYLKAPOV

Department : Petroleum and Natural Gas Engineering

Programme: Petroleum and Natural Gas

JUNE 2010

ISTANBUL TECHNICAL UNIVERSITY ★ INSTITUTE OF SCIENCE AND TECHNOLOGY

OIL PRODUCTION BY WATERFLOODING

M.Sc. Thesis by
Nurbol ZHARYLKAPOV
(505061505)

Date of submission : **07 May 2010**
Date of defence examination: **10 June 2010**

Supervisor (Chairman) : **Prof. Dr. Mustafa ONUR (ITU)**
Members of the Examining Committee : **Prof. Dr. Fatma ARSLAN (ITU)**
Assist. Prof. Dr. Ö. İnanç TÜREYEN (ITU)

JUNE 2010

<u>İSTANBUL TEKNİK ÜNİVERSİTESİ ★ FEN BİLİMLERİ ENSTİTÜSÜ</u>

SU ÖTELEMESI İLE PETROL ÜRETIMI

YÜKSEK LİSANS TEZİ
Nurbol JARILKAPOV
(505061505)

Tezin Enstitüye Verildiği Tarih : 07 Mayıs 2010
Tezin Savunulduğu Tarih : 10 Haziran 2010

Tez Danışmanı : Prof. Dr. Mustafa ONUR (İTÜ)
Diğer Jüri Üyeleri : Prof. Dr. Fatma ARSLAN (İTÜ)
Yrd. Doç. Dr. Ö. İnanç TÜREYEN (İTÜ)

HAZİRAN 2010

FOREWORD

I express my deep gratitude to my supervisor, head of Petroleum and Natural Gas Department, Prof. Dr. Mustafa Onur for his patience, support, encouragement, advice and guidance throughout the study.

In addition, I would like to express my appreciations to all staff of Petroleum and Natural Gas Engineering Department of Istanbul Technical University for their interesting and valuable lessons that I attended. I would also like to thank to my thesis committee members, Prof. Dr. Fatma Arslan and Assist. Prof. Dr. Ö. İnanç Türeyen for their constructive comments.

I would like to express my deepest gratitude to my family and friends for being always beside me with their love, support and guidance throughout all my life and throughout this study. Especially, I wish to thank my friends, Sabit Bidaibaev, Abbas N. Tahir and Fuad Mamadov, them unconditional support and care, patience and understanding and explicit belief in me.

May 2010

Nurbol Zharylkapov

Petroleum Engineer

TABLE OF CONTENTS

Page

ABBREVIATIONS

A	: cross-sectional area, ft^2
a	: coefficient
B_o	: oil formation volume factor, RB/STB
B_w	: water formation volume factor, RB/STB
b	: coefficient
E_A	: areal sweep efficiency, fraction
E_{Abt}	: areal sweep efficiency at breakthrough, fraction
f_w	: fractional flow of water
f_{wf}	: fractional flow of water
g	: gravity constant
h	: thickness of reservoir zone, ft
k	: permeability, darcies
k_o	: permeability to oil, darcies
k_w	: permeability to water, darcies
k_{ro}	: relative permeability to oil
k_{rw}	: relative permeability to water
k_{ro}^{o}	: end-point relative permeability to oil
k_{rw}^{o}	: end-point relative permeability to water
L	: length, ft
M	: mobility ratio
M^*	: end-point mobility ratio
N	: total number of piecewise constant flow rate steps
N_p	: cumulative oil production, bbl
N_{pbt}	: cumulative oil production at breakthrough, bbl
OIIP	: oil initially in place, STB
P_c	: capillary pressure, psi
q_o	: oil production rate, RB/D
q_t	: total injection or production rate, RB/D
q_w	: water injection rate, RB/D
RF	: recovery factor
r_w	: effective well bore radius, ft
S_i	: skin factor at the injection well
S_{iw}	: interstitial water saturation
S_{or}	: residual oil saturation
S_p	: skin factor at the production well
STB/D	: stock tank barrel per day
S_w	: water saturation, fraction
$\bar{S}_w$	: average water saturation, fraction
S_{wc}	: connate water saturation
S_{wD}	: dimensionless water saturation
S_{wf}	: water saturation at breakthrough, fraction
S_{wi}	: initial water saturation

t	: time, day
t_{bt}	: time at breakthrough, day
t_f	: time to fill up, day
t_{int}	: time to interference, day
V_p	: total pore volume, bbl
W_i	: cumulative water injected, bbl
W_{ibt}	: cumulative water injected at breakthrough, bbl
WOR	: water-oil ratio
x_{Sw}	: location of water saturation on the *x* axis, ft
x_{Sfw}	: location of the flood front saturation on the *x* axis, ft
λ_t	: total mobility
μ_{app}	: apparent viscosity, cp
μ_o	: oil viscosity, cp
μ_w	: water viscosity, cp
ρ_o	: oil density, lb/ ft^3
ρ_w	: water density, lb/ ft^3
ϕ	: porosity, fraction

LIST OF TABLES

LIST OF FIGURES

Page

OIL PRODUCTION BY WATERFLOODING

SUMMARY

In this thesis, we consider the application of frontal advance theory to displacement processes by water injection in homogeneous porous media. The assumptions under which a generalized frontal advance equation can be used to describe a flow process in a homogeneous porous medium are examined. Material balance equations are derived based on these assumptions, and the theory is illustrated by application to the Bukley-Leverett model.

Using the Buckley-leverett theory, we consider three example applications of waterflood performance in 1D linear system before and after breakthrough for both constant-rate water injection rate and constant-pressure injection cases.

It is well-known that pattern geometry plays a major role in determining oil recovery during waterflooding and enhanced oil recovery operations. In addition, in the fourth example we consider waterflood performance for a 2D performance calculation for an areal five-spot pattern.

SU ÖTELEMESI İLE PETROL ÜRETIMI

ÖZET

Bu tez çalışmasında, öteleme işlemleri için homojen gözenekli ortamda cephesel ilerleme teorilerinin uygulaması düşünülmüştür. Homojen bir gözenekli ortamda bir akış süreci tanımlamak için genelleştirilmiş cephesel ilerleme denklemi kullanılarak varsayımları incelenmiştir. Kütle-korunum denklemleri bu varsayımlara dayalı türetilmiştir ve Bukley-Leverett teorisinin 1B ve 2B modellere uygulamalarla gösterilmektedir.

Buckley-leverett teorisini kullanarak, su öteleme performansının uygulamasını üç örnekle, 1 boyutlu lineer sistemi su varış öncesi ve sonrası hem sabit debide su enjeksiyonu hem de sabit basınçta su enjeksiyonu olguları için düşünülmüştür.

İki boyutlu desen ("pattern") geometrisinin su ötelemesi sırasında petrol kurtarımının belirlemesinde ve gelişmiş petrol kurtarma işlemlerinde önemli bir rol oynadığı bilinmektedir. Buna ek olarak, dördüncü örnek uygulamada, cephesel ilerleme teoremi kullanılarak beş-nokta deseni 2B bir sistem için su öteleme performansını hesaplamalarının nasıl yapılacağı gösterilmiştir.

1. INTRODUCTION

Today, waterflooding is still the recovery process responsible for most of the oil production by secondary recovery. Water injected into the reservoir displaces almost all of the oil except the residual oil saturation from the portions of the reservoir contacted or swept by water. The fraction of oil displaced from a contacted volume is known as the displacement efficiency and depends on the relative permeability characteristics of the rock as well as the viscosities of the displacing and displaced fluids.

In this thesis, we used the Buckley-Leverett theory. Buckley and Leverett (1942) presented a method for constructing displacing fluid saturation and predicting the performance of the displacement process by using the law of conservation of mass to the flow of two fluids (oil and water) in one direction *(x)* and we used this model in different applications. First at constant rate injection and second at constant pressure injection. In addition, we use the Graig-Geffen-Morse method (1955) which considers a fully developed 5-spot pattern, i.e., all wells produce and inject at the same rate. The method is for a quadrant of five-spot pattern.

1.1 Purpose of the Thesis

The purpose of this thesis is to use the Buckley-Leverett frontal advance theory to design and predict the waterflood performance. It is one of the simplest and most widely used methods of estimating the advance of a fluid displacement front in an immiscible displacement process under constant rate injection and constant pressure injection to determine performance times before and after breakthrough. In addiction, our objective is to determine the areal sweep efficiency, mobility ratio and WOR distribution for different aspect ratios by using the Craig-Geffen-Morse method for a 2D 5-spot pattern.

1.2 Scope of the Thesis

In a waterflood, water is injected in a well or pattern of wells to displace oil towards a producer. When the leading edge of the waterflood front reaches the producer breakthrough occurs. After breakthrough, both oil and water are produced and the water cut increases progressively.

There are many different methods for predicting waterflood performance. These methods range from the simple analytical methods to the complex numerical methods. In this thesis, we propose an exact analytical solution for predicting waterflood performance in one-dimensional linear flow and an areal five-spot pattern.

The main assumptions used in developing the analytical models are: (i) two-phase reservoir (ii) the reservoir is homogeneous, i.e., there is no spatial variability in porosity and permeability,(iii) flow is linear and horizontal, (iv) flow in the reservoir from the start of production to the end of production is under unsteady-steady state conditions.

In Chapter 2, we consider the methods, which are related to one-dimensional (1D) fluid displacement processes and review the frontal advance theory introduced by Buckley-Leverett (1942). We show how this method can be used for prediction performance both the constant-rate water injection and the constant-pressure water injection cases.

In Chapter 3, we extend the prediction methods based on 1D linear flow in Chapter 2 to two-dimensional problems (*x*-*y*) and describe the performance prediction for a five-spot pattern, based on the method of Craig-Geffen-Morse (1955).

In Chapter 4, we present four example applications; three for 1D case, and one for 2D 5-spot pattern.

Chapter 5 presents the conclusions reached during the course of this study, and also makes recommendations for future studies that may be conducted on oil production by waterflooding.

1.3 Literature Review

In 1946, Buckley and Leverett presented the frontal advance equation. Applying mass balance to a small element within the continuous porous medium, they expressed the difference at which the displacing fluid enters this element and the rate at which it leaves it in terms of the accumulation of the displacing fluid. By transforming this material balance equation, the frontal advance equation can be obtained:

$$\left(\frac{\partial L}{\partial t}\right)_{Sw} = \frac{q_t}{A\phi}\left(\frac{\partial f_w}{\partial S_w}\right)_t \tag{1.1}$$

The only assumptions necessary for the derivation are that there is no mass transfer between phases, and the phases are incompressible.

This equation states that the rate of advance of a plane of fixed water saturation is equal to the total fluid velocity multiplied by the change in composition of the flowing stream caused by a small change in the saturation of the displacing fluid. That is, any water saturation, S_w, moves along the flow path at a velocity equal to $\frac{q_t}{A\phi}\frac{df_w}{dS_w}$. As the total flow rate q_t increases, the velocity of the plane of saturation correspondingly increases. As the total flow rate is reduced, the velocity of the saturation is correspondingly reduced. Eq. 1.1 can be integrated to yield

$$L = \frac{W_i}{A\phi}\left(\frac{\partial f_w}{\partial S_w}\right) \tag{1.2}$$

where *L* is the total distance that the plane of given water saturation moves.

Buckley and Leverett pointed out that Eq. 1.2 can be used calculate the saturation distribution existing during a flood. The value of $\frac{\partial f_w}{\partial S_w}$ is slope of the curve of fractional flow vs. water saturation. Most fractional flow curves exhibit two saturations having the same value of $\frac{\partial f_w}{\partial S_w}$. The consequence of this is that according to Eq. 1.1, two different saturations would exist at the same point in the formation at the same time. To make the situation even more absurd, if an initial saturation gradient exists above the water-oil contact prior to flooding, the computed saturation distribution is triple-valued over a portion of its length.

In 1952 in another paper of fundamental importance, Welge engaged upon Buckley and Leverett's work. He showed that construction of a tangent to the fractional flow curve equivalent to the "balancing of areas" technique suggested by Buckley and Leverett for finding the saturation at the "discontinuity". Welge further went on to derive an equation that rates the average displacing fluid saturation to that saturation at the production end of system.

The 1950 paper of Dykstra and Parsons presented a correlation between waterflood recovery and both mobility ratio and permeability distribution. This correlation was based on calculations applied to a layered linear model with no cross flow. This first work on vertical stratification with inclusion of mobility ratios other than unity was presented in the work of Dykstra and Parsons who have developed an approach for handling stratified reservoirs, which allows calculating waterflood performance in multi-layered systems. But their method requires the assumption that the saturation behind the flood front is uniform, i.e. only water moves behind the waterflood front. There are other assumptions involved such as: linear flow, incompressible fluid, piston-like displacement, no cross flow, homogeneous layers, constant injection rate, and the pressure drop (ΔP) between injector and producer across all layers is the same.

In 1955, Craig et al. presented the results of waterflood model in five-spot pattern. A variety of oil viscosities used to obtain a range of saturation gradients and it was found that if the water mobility was defined at the average water saturation behind the flood front at water breakthrough, the data on areal sweep versus mobility ratio would match those obtained by using immiscible fluids. As a result of those studies, the water mobility is defined as that at the average water saturation in the water-contacted portion of the reservoir and this definition has been widely accepted.

2. FRONTAL ADVANCE THEORY FOR UNSTEADY STATE DISPLACEMENT FOR 1D FLOW

In this chapter, we consider the methods, which are related to one-dimensional (1D) fluid displacement processes. The most of the theory given in this chapter are based the well-known Buckley-Leverett model. Buckley and Leverett (1942) presented a method for constructing displacing fluid saturation and predicting the performance of the displacement process by using the law of conservation of mass to the flow of two fluids (oil and water) in one direction *(x).*

Before giving the details of the Buckley-Leverett model, it is important to note that displacement of one fluid with another fluid (e.g., displacing oil with water or displacing oil with gas) is an unsteady-state process because the saturations of fluids change with time. This is mainly due to the changes in relative permeabilities and hence due to changes in phase pressures or phase velocities. Figure 2.1 shows four representative stages of a linear waterflood at initial (or interstitial) water saturation.

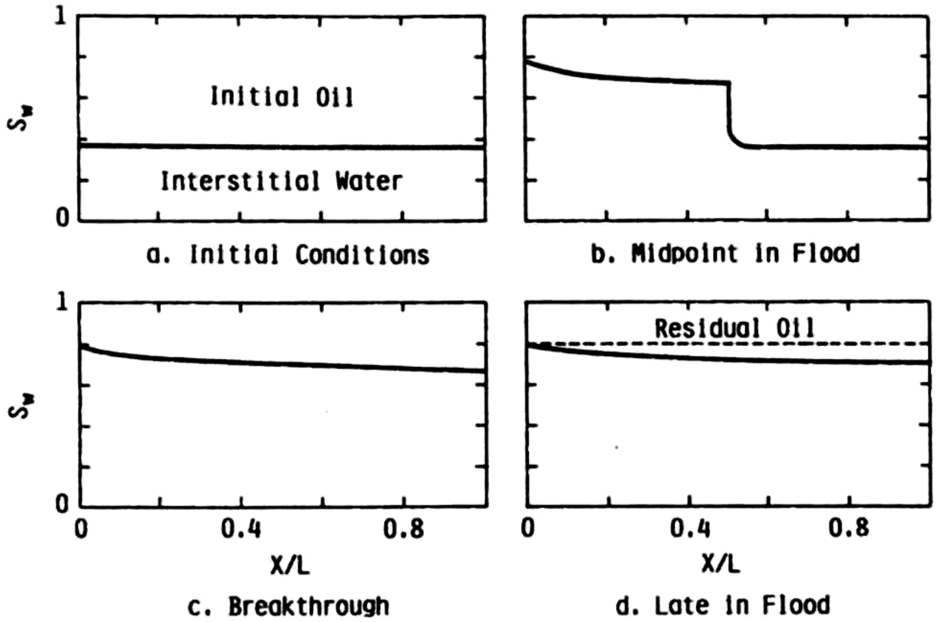

Figure 2.1: Saturation distributions during different stages of a waterflood, adapted from Willhite (1986).

As explained by Willhite (1986), at time $t = 0$, i.e., at the onset of displacement, initial water and oil saturations are uniform, as shown in Figure 2.1a. Injection of water at a flow rate q_w causes oil to be displaced from the reservoir. A sharp water saturation gradient develops, as in Figure (2.1b). Water and oil flow simultaneously in the region behind the saturation change. There is no flow of water ahead of the saturation change because the permeability to water is essentially zero. Eventually, water arrives at the end of the reservoir, as shown in Figure 2.1c. This point is called "breakthrough". After breakthrough, the fraction of water in the effluent increases as the remaining oil is displaced. Figure 2.1d depicts the water saturation in a linear system late in the displacement.

Using the Buckley-Leverett theory, we can predict displacement performance, which can be solved easily with graphical techniques. One of the simplest and most widely used methods of estimating the advance of a fluid displacement front in an immiscible displacement process is the Buckley-Leverett method. The Buckley-Leverett theory [1942] estimates the rate at which an injected water bank moves through a porous medium. The Buckley-Leverett model discussed in this section is based on the following:

- Flow is linear and horizontal
- Water is injected into an oil reservoir
- Oil and water are both incompressible. Under this assumption, the total flow rate is equal to q_t at all points in the reservoir; i.e., q_t does not vary with position x.
- Oil and water are immiscible.
- Gravity and capillary pressure effects are negligible
- Homogeneous reservoir, i.e., there is no spatial variability in porosity and permeability.
- Uniform initial (irreducible or mobile) water saturation exists throughout the reservoir.
- No free gas exist in the reservoir.

So before describing the Buckley-Leverett theory of immiscible displacement in one dimension, the fractional flow equation that relates the ratio of relative permeabilities to the experimental data that is measured in a typical displacement experiment must be derived. We derive the fractional flow equation for a one-dimensional oil-water system. As considering the displacement of oil by water in a system of dip angle α , by Figure 2.2.

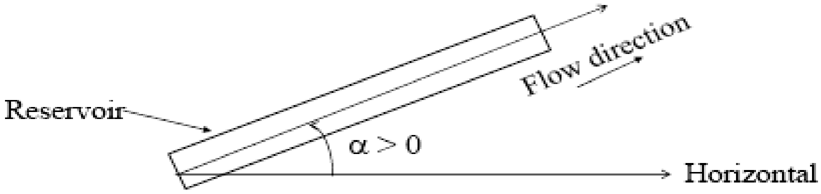

Figure 2.2: Displacement of oil by water in a system of dip angle

We are starting with the well-known Darcy's law (in consistent units, e.g., SI or CGS), for the two phases, oil and water. Then, we can express oil and water flow rate as follows:

$$q_o = -\frac{kk_{ro}A}{\mu_o}\left(\frac{\partial P_o}{\partial x} + \rho_o g \sin\alpha\right) \quad \textbf{(2.1)}$$

$$q_w = -\frac{kk_{rw}A}{\mu_w}\left(\frac{\partial P_w}{\partial x} + \rho_w g \sin\alpha\right) \quad \textbf{(2.2)}$$

M The phase pressures are different because of the capillary pressure, and hence, we can replace the water pressure by $P_w=P_o-P_c$ in Eq. 2.2 to obtain:

$$q_w = -\frac{kk_{rw}A}{\mu_w}\left(\frac{\partial (P_o - P_c)}{\partial x} + \rho_w g \sin\alpha\right) \quad \textbf{(2.3)}$$

After rearranging, Eqs. 2.1 and 2.2 may be written, respectively, as:

$$-q_o \frac{\mu_o}{kk_{ro}A} = \frac{\partial P_o}{\partial x} + \rho_o g \sin\alpha \quad \textbf{(2.4)}$$

$$-q_w \frac{\mu_w}{kk_{rw}A} = \frac{\partial P_o}{\partial x} - \frac{\partial P_c}{\partial x} + \rho_w g \sin\alpha \quad \textbf{(2.5)}$$

Subtracting Eq. 2.5 from Eq. 2.4, we obtain:

$$-\frac{1}{kA}\left(q_w\frac{\mu_w}{k_{rw}}-q_o\frac{\mu_o}{k_{ro}}\right)=-\frac{\partial P_c}{\partial x}+\Delta\rho g\sin\alpha \tag{2.6}$$

Substituting for

$$q_t=q_w+q_o \tag{2.7}$$

and defining the water cut as:

$$f_w=\frac{q_w}{q_t} \tag{2.8}$$

in Eq. 2.6, and solving the resulting equation for the fraction of water flowing, we obtain the following expression for the fraction of water flowing:

$$f_w=\frac{1+\dfrac{kk_{ro}A}{q_t\mu_o}\left(\dfrac{\partial P_c}{\partial x}-\Delta\rho g\sin\alpha\right)}{1+\dfrac{k_{ro}}{\mu_o}\dfrac{\mu_w}{k_{rw}}} \tag{2.9}$$

The other forms of f_w that you may see in other books are:

$$f_w=\frac{\dfrac{k_w}{\mu_w}}{\left(\dfrac{k_w}{\mu_w}+\dfrac{k_o}{\mu_o}\right)}+\frac{\dfrac{A}{q_t}\dfrac{k_w}{\mu_w}\dfrac{k_o}{\mu_o}\left[\dfrac{\partial P_c}{\partial x}+\Delta\gamma\sin\alpha\right]}{\left(\dfrac{k_w}{\mu_w}+\dfrac{k_o}{\mu_o}\right)} \tag{2.10}$$

and

$$f_w=\frac{1}{1+\left(\dfrac{k_o}{k_w}\right)\left(\dfrac{\mu_w}{\mu_o}\right)}+\frac{\dfrac{k_oA}{\mu_oq_t}\left[\dfrac{\partial P_c}{\partial x}+(\rho_o-\rho_w)g\sin\alpha\right]}{1+\left(\dfrac{k_o}{k_w}\right)\left(\dfrac{\mu_w}{\mu_o}\right)} \tag{2.11}$$

In oilfield units, Eq. 2.11 becomes

$$f_w = \frac{1}{1+\left(\frac{k_o}{k_w}\right)\left(\frac{\mu_w}{\mu_o}\right)} + \frac{\frac{1.127 k_o A}{\mu_o q_t}\left[\frac{\partial P_c}{\partial x} + 0.4333(\rho_o - \rho_w) g \sin\alpha\right]}{1+\left(\frac{k_o}{k_w}\right)\left(\frac{\mu_w}{\mu_o}\right)} \quad \textbf{(2.12)}$$

When x is in the horizontal plane, α=0, there is no gravity term and we neglect capillary pressure, then Eqs. 2.9-2.11 becomes:

$$f_w = \frac{1}{1+\left(\frac{k_o}{k_w}\right)\left(\frac{\mu_w}{\mu_o}\right)} \quad \textbf{(2.13)}$$

or in terms of relative perms, the previous equation can be rewritten as:

$$f_w = \frac{1}{1+\frac{k_{ro}}{\mu_o}\frac{\mu_w}{k_{rw}}} \quad \textbf{(2.14)}$$

Note that Eq. 2.12 can also be well approximated by Eq. 2.13 (or Eq. 2.14) if the water injection rate or total flow rate qt in Eq. 2.12 is sufficiently large so that the second term in the right-hand side of Eq. 2.12 is much smaller than the first term and hence it can be neglected.

As can be realized from Eq. 2.14, f_w is a function of S_w (due to effective or relative perms) and viscosity ratio, i.e.

$$f_w = f_w\left(S_w, \frac{\mu_w}{\mu_o}\right) \quad \textbf{(2.15)}$$

Under the assumption that capillary and gravity does not have effect on f_w, a typical f_w vs. S_w curve is a ‘’*S*’’ shaped curve as shown in Fig. 2.3.

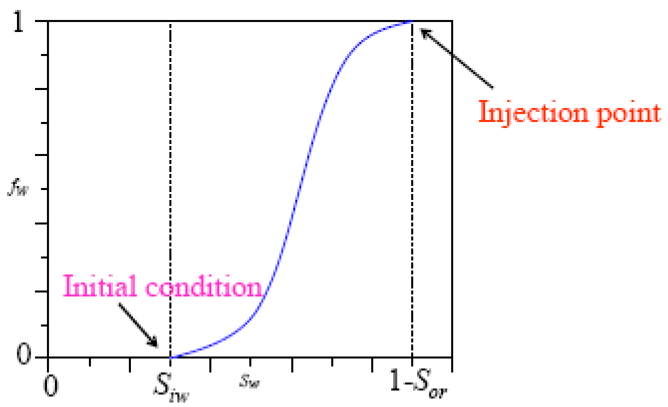

Figure 2.3: Fractional flow curve expressed with the initial and injection point conditions.

At the injection point, oil rate is zero and the total rate is equal to water injection rate, so

$$f_w = \frac{q_w}{q_t} = \frac{q_w}{q_o + q_w} = \frac{q_w}{0 + q_w} = 1 \qquad \textbf{(2.16)}$$

Initially, if we have irreducible water saturation (S_{iw}) in the reservoir prior to flood (as shown in figure 2.3), then f_w = 0 because effective (or relative) water perm is zero at this saturation (see Eq. 2.13 or 2.14).

Fractional flow equation given by Eq. 2.13 (or 2.14) or in general Eq. 2.9 can be used to calculate the fraction of flow of water, at any point in the reservoir if the water saturation is known at that point. In a water flooding operation, we want to have a small fractional flow of water at a given water saturation. Thus, as fractional flow curve shifts to right (Curve 2 in Fig. 2.4), we expect to have a better oil recovery, as shown in Fig. 2.4.

The effect of various parameters (viscosity of water and oil, mobility ratio, wettability and capillary pressure) on the water fractional flow curve are discussed next.

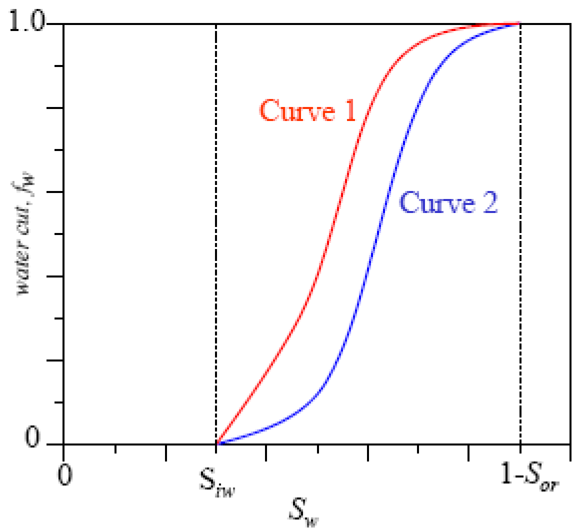

Figure 2.4: Fractional flow curves for two different cases; the fractional a flow curve for Curve 2 provides better oil recovery than that for Curve 1.

The effect of mobility ratio on the fractional flow curve: The efficiency of a water flood depends greatly on the mobility ratio of the displacing fluid to the displaced fluid at a given water saturation S_w, defined by

$$M = \frac{\left(\dfrac{k_{rw}}{\mu_w}\right)_{S_w}}{\left(\dfrac{k_{ro}}{\mu_o}\right)_{S_w}} \qquad \textbf{(2.17)}$$

or in terms of end point effective or relative permeabilities, we can defined end-point mobility ratio, M^*, as:

$$M^* = \frac{k_{rw}^0}{k_{ro}^0}\frac{\mu_o}{\mu_w} = \frac{\left(\dfrac{k_{rw}^0}{\mu_w}\right)}{\left(\dfrac{k_{ro}^0}{\mu_o}\right)} = \frac{\dfrac{k_{rw}(1-S_{or})}{\mu_w}}{\dfrac{k_{ro}(S_{iw})}{\mu_o}} \qquad \textbf{(2.18)}$$

where k_{rw}^0 and k_{ro}^0 represent the end-point relative permeabilities to water and oil, respectively. If $M^* < 1$, the displacement is called as the "favorable" displacement, while if $M^* > 1$, the displacement is called as the "unfavorable displacement.

It should be noted that the lower the mobility ratio, the more efficient displacement, and the curve is shifted right. Typical fractional flow curves for high and low oil viscosities, and thus high or low mobility ratios, are shown in the figure below. In addition to the two curves, an extreme curve for perfect displacement efficiency.

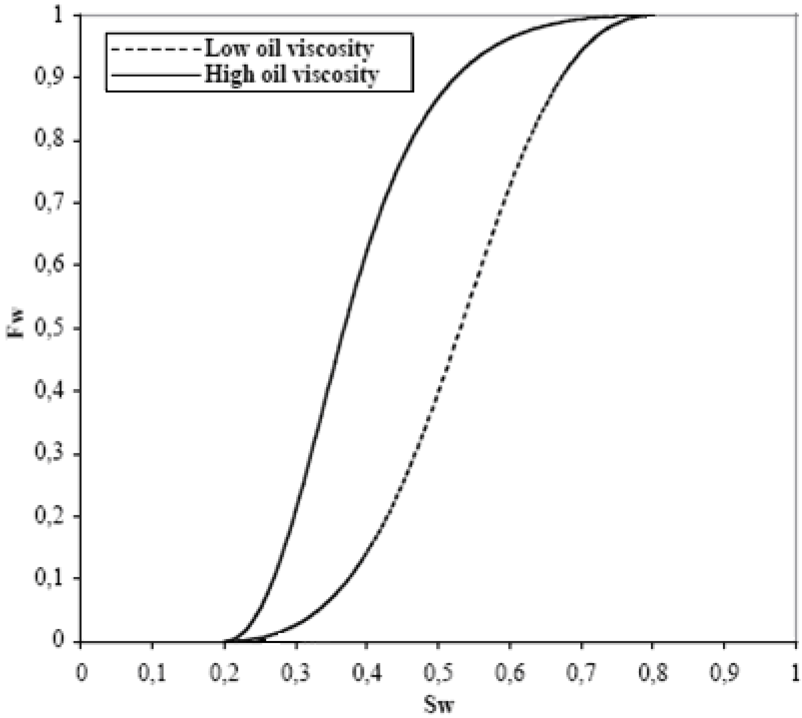

Figure 2.5: Effect of mobility ratio on fractional flow, after Kleppe (2009).

<u>Effect of gravity on fractional flow curve.</u> In a non-horizontal system, with water injection at the bottom and production at the top, gravity forces will contribute to higher recovery efficiency. Typical curves for horizontal (α = 0^o) and vertical (α = 90^o) flow are shown below.

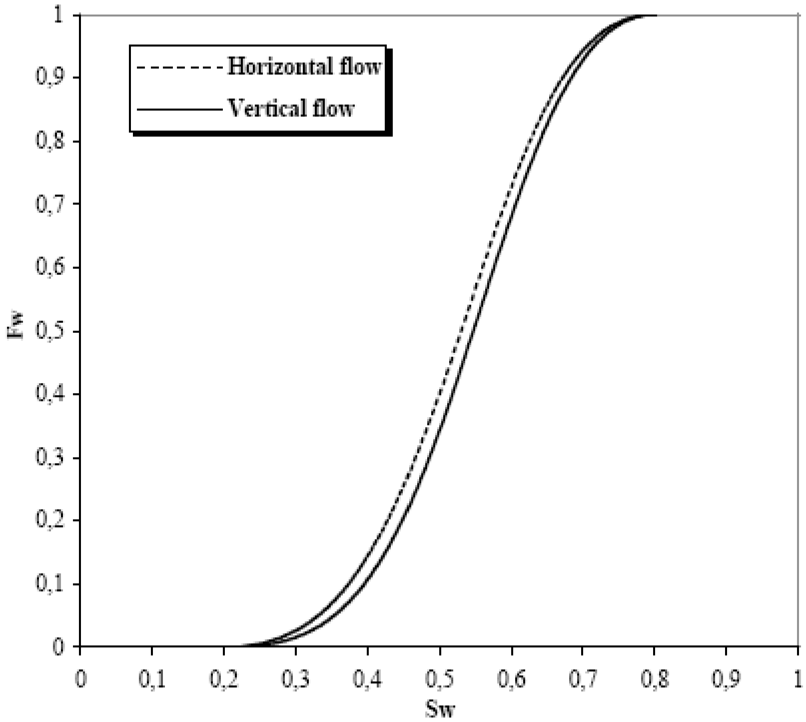

Figure 2.6: Effect of gravity on fractional flow**,** after Kleppe (2009)

Effect of capillary pressure on fractional flow curve. As may be observed from the fractional flow expression:

$$f_w = \frac{1 + \frac{k k_{ro} A}{q_t \mu_o}\left(\frac{\partial P_c}{\partial x} - \Delta \rho g \sin \alpha\right)}{1 + \frac{k_{ro}}{\mu_o}\frac{\mu_w}{k_{rw}}} \qquad \textbf{(2.19)}$$

the capillary pressure will contribute to a higher f_w (since $\frac{\partial P_c}{\partial x} > 0$), and thus to a less efficient displacement. However, this argument alone is not really valid, since the Buckley-Leverett solution assumes a discontinuous water-oil displacement front. If capillary pressure is included in the analysis, such a front will not exist, since capillary dispersion (i.e. imbibitions) will take place at the front. Thus, in addition to a less favorable fractional flow curve, the dispersion will also lead to an earlier water break-through at the production well.

In the next section we develop an expression for the Buckley-Leverett equation. Buckley and Leverett (1942) presented what is recognized as the basic equation for describing two-phase, immiscible displacement in a linear system. The equation is derived based on developing a material balance for the displacing fluid as it flows through any given element in the porous media:

Volume entering the element – Volume leaving the element = change in fluid volume **(2.20)**

Let's consider a differential element of porous media, as shown in Figure 2.7, having a differential length dx, an area *A*, and a porosity ϕ. During a differential time period dt, the total volume of water entering the element is given by:

Volume of water entering the element = $q_t f_w dt$ **(2.21)**

The volume of water leaving the element has differentially smaller water cut $(f_w - df_w)$ and is given by:

Volume of water leaving the element = $q_t (f_w - df_w) dt$ **(2.22)**

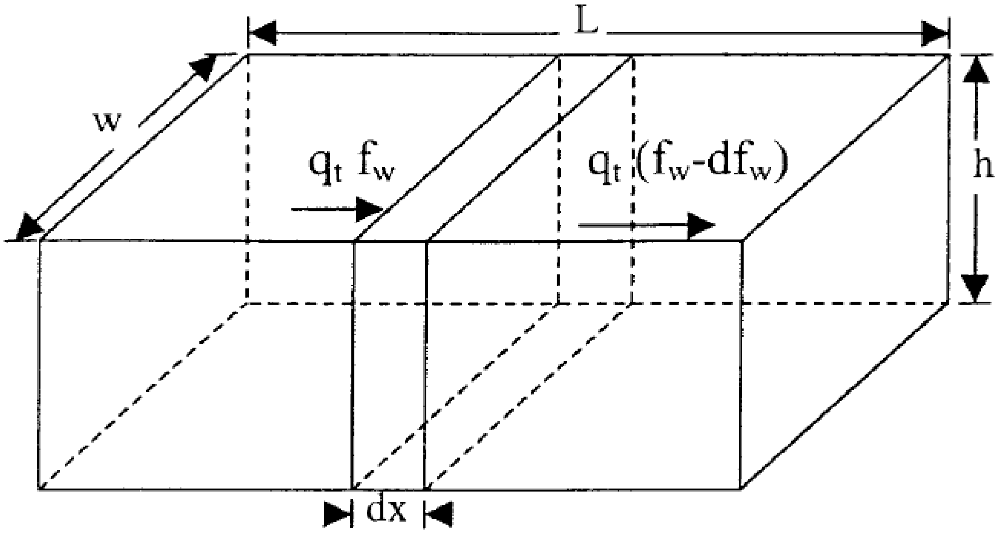

Figure 2.7: Water flow through a linear differential element, adapted from Tarek (2006).

Subtracting the above two expressions gives the accumulation of the water volume within the element in terms of the differential changes of the saturation dS_w:

$$q_t f_w dt - q_t\left(f_w - df_w\right)dt = A\phi(dx)(dS_w)/5.615 \quad \textbf{(2.23)}$$

Simplifying:

$$q_t df_w dt = A\phi(dx)(dS_w)/5.615 \quad \textbf{(2.24)}$$

Separating the variables gives:

$$v_{S_w} = \left(\frac{dx}{dt}\right)_{S_w} = \frac{5.615 q_t}{A\phi}\left(\frac{df_w}{dS_w}\right)_{S_w} \quad \textbf{(2.25)}$$

where v_{S_w} is velocity of any specified value of S_w, ft/day, $\left(\frac{df_w}{dS_w}\right)_{S_w}$ is the slope of the f_w vs. S_w curve at S_w.

The above relationship given by Eq. 2.25 suggests that the velocity of any specific water saturation S_w is directly proportional to the value of the slope of the f_w vs. S_w curve, evaluated at S_w. Note that for two-phase incompressible flow, the total flow rate q_t is essentially equal to the injection rate q_w, or:

$$v_{S_w} = \left(\frac{dx}{dt}\right)_{S_w} = \left(\frac{5.615 q_w}{A\phi}\right)\left(\frac{df_w}{dS_w}\right)_{S_w} \quad \textbf{(2.26)}$$

where q_w is water injection rate, bbl/day.

To calculate the total distance any specified water saturation will travel during a total time t, Eq. 2.26. must be integrated:

$$\int_0^x dx = \left(\frac{5.615 q_w}{A\phi}\right)\left(\frac{df_w}{dS_w}\right)_{S_w} \int_0^t dt \quad \textbf{(2.27)}$$

or

$$(x)_{S_w} = \left(\frac{5.615 q_w t}{A\phi}\right)\left(\frac{df_w}{dS_w}\right)_{S_w} \quad \textbf{(2.28)}$$

In deriving Eq. 2.27 and 2.28 we assumed that water injection rate q_w is constant with time. However, this assumption is not necessary because starting from Eq. 2.26, we can show that Eq. 2.8 can also be expressed in terms of total volume of water injected by recognizing that the cumulative water injected is given by:

$$W_i(t) = \int_0^t q_w(\tau) d\tau \quad \textbf{(2.29)}$$

and hence we obtain:

$$(x)_{Sw} = \frac{5.615 W_i(t)}{A\phi} \left(\frac{df_w}{dS_w} \right)_{S_w} \quad \textbf{(2.30)}$$

where W_i is cumulative water injected, bbl, t is time, day and $(x)_{Sw}$ is distance from the injection for any given saturation S_w, ft. Note that if q_w is constant and equal to q_w for all times, then Eq. 2.29 is simply given by $W_i(t) = q_w t$. Using this equation in Eq. 2.30 gives Eq. 2.28, which assumes a constant water injection rate of q_w.

Equation 2.28 or 2.30 suggests that the position of any value of water saturation S_w at given cumulative water injected W_i is proportional to the slope (df_w / dS_w) for this particular S_w. At any given time *t*, the water saturation profile can be plotted by simply determining the slope of the f_w curve at each selected saturation and calculating the position of S_w from Equation 2.28 or 2.30.

Shown in Figure 2.8 is the typical *S* shape of the f_w curve and its derivative curve (df_w / dS_w). However, a mathematical difficulty arises when using the derivative curve to construct the water saturation profile at any given time because there exists two saturation values that satisfy the given derivative value of (df_w / dS_w) as illustrated in Fig. 2.8 (see saturation values designated as *A* and *B* in the horizontal axis of Fig. 2.8). Evaluating Eq. 2.30 for the saturations *A* and *B* gives:

$$(x)_A = \frac{5.615 W_i}{A\phi} \left(\frac{df_w}{dS_w} \right)_A \quad \textbf{(2.31)}$$

and

$$(x)_B = \frac{5.615W_i}{A\phi}\left(\frac{df_w}{dS_w}\right)_B \tag{2.32}$$

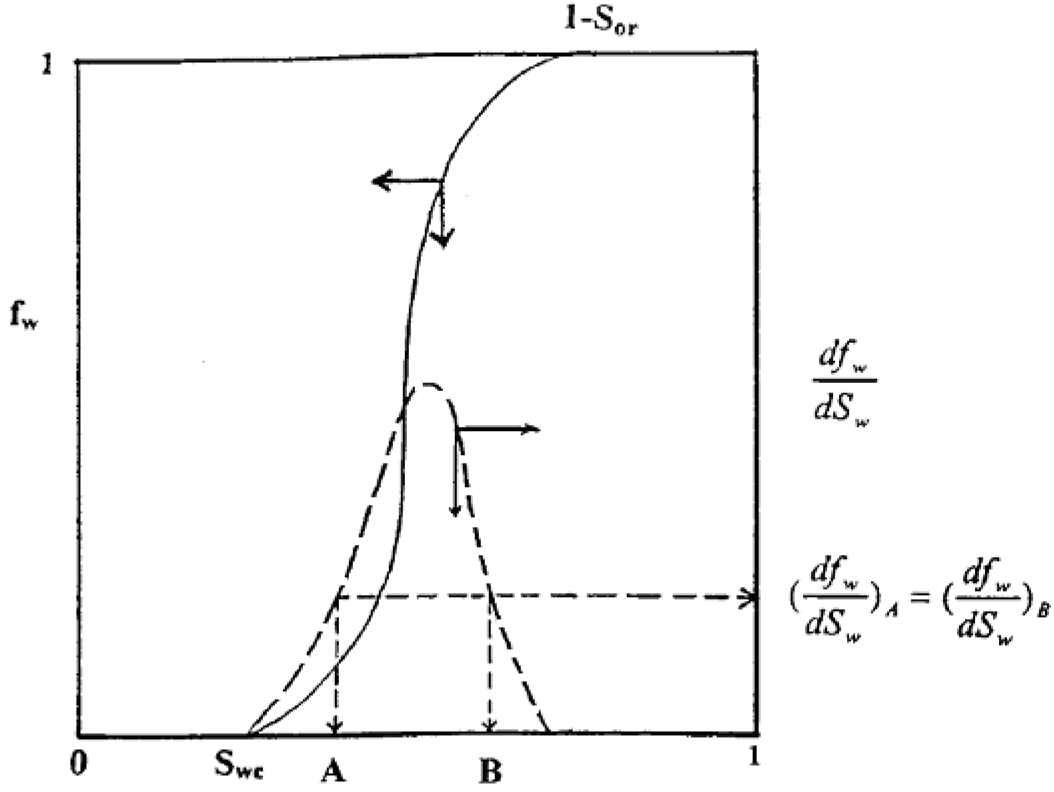

Figure 2.8: The f_w curve with its saturation derivative curve, adapted from Tarek (2006).

As shown in Fig. 2.8 both derivatives are identical, i.e. $\left(df_w / dS_w\right)_A = \left(df_w / dS_w\right)$, implying that multiple water saturations can coexist at the same position—but this is physically impossible, though mathematically permissable. Buckley and Leverett (1942) recognized the physical impossibility of such a condition. They pointed out that this apparent problem is due to the neglect of the capillary pressure gradient term in the fractional flow equation. This capillary term (see Eq. 2.12) is given by:

$$\text{Capillary term} = \left(\frac{0.001127\,k_o A}{\mu_o q_t}\right)\left(\frac{dP_c}{dx}\right) \tag{2.33}$$

As shown in Fig. 2.9, neglecting capillary term when constructing the fractional flow curve would produce a graphical relationship that is characterized by the following two segments of lines:

- A straight line segment with a constant slope of $\left(\frac{df_w}{dS_w}\right)_{Swf}$ from S_{wc} to S_{wf}
- A concaving curve with decreasing slopes from S_{wf} to $\left(1-S_{or}\right)$

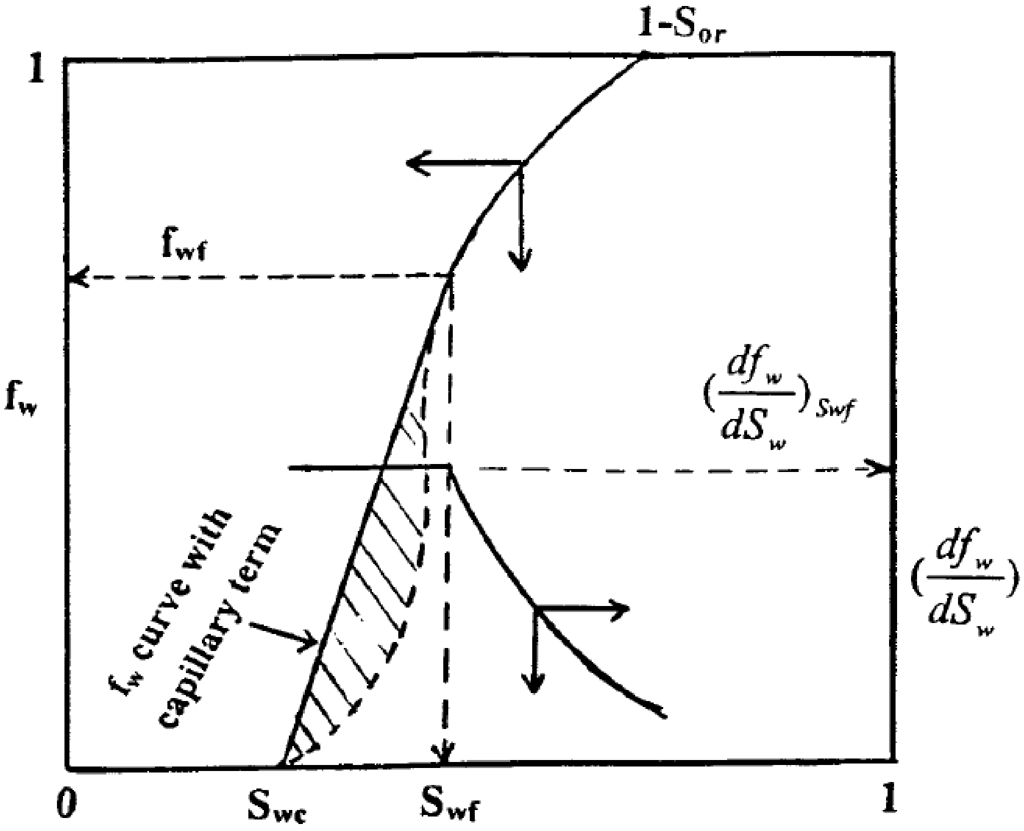

Figure 2.9: Effect of the capillary term on the f_w curve, adapted from Tarek (2006).

Terwilliger et al. (1951) found that at the lower range of water saturations between S_{wc} and S_{wf}, all saturations move at the same velocity as a function of time and distance. Notice that all saturations in that range have the same value for the slope and, therefore, the same velocity as given by Equation 2.26:

$$(v)_{S_w<S_{wf}} = \left(\frac{5.615 q_w}{A\phi}\right)\left(\frac{df_w}{dS_w}\right)_{S_{wf}} \tag{2.34}$$

We can also conclude that all saturations in this particular range will travel the same distance *x* at any particular time *t*, as given by Equation 2.30:

$$(x)_{S_w<S_{wf}} = \left(\frac{5.615W_i(t)}{A\phi}\right)\left(\frac{df_w}{dS_w}\right)_{Swf} \qquad \textbf{(2.35)}$$

The water saturation profile will maintain a constant over the range of saturation between S_{wc} and S_{wf} with time. According to Terwilliger et al. (1951), the reservoir flooded zone with this range of saturation is the stabilized zone. This zone is defined as the particular saturation interval where all points of saturation travel at the same velocity. From Figure 2.10 there is another saturation zone between S_{wf} and $(1-S_{or})$ which is named the nonstabilized zone. In this zone, the velocity of any water saturation is variable, and hence we will calculate the distance to a given saturation in the nonstabilized zone such that $S_{wf} \leq S_w \leq 1-S_{or}$ from:

$$(x)_{S_w>S_{wf}} = \left(\frac{5.615W_i(t)}{A\phi}\right)\left(\frac{df_w}{dS_w}\right)_{Sw} \qquad \textbf{(2.36)}$$

Experimental core flood data show that the actual water saturation profile during water flooding is similar to that of Figure 2.10. There is a distinct front, or shock front**,** at which the water saturation abruptly increases from S_{wc} to S_{wf}. Behind the flood front there is a gradual increase in saturations from S_{wf} up to the maximum value of $1-S_{or}$. Therefore, the saturation S_{wf} is called the water saturation at the front or, alternatively, the water saturation of the stabilized zone. In Fig. 2.10, the value of S_{wc} is equal to 0.

According to Welge (1952) showed that by drawing a straight line from S_{wc} (or from S_{wi} if it is different from S_{wc}) tangent to the fractional flow curve, the saturation value at the tangent point is equivalent to that at the front S_{wf}. The coordinate of the point of tangency represents also the value of the water cut at the leading edge of the water front f_{wf}.

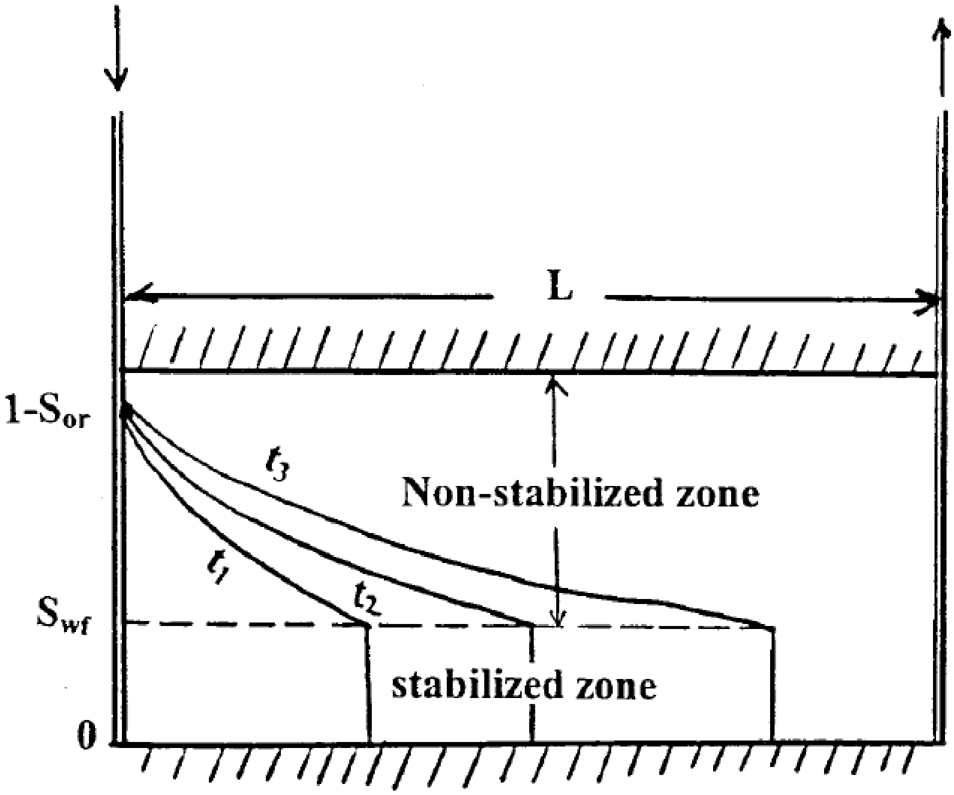

Figure 2.10: Water saturation profile as a function of distance and time, adapted from Tarek (2006).

From the above discussion, the water saturation profile at any given time t_1 can be easily developed using the procedure given in the following steps:

Step 1. Ignoring the capillary pressure term, construct the fractional flow curve, i.e., f_w vs. S_w.

Step 2. Draw a straight-line tangent from S_{wc} to the curve.

Step 3. Identify the point of tangency and read off the values of S_{wf} and f_{wf}.

Step 4. Calculate graphically the slope of the tangent as $\left(\frac{df_w}{dS_w}\right)_{Swf}$

Step 5. Using Equation 2.30, we calculate the distance of the leading edge of the waterfront from the injection well (simply called the location of front) as:

$$(x)_{S_{wf}} = \left(\frac{5.615 W_i(t_1)}{A\phi}\right)\left(\frac{df_w}{dS_w}\right)_{S_{wf}} \tag{2.37}$$

Step 6. Select several values for water saturation S_w greater than S_{wf} and determine $\left(\frac{df_w}{dS_w}\right)_{Sw}$ by graphically drawing a tangent to the f_w curve at each selected water saturation (as shown in Figure 2.11).

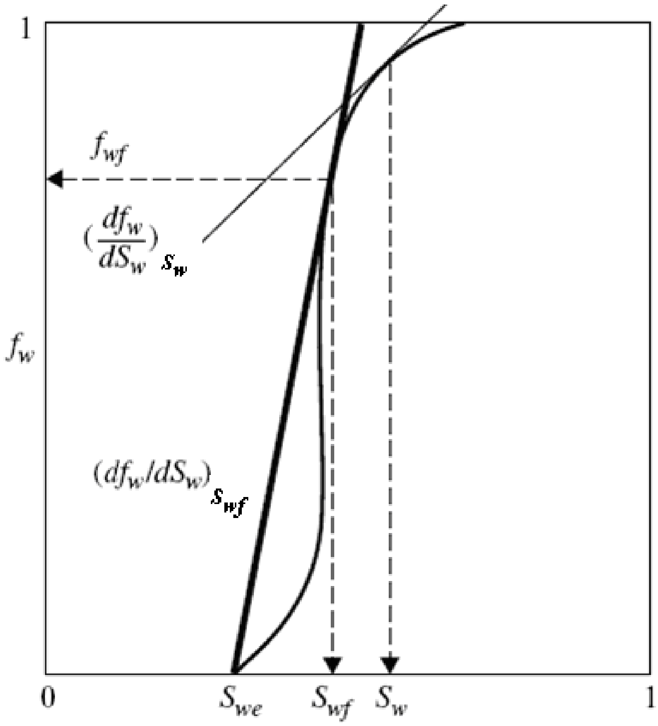

Figure 2.11: Fractional flow curve.

Step 7. Using Equation 2.36 we calculate the distance from the injection well to each selected saturation or:

$$(x)_{S_w} = \left(\frac{5.615 W_i(t_1)}{A\phi}\right)\left(\frac{df_w}{dS_w}\right)_{S_w} \qquad \textbf{(2.38)}$$

Step 8. Establish the water saturation profile after t_1 days by plotting results obtained in step 7.

Step 9. Select a new time t_2 and repeat steps 5 through 7 to generate a family of water saturation profiles as shown schematically in Figure 2.10.

Some erratic values of $\left(\frac{df_w}{dS_w}\right)_{S_w}$ might result when determining the slope graphically at different saturations. A better way is to determine the derivative mathematically by recognizing that the relative permeability ratio $\frac{k_{ro}}{k_{rw}}$ can be expressed by Equation below:

$$\frac{k_{ro}}{k_{rw}} = ae^{bS_w} \tag{2.39}$$

Notice that the slope b in the above expression has a negative value. The above expression can be substituted into Equation 2.14 to give:

$$f_w = \frac{1}{1+\left(\frac{\mu_w}{\mu_o}\right)ae^{bS_w}} \tag{2.40}$$

The derivative of $\left(\frac{df_w}{dS_w}\right)_{S_w}$ may be obtained mathematically by differentiating the above equation with respect to S_w to give:

$$\left(\frac{df_w}{dS_w}\right)_{S_w} = \frac{-\left(\frac{\mu_w}{\mu_o}\right)abe^{bS_w}}{\left[1+\left(\frac{\mu_w}{\mu_o}\right)ae^{bS_w}\right]^2} \tag{2.41}$$

The above steps are general for computing the water saturation profile as function of time for a specified value of time or cumulative water injection for the cases of constant-rate water injection or injection at constant pressure. In the next two subsections, we will outline the procedure for performance predictions before and after breakthrough for both constant-rate water injection rate and constant-pressure injection cases.

2.1 Constant Rate Injection

Here, we provide the performance calculation for the case of constant-rate injection case before and after breakthrough. First, we present the calculation procedure for times before breakthrough and then the calculation procedure for times after breakthrough. For simplicity, we denote breakthrough as BT.

<u>Performance Calculations Before BT Times.</u> The following steps are followed:

Step 1: Determine water saturation at the front and average saturation behind the front (i.e., S_{wf} and $\overline{S}_{wf}$) as we discussed earlier (graphical procedure, analytical, etc.). Here, $\overline{S}_{wf}$ represents the average water saturation behind the front at any time up to breakthrough or also called as the average saturation in the reservoir at the time of breakthrough. It is determined by the extrapolation of the tangent line to $f_w = 1$ line on f_w-S_w curve (see Fig. 2.11).

Step 2. Compute the time of BT (t_{bt}). This time value is computed from:

$$t_{bt} = \frac{AL\phi}{5.615 q_t \left(\dfrac{\partial f_w}{\partial S_w} \right)_{S_{wf}}} \qquad \textbf{(2.42)}$$

Step 3: Computing oil production prior to BT. Let $Q_o(t)$ denote the cumulative oil production in RB from time zero (beginning of the flood) to t. Then, from material balance, we

$$Q_o(t) = \left[1 - f_w\left(S_{wi}\right)\right] \frac{AL\phi Q_i(t)}{5.615} \qquad \textbf{(2.43)}$$

where $Q_i(t)$ is the fraction of the cumulative pore volumes of water injected (a fraction) up to time t and for the constant-rate injection case, it is given by

$$Q_i(t) = \frac{5.615 q_t t}{A\phi L} \qquad \textbf{(2.44)}$$

Using Eq. 2.44 in Eq. 2.43 gives:

$$Q_o(t) = \left[1 - f_w\left(S_{wi}\right)\right]\left(q_t t\right) \qquad \textbf{(2.45)}$$

where q_t is the water injection rate in RB/D.

If we wish to compute cumulative oil produced in terms of stock tank rates, then we denote $N_p(t)$ to represent the cumulative oil production in STB up to time t and compute $N_p(t)$ from:

$$N_p(t) = \frac{Q_o(t)}{B_o} = [1 - f_w(S_{wi})]\frac{AL\phi Q_i(t)}{5.615B_o} \quad \text{for } t < t_{bt} \tag{2.46}$$

where B_o represents the oil formation volume factor (RB/STB) and should evaluated at average reservoir pressure.

It is important to note that Eqs. 2.45 and 2.46 apply only up to BT because at t_{bt} the saturation at $x = L$ jumps to S_{wf} and then continues to increase. In Eqs. 2.45 and 2.46, we have $f_w(S_{wi})$ value. Here, S_{wi} represents the initial water saturation and in some cases, this saturation value may exceed the value of irreducible water saturation S_{iw} (or S_{wc} used interchangeably in this thesis) and hence $f_w(S_{wi})$ may be greater than zero. In cases, $S_{wi} = S_{iw}$, then $f_w(S_{wi})$=0, and hence Eqs. 2.45 and 2.46 simply become:

$$Q_o(t) = q_t t \tag{2.47}$$

and

$$N_p(t) = \frac{Q_o(t)}{B_o} = \frac{q_t t}{B_o} \quad \text{for } t < t_{bt} \tag{2.48}$$

Step 4: Computation of average water saturation in reservoir prior to BT. We let $\overline{S_w}$ to denote the average water saturation in the reservoir at any time before BT time. It will be computed from:

$$\overline{S_w} = S_{wi} + \frac{5.615 q_t t}{A\phi L}[1 - f_w(S_{wi})] \tag{2.49}$$

If $S_{wi} = S_{iw}$, then Eq. 2.49 simplifies to:

$$\overline{S_w} = S_{iw} + \frac{5.615 q_t t}{A\phi L} \tag{2.50}$$

Step 5: Computation of cumulative oil production at the time of BT. It is computed from:

$$N_p(t_{bt}) = \frac{Q_o(t_{bt})}{B_o} = \frac{AL\phi(\overline{S}_w - S_{wi})}{5.615B_o} \tag{2.51}$$

Another parameter of interest at time of BT is the recovery factor (*RF*) which is defined as the cumulative oil produced in STB up to time t_{bt} divided by the oil initially in place (OIIP) in STB, that is,

$$RF = \frac{N_p(t_{bt})}{OIIP} \qquad \textbf{(2.52)}$$

where *OIIP* is computed from:

$$OIIP = \frac{A\phi L(1 - S_{wi})}{5.615 B_{oi}} \qquad \textbf{(2.53)}$$

where B_{oi} is the formation volume factor at initial reservoir pressure. It may be worth noting that Eq. 2.52 can also be used to compute the values of *RF* for any time before the time of BT.

Step 6: Computation of water oil ratio at the time of BT. WOR at the instant of BT (in STB/STB) is to be computed from:

$$WOR(t_{bt}) = \frac{q_w(t_{bt})/B_w}{q_o(t_{bt})/B_o} = \frac{f_w(S_{wf})}{B_w}\,\frac{B_o}{\left[1 - f_w(S_{wf})\right]} \qquad \textbf{(2.54)}$$

At any time *t* prior to BT, WOR is to be determined from

$$WOR(t) = \frac{q_w(t)}{q_o(t)} = \frac{f_w(S_{wi})}{B_w}\,\frac{B_o}{\left[1 - f_w(S_{wi})\right]} \qquad \textbf{(2.55)}$$

If $S_{wi} = S_{iw}$, then Eq. 2.55 gives zero water-oil-ratio for any time *t* before BT, as expected.

Performance Calculations After BT. The following steps are followed:

Step 1: Select a set of 10 or more values of S_w between S_{wf} and 1-S_{or} (as shown in Fig. 2.12). Denote each of these S_w values by S_{w2} and denote the corresponding values of f_w by f_{w2}. Let $\overline{S_{w2}}$ to denote the average water saturation in the reservoir when the water saturation at $x = L$ is equal to S_{w2}.

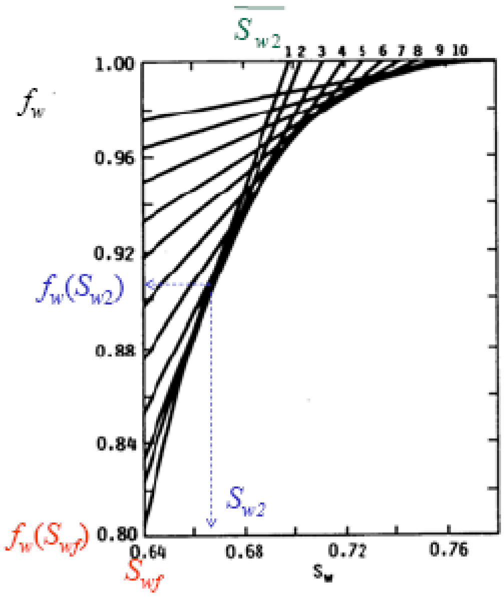

Figure 2.12: Selection of water saturation values of S_{w2} for performance calculations after BT, after Willhite (1986).

Step 2: Then for each value of S_{w2}, compute the slope df_w/dS_w at S_{w2} from the table or graph. Then compute the time t_2 when the saturation S_{w2} reaches $x=L$. Recall (Eq. 2.36) that any saturation between $S_{wf}<S_{w2}<1-S_{or}$, S_{w2} reaches the right-end ($x=L$) at time t_2 such that

$$L = \frac{5.615 q_t t_2}{A\phi}\left(\frac{\partial f_w}{\partial S_w}\right)_{S_{w2}} \tag{2.56}$$

Solving Eq. 2.56 for t_2 gives:

$$t_2 = \frac{A\phi L}{5.615 q_t \left(\frac{\partial f_w}{\partial S_w}\right)_{S_{w2}}} \tag{2.57}$$

Step 3: Estimate $\overline{S_{w2}}$, which is the average water saturation in the reservoir when S_{w2} reaches $x = L$. This value can estimated graphically by drawing a tangent line to the f_w curve at $Sw2$, as shown in Fig. 2.12. The saturation value where this tangent line intersects the $f_w = 1$ horizontal line is $\overline{S_{w2}}$.

We can also analytically compute the value of $\overline{S_{w2}}$ from Eq. 2.58. If we prepare a head of time a graph of df_w/dS_w vs. S_w, we can find the value of df_w/dS_w at S_{w2}, then compute the average saturation from

$$\overline{S_{w2}} = S_{w2} + \frac{[1 - f_w(S_{w2})]}{\left(\frac{\partial f_w}{\partial S_w}\right)_{S_{w2}}} \quad \textbf{(2.58)}$$

Step 4: Computations of N_p, and *WOR* at t_2. Cumulative oil produced (displaced), N_p, up to time t_2 in STB can be computed from:

$$N_p(t_2) = \frac{Q_o(t_2)}{B_o} = \frac{AL\phi\left(\overline{S_{w2}} - S_{wi}\right)}{5.615B_o} \quad \textbf{(2.59)}$$

where B_o is evaluated at our best estimate of average reservoir pressure. Then, we can compute the recovery factor *RF* at t_2 from

$$RF = \frac{N_p(t_2)}{OIIP} \quad \textbf{(2.60)}$$

The producing WOR ratio at t_2 is given by

$$WOR(t_2) = \frac{f_w(S_{w2})}{B_w} \frac{B_o}{[1 - f_w(S_{w2})]} \quad \textbf{(2.61)}$$

Step 5: Computing cumulative water produced at t_2. It (denoted by $Q_{w,cum}$) can be computed from:

$$Q_{w,cump}(t_2) = \frac{Q_{w,inj}(t_2) - \Delta V_w}{B_w} \quad \textbf{(2.62)}$$

where $Q_{w,inj}$ represents the cumulative water injected up to time t2, and can be computed from

$$Q_{w,inj}(t_2) = \frac{A\phi L}{5.615\left(\frac{\partial f_w}{\partial S_w}\right)_{S_{w2}}} \quad \textbf{(2.63)}$$

and ΔV_w represents the increase in water volume (in RB) in the reservoir at time t_2 and can be computed from:

$$\Delta V_w = \frac{A\phi L\left(\overline{S_{w2}} - S_{wi}\right)}{5.615} \qquad \textbf{(2.64)}$$

The above given steps (Steps 2-5) are repeated for each value of S_{w2}.

2.2 Constant Pressure Injection

Here, we provide the performance calculations for the case of constant pressure injection case before and after breakthrough. First, we present the calculation procedure for times before BT and then the calculation procedure for times after BT. It should be noted that the performance calculations for the constant pressure injection case is computationally more intensive than the performance prediction for the constant-rate injection case.

Before giving the calculation procedure, we should state why one should consider the constant pressure injection case for predicting the waterflood performance.

So far, we have considered constant rate injection. However, economic and technical considerations usually lead to waterflooding a reservoir at the rate maximum possible. In field applications, operation at constant pressure change between injection and production wells is frequently used due to reasons listed below:

- Pressure in the injection well may be limited by the operator’s desire to operate below the fracture (or also called parting) pressure of the formation. For instance, if we fracture the well, we no longer have the control over the sweep as shown in Figure 2.13.
- At the producing well, control of gas and sand or other operating problems may also lead to maintenance of a specified back pressure.

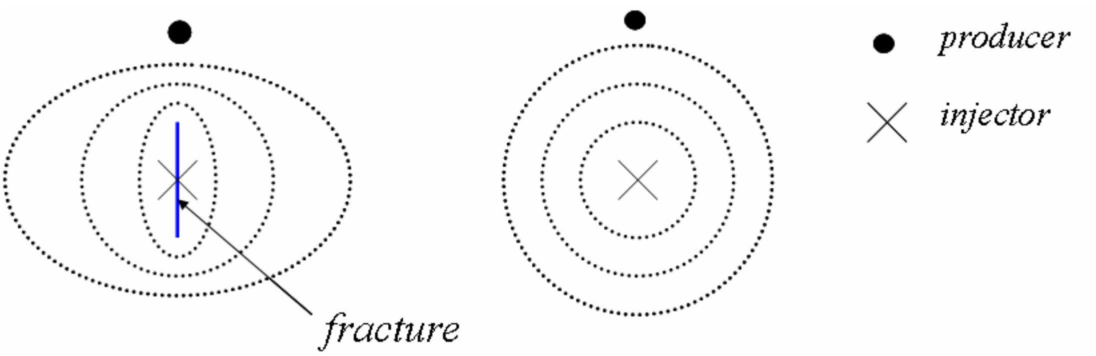

Figure 2.13: Sweep with and without fracture at the injector, after Onur (2008).

It is important to note that the frontal advance equation that we derived earlier is given by

$$\left(\frac{dx}{dt}\right)_{\hat{S}_w} = \frac{5.615 q_t}{\phi A}\left(\frac{\partial f_w}{\partial S_w}\right)_{\hat{S}_w} \tag{2.65}$$

When deriving this equation, we made no assumption regarding the variation of q_t with time. So, Eq. 2.65 is quite general in the sense that q_t in Eq. 2.65 can be treated as a function of time, t, i.e., $q_t = q_t(t)$.

Assuming no capillary pressure and gravity effects, the total flow rate, q_t, is given the Darcy's equation for 1D flow as:

$$q_t(t) = -1.127 \times 10^{-3} kA\left[\frac{k_{ro}}{\mu_o} + \frac{k_{rw}}{\mu_w}\right]\frac{\partial p}{\partial x} \tag{2.66}$$

or

$$q_t(t) = -1.127 \times 10^{-3} kA\lambda_t \frac{\partial p}{\partial x} \tag{2.67}$$

where λ_t is called the total mobility and is defined as

$$\lambda_t = \frac{k_{ro}}{\mu_o} + \frac{k_{rw}}{\mu_w} = \lambda_o + \lambda_w \tag{2.68}$$

Because of the incompressible flow assumption, q_t in Eq. 2.67 is constant for every x at a given time t. Then, we can integrate Eq.2.66 with respect to x from x = 0 to x =L to obtain:

$$q_t = 1.127 \times 10^{-3} \frac{kA}{\left(\int_0^L \frac{1}{\lambda_t} dx\right)}\left(p_{inj} - p_{wf}\right) \tag{2.69}$$

where p_{inj} and p_{wf} represent the pressures at the injector and the producer, respectively. It is worth noting that as S_w changes with position x (see Fig. 2.10), and the total mobility λ_t is a function of water saturation, then λ_t is a function of position x.

If we define an apparent viscosity given by

$$\mu_{app} = \frac{1}{L}\int_0^L \frac{1}{\lambda_t} dx \qquad \textbf{(2.70)}$$

which represents an average of inverse of total mobility over the total length *L*, then we can express Eq. 2.69 as:

$$q_t = 1.127 \times 10^{-3} \frac{kA}{\mu_{app}} \frac{\left(p_{inj} - p_{wf}\right)}{L} \qquad \textbf{(2.71)}$$

It should be noted that apparent viscosity is a function of water saturation because it depends on the mobility profile and time, t. So, q_t is a function of time for the constant pressure injection case. So, to compute the flood performance at any time t, we need to compute the apparent viscosity, μ_{app}, at any time t. This requires that we need to compute the saturation profile as a function of x in the reservoir at a given time t. There are two approaches that can be used:

- Numerical solution procedure
- Concept of the average of apparent viscosity, μ_{app}

In this thesis, we will consider the latter approach. Before proceeding with this approach, we have several remarks to make regarding the behavior of q_t for the constant pressure injection case, in comparison with the constant-rate injection case.

In the case of favorable mobility ratio, i.e., typically water viscosity is bigger than oil viscosity, the total mobility tends to decrease, hence the apparent viscosity, μ_{app}, increases at least up to breakthrough. Thus, the total flow rate, q_t, tends to decrease up to breakthrough for this case. After breakthrough, the preference flow path is for water and thus the total mobility tends to increase and thus, the apparent viscosity tends to decrease. So, q_t tends to increase for the favorable case after the breakthrough. Turning the statement around, for the constant-rate injection case, we expect the injection pressure, p_{inj}, to increase before the breakthrough and to decrease after the breakthrough for the favorable case. These results are schematically illustrated in Figure 2.14.

For the unfavorable case, we would expect that the q_t increases both before and after breakthrough under constant pressure case. Turning the statement around, for the constant-rate injection case, the injection pressure will decrease before and after breakthrough for the unfavorable case. These results are schematically illustrated in Figure 2.15.

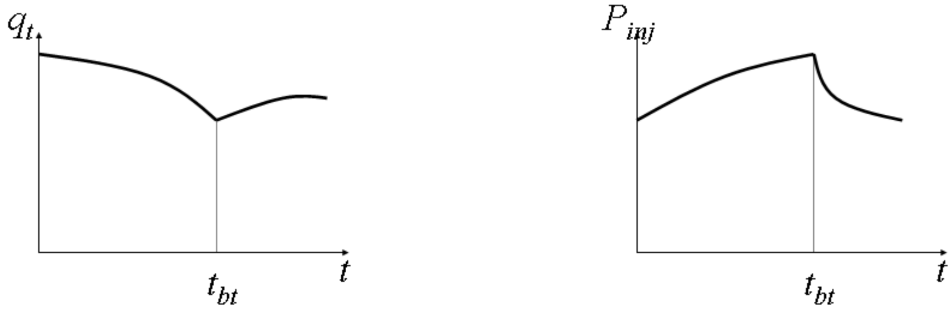

(a) Constant pressure injection case **(b) constant-rate injection case**

Figure 2.14: The behavior of q_t and p_{inj} for the constant pressure injection and constant-rate injection cases; favorable mobility ratio, after Onur (2008).

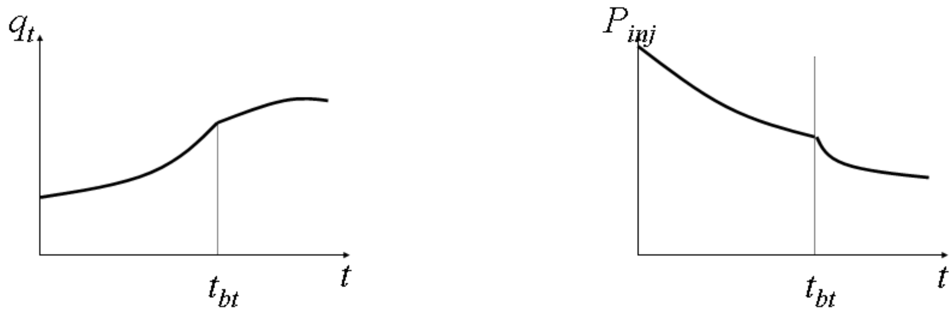

(a) Constant pressure injection case **(b) constant-rate injection case**

Figure 2.15: The behavior of q_t and p_{inj} for the constant pressure injection and constant-rate injection cases, unfavorable mobility ratio, after Onur (2008).

Now, we give the performance calculation procedure for the constant pressure injection case based on the frontal advance theory. Earlier we showed that the advance frontal equation can be written as

$$x_{\hat{S}_w}(t) = LQ_i(t)\left(\frac{\partial f_w}{\partial S_w}\right)_{\hat{S}_w} \quad \textbf{(2.72)}$$

where $\hat{S}_w$ is the given water saturation value, and $Q_i(t)$ is the number of cumulative pore volumes of water injected up to time t.

$$Q_i(t) = \frac{5.615\int_0^t q_t(\tau)d\tau}{A\phi L} = \frac{\int_0^t q_t(\tau)d\tau}{V_p} \quad \textbf{(2.73)}$$

where V_p represents the reservoir pore volume in RB.

It should be noted that Eq. 2.73 provides a direct relationship, though implicit, between $q_t(t)$ and $Q_i(t)$. This suggests that if we specify values of $Q_i(t)$, then a value of $q_t(t)$ can be computed for each value of $Q_i(t)$ specified. Before we give the procedure, we should note that we can rearrange Eq. 2.73 as

$$V_p Q_i(t) = \int_0^t q_t(\tau) d\tau \qquad \textbf{(2.74)}$$

Suppose that we know the values of q_t at n discrete time points, $0=t_0<t_1<t_2<\ldots<t_n=t_e$, and we wish to compute $V_pQ_i(t_e)$. One way to do this is to write Eq. 2.74 as

$$V_p Q_i(t_e) = \sum_{l=1}^{n} \int_{t_{l-1}}^{t_l} q_t(\tau) d\tau \qquad \textbf{(2.75)}$$

The if we apply the trapezoidal rule of integration for each integral in the sum in Eq. 2.75, we can obtain

$$\begin{aligned} V_p Q_i(t_e) &= \sum_{l=1}^{n-1} \left[\frac{q_t(t_l) + q_t(t_{l-1})}{2} \right] (t_l - t_{l-1}) \\ &+ \left[\frac{q_t(t_e) + q_t(t_{n-1})}{2} \right] (t_e - t_{n-1}) \end{aligned} \qquad \textbf{(2.76)}$$

Performance Calculations Before BT Times. The following steps are followed:

Step 1: First, compute $Q_i(t_{bt})$, which can be computed from

$$\frac{1}{Q_i(t_{bt})} = \left(\frac{df_w}{dS_w} \right)_{S_{wf}} \qquad \textbf{(2.77)}$$

Then, we solve for $Q_i(t_{bt})$ as:

$$Q_i(t_{bt}) = \frac{1}{\left(\dfrac{df_w}{dS_w} \right)_{S_{wf}}} \qquad \textbf{(2.78)}$$

Step 2: Specify a sequence of $Q_i(t_{bt})$. Note we can generate a sequence by diving $Q_i(t_{bt})$ into say k (e.g. 10) increments;

$$0 = Q_i(t_0) < Q_i(t_1) < Q_i(t_2) < \cdots < Q_i(t_{k-1}) < Q_i(t_k = t_{bt}) \qquad \textbf{(2.79)}$$

Note that we we don't know the values of time corresponding to each Q_i at this stage.

Step 3: Now, given $Q_i(t_j)$, we can compute the saturation profile from

$$x_{\hat{S}_w}(t_j) = LQ_i(t_j)\left(\frac{\partial f_w}{\partial S_w}\right)_{\hat{S}_w} \qquad for\ S_{wf} \le \hat{S}_w \le 1 - S_{or} \qquad \textbf{(2.80)}$$

Here, we take several values of $\hat{S}_w$ between S_{wf} and $1\text{-}S_{or}$, say a total of r values, then solve Eq. 2.80 for x. Repeating this procedure several times, we can construct $\hat{S}_w$ vs. x profile at a given $Q_i(t_j)$.

Step 4: Using the saturation values determined in Step 3, compute the total mobility profile, λ_t as a function of x.

Step 5: Now, we can compute the apparent viscosity, μ_{app} at $Q_i(t_j)$ from Eq. 2.70 by the application of the trapezoidal rule as:

$$\mu_{app} = \frac{1}{2L}\sum_{m=1}^{r}\left[\frac{1}{\lambda_t(x_m)} + \frac{1}{\lambda_t(x_{m-1})}\right](x_m - x_{m-1}) \qquad \textbf{(2.81)}$$

where $x_0 = 0$ and $x_r = L$ and r is the total number of increments chosen between 0 and L.

Step 6: Compute $q_t(t_j)$, though we don't know the specific value of t_j, from Eq. 2.71 with the given values of p_{inj} and p_{wf}.

Step 7: Now using $t_e = t_j$ in Eq. 2.76 gives

$$\begin{aligned} V_p Q_i(t_j) = &\sum_{l=1}^{n-1}\left[\frac{q_t(t_l) + q_t(t_{l-1})}{2}\right](t_l - t_{l-1}) \\ &+ \left[\frac{q_t(t_e) + q_t(t_{n-1})}{2}\right](t_j - t_{n-1}) \end{aligned} \qquad \textbf{(2.82)}$$

In Eq. 2.82, everything is known except the time t_j, so we can rearrange Eq. 2.82 to compute t_j as

$$t_j = t_{j-1} + \frac{V_p Q_i(t_j) - \sum_{l=1}^{j-1} \left[\frac{q_t(t_l) + q_t(t_{l-1})}{2} \right] (t_l - t_{l-1})}{\left[\frac{q_t(t_j) + q_t(t_{j-1})}{2} \right]} \qquad \textbf{(2.83)}$$

for j=1, 2,

It is important to note that $q_t(0^+)$ in Eq. 2.83 is computed from

$$q_t(0) = 1.127 \times 10^{-3} \frac{kA}{\mu_{app}(0)} \frac{(p_{inj} - p_{wf})}{L} \qquad \textbf{(2.84)}$$

where $\mu_{app}(0) = k_{ro}(S_{wi}) / \mu_o$.

Step 8: Calculate the average saturation in the reservoir at t_j from,

$$\bar{S}_w(t_j) = S_{wi} + [1 - f_w(S_{wi})] Q_i(t_j) \qquad \textbf{(2.85)}$$

Step 9: Calculate $N_p(t_j)$, WOR(t_j), etc. For example, $N_p(t_j)$ is calculated from

$$N_p(t_j) = V_p \left[\frac{\bar{S}_w(t_j) - S_{wi}}{B_o} \right] \qquad \textbf{(2.86)}$$

and WOR is computed at the t_{bt} is computed from:

$$WOR(t_{bt}) = \frac{q_w(t_{bt}) / B_w}{q_o(t_{bt}) / B_o} = \frac{f_w(S_{wf})}{B_w} \frac{B_o}{[1 - f_w(S_{wf})]} \qquad \textbf{(2.87)}$$

Performance Calculations After BT. The following steps are followed:

Here, specify Q_i values after BT such that

$$Q_i(t_k = t_{bt}) < Q_i(t_{k+1}) < Q_i(t_{k+2}) < Q_i(t_{k+3}) < \cdots \qquad \textbf{(2.88)}$$

Then, we perform a similar process to performance calculations as the performance before breakthrough. An easier way to the above procedure is to specify a set of $S_w(x=L)$ (or with the same notation used for the constant-rate injection case as S_{w2}) such that

$$S_{wf} = S_{w2}(t_k = t_{bt}) < S_{w2}(t_{k+1}) < S_{w2}(t_{k+2}) < S_{w2}(t_{k+3}) < \cdots \quad \textbf{(2.89)}$$

Then, we compute $Q_i(t_{k+j})$ corresponding to each specified value of saturation at $x=L$ from:

$$Q_i(t_{k+j}) = \frac{1}{\left(\dfrac{df_w}{dS_w}\right)_{S_{w2}(t_{k+j})}} \quad \textbf{(2.90)}$$

Next, we compute the average water saturation in the reservoir from

$$\overline{S_w}(t_{k+j}) = S_{w2}\left(t_{k+j}\right) + \left[1 - f_w(S_{w2}(t_{k+j}))\right]Q_i(t_{k+j}) \quad \textbf{(2.91)}$$

The cumulative oil production is then computed from

$$N_p(t_{k+j}) = V_p\left[\frac{\overline{S_w}(t_{k+j}) - S_{wi}}{B_o}\right] \quad \textbf{(2.92)}$$

Water production after BT is computed using the same equations given for the constant-rate injection case.

In Chapter 4, we will present example applications of performance calculations for both the constant-rate and constant-injection pressure cases.

3. IMMISCIBLE DISPLACEMENT TWO DIMENSIONS-AREAL OR PATTERN FLOODING

In this chapter, we extend the prediction methods based on 1D linear flow in Chapter 2 to two-dimensional problems (*x*-*y*). Reservoir displacement processes are frequently conducted in patterns (see Fig. 3.1) where a specific configuration of injection and production wells is repeated across the field.

If the reservoir has been developed on a regular pattern, commonly used patterns for injection are the five spot, nine spot and staggered and line drive patterns.

Typically, approximate methods are used to correlate results of 1D linear flow to 2D flow in terms of the mobility ratio, *M*, which is defined by

$$M = \frac{\left(k_{rw}\right)_{\overline{S_{wf}}}}{\left(k_{ro}\right)_{S_{wi}}} \frac{\mu_o}{\mu_w} \qquad \textbf{(3.1)}$$

In cases where mobility ratio (*M*) is less than one, it tends to be harder to inject water. So for such cases, we may need more injectors than producers.

In this thesis, we will restrict the methods developed only for 5-spot pattern shown in Fig. 3.1 because of its common use. In addition, we consider only the liquid filled reservoirs, i.e., we do not consider that free gas exist in the reservoir prior to water flood. The prediction procedures for other patterns shown in Fig. 3.1 as well as for the reservoirs with free gas cases can be found in Willhite's book. It should be noted that the analytical models for areal flooding assume that no variation of saturation in the vertical direction (i.e., vertical sweep is 100%), and the 1D case considered in the previous chapter assumes that at the breakthrough the whole reservoir area has been contacted by injection (i.e., the areal sweep efficiency is 100%). However, for 2D displacement case, this assumption does not hold.

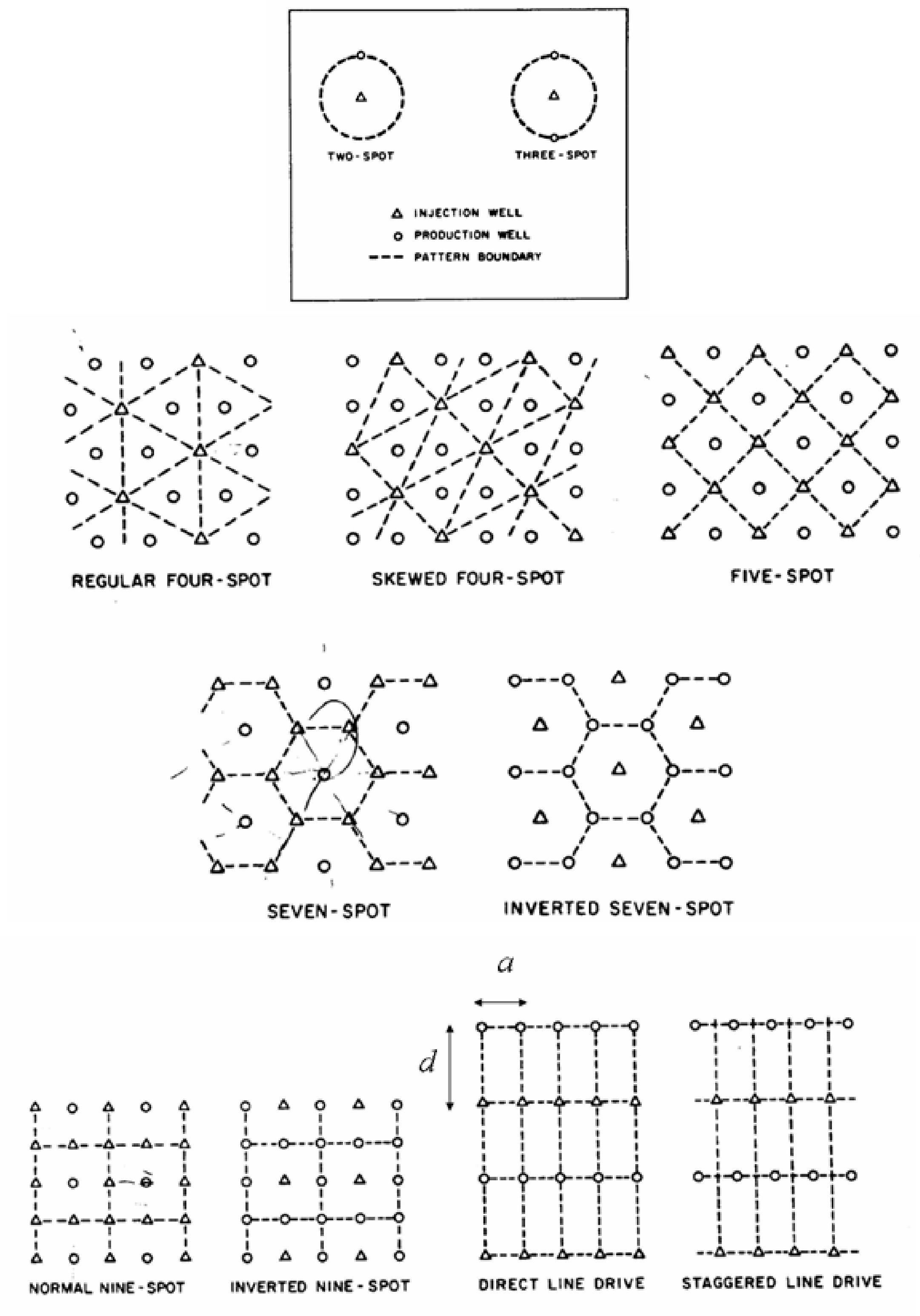

Figure 3.1: Patterns considered for 2D displacement, taken from Willhite (1986).

In the 2D areal case, in general, at the breakthrough (BT) the whole area will not be contacted by the injected water as shown in Fig. 3.2.

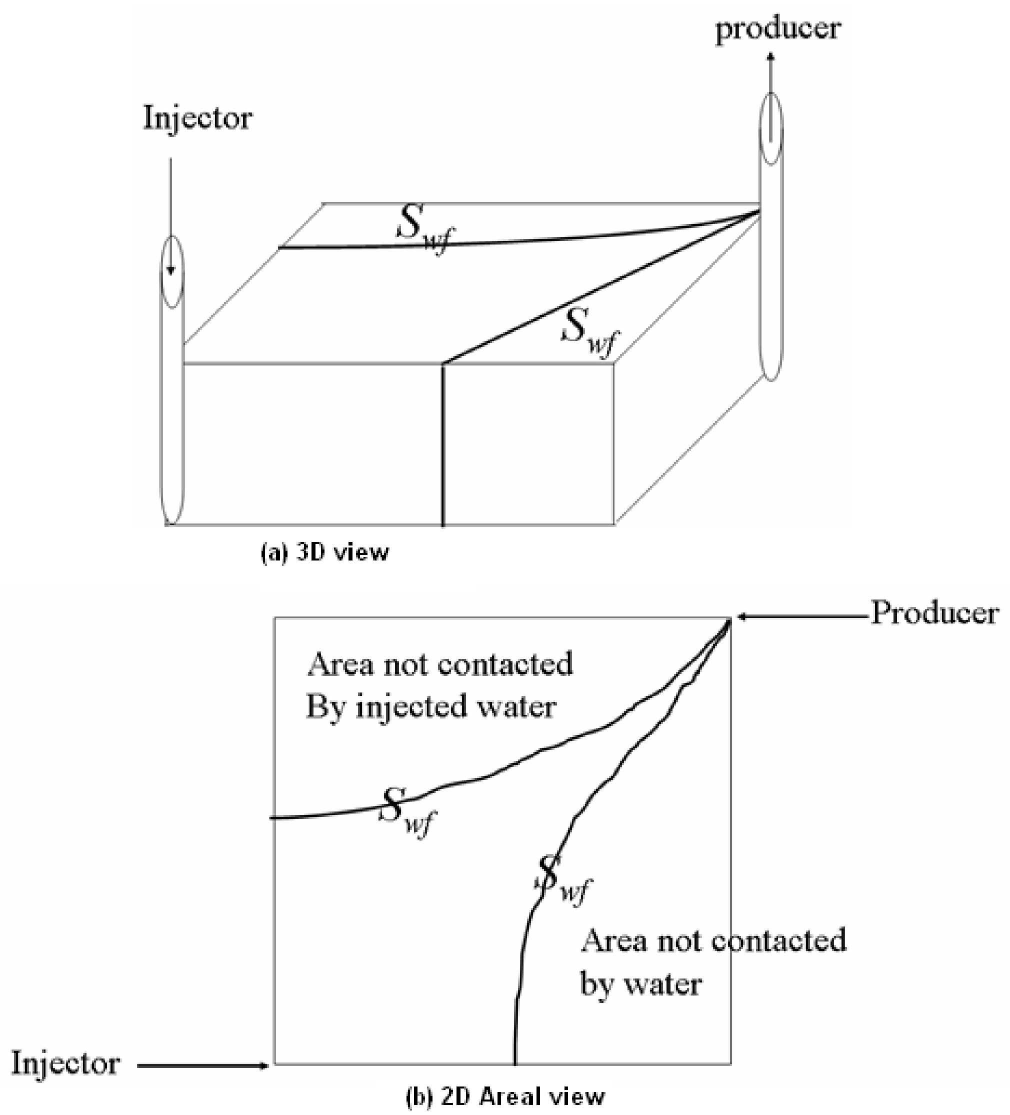

Figure 3.2: The movement of injected water at breakthrough for 2D displacement, after Onur (2008).

The behavior shown in Fig. 3.2 is usually explained by inspecting streamlines. Streamlines are paths followed by fluid particles as they traverse from an injection well to production well. The region bounded by two streamlines is called a stream tube or stream channel because there is no fluid flow across streamlines (see Fig. 3.3). Studies for incompressible flow in symmetrical well patterns also show that a straight line connecting the injector and producer is the shortest streamline between these two wells, and as result, the pressure gradient along this line is the highest. So, injected water moving areally along this shortest streamline reaches the producing well before the water moving along any other streamline. This is also depicted on Fig. 3.4 for a quarter of a 5-spot pattern.

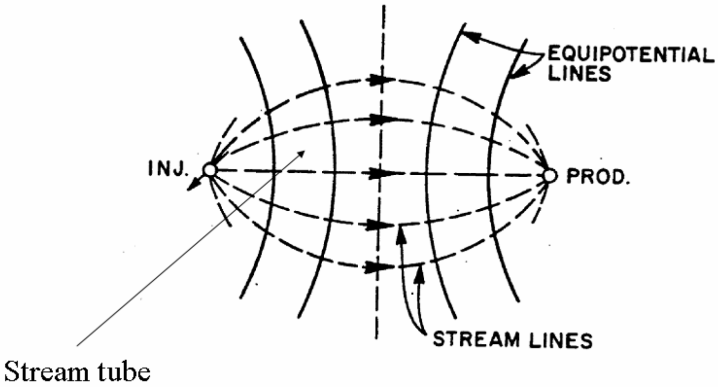

Figure 3.3: Streamlines and stream tube between an injector and producer, taken from Willhite (1996) with modification.

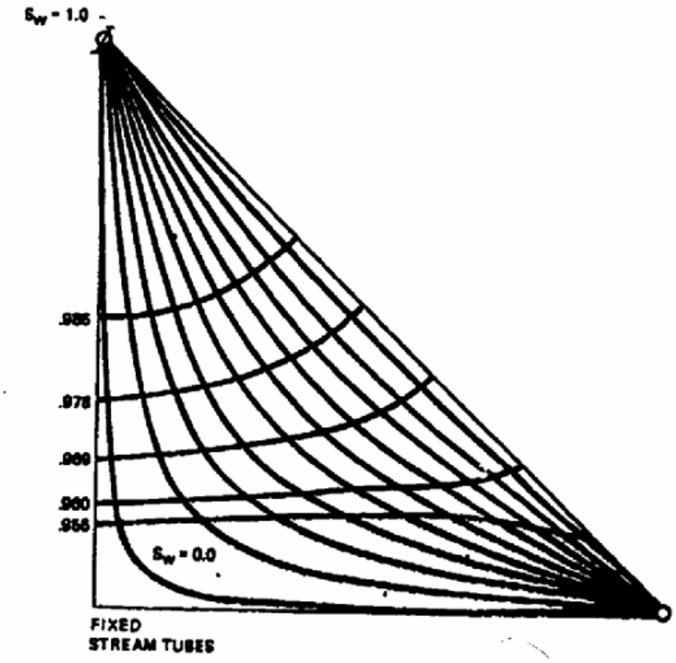

Figure 3.4: Streamlines for a quarter of 5-spot pattern, after Willhite (1996).

For two different mobility ratios, the stages of a waterflood in a five-spot pattern are shown in Fig. 3.5. As can be seen from this figure, if the mobility ratio is less than 1, we have a better sweep, i.e., most of the area is contacted by the water.

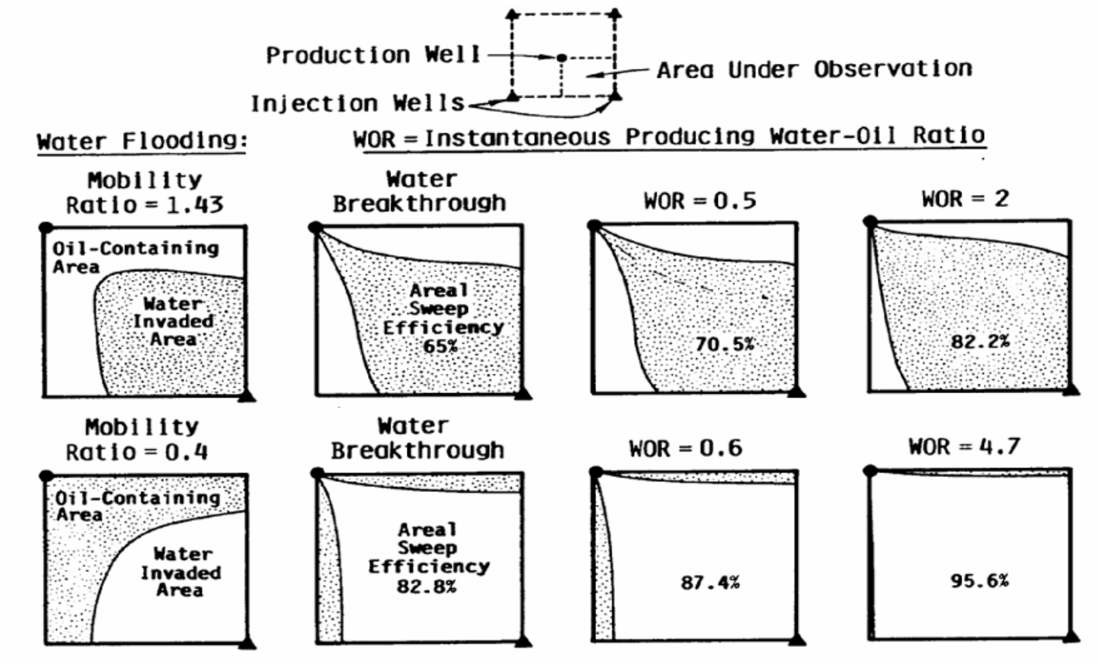

Figure 3.5: The stages of waterflood for a five-spot pattern, after Willhite (1996).

For areal displacement, one of the key parameter in performance calculations is the areal sweep efficiency denoted by E_A and defined as:

$$E_A = \frac{Pore\,volume\,contaced\,by\,injected\,water}{Total\ pore\,volume} \tag{3.2}$$

which is nothing more than the fraction of pore volume contacted by the injected water. Areal sweep efficiency at BT is denoted by E_{Abt}. So at BT, we have

$$E_A = E_{Abt} \ < 1 \tag{3.3}$$

After BT, E_A continues to increase until E_A =1.

Areal sweep efficiency at BT, E_{Abt} (or in general E_A) depends on the pattern geometry and mobility ratio (M) for homogeneous isotropic systems. If the system is anisotropic, it will also depend on the anisotropy ratio k_x/k_y. As shown by Mortada and Nabor (1961), The best areal sweep efficiency is obtained when the direction of maximum permeability is parallel to a line connecting adjacent injection wells. For five-spot pattern, the sweep efficiencies as a function of k_x/k_y are shown in Fig. 3.6. In this thesis, we restrict ourselves with the prediction methods for isotropic systems. The treatment for anisotropic systems can be found in Mortada and Nabor (1961) and Willhite (1986).

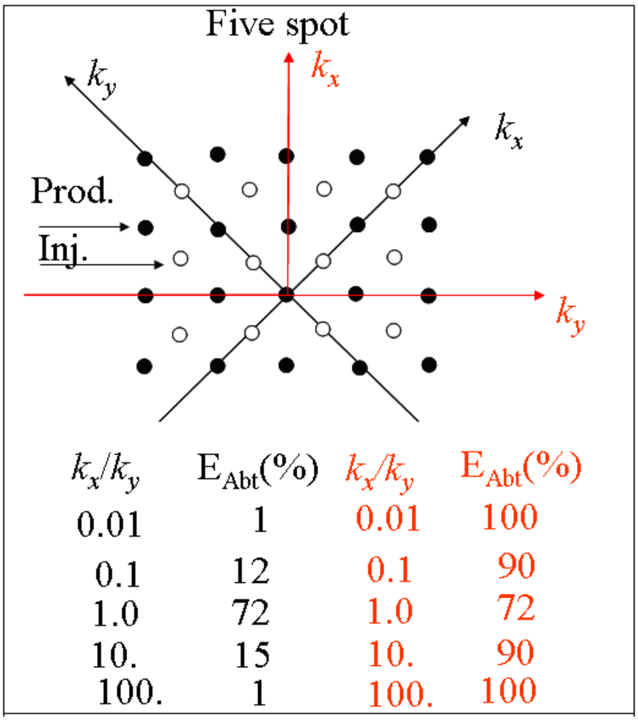

Figure 3.6: Effect of anisotropy ratio on areal sweep efficiency, after Mortada and Nabor (1961) with modification.

Assuming piston-like displacement, Dyes et al (1954) presented correlations for areal sweep as a function of mobility ratio and fraction of pore volume injected (Q_i) for various patterns. For instance, Fig. 3.7 shows their correlation for a five-spot pattern.

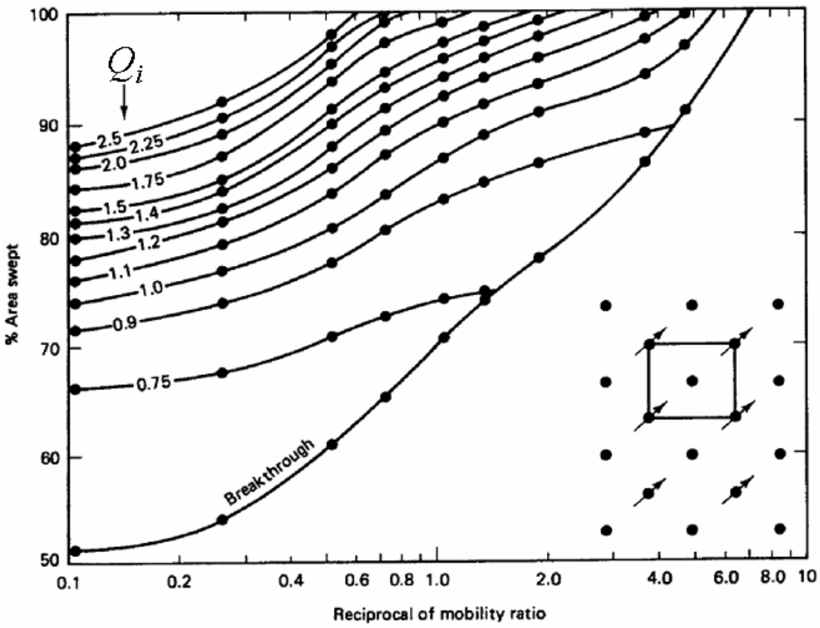

Figure 3.7: Areal sweep efficiency for a five-spot pattern under the assumption of piston-like displacement Dyes et al. (1954).

Because a common pattern used for both pilot and field projects is the five-spot, we will consider performance predictions for a five-spot using the Craig-Geffen-Morse (CGM) procedure as described in Craig *et al.* (1955). This method is given in the next section

3.1 Craig-Geffen-Morse (GGM) Procedure

CGM method considers developed (or confined) 5-spot pattern, i.e., wells produce and inject at the same rate. So, the confined 5-spot reduces to a simpler problem due to symmetry as shown in Fig. 3.8. Hence, we can apply the method for a quadrant of five-spot pattern.

CGM gives a correlation for E_{Abt} vs. M (as shown in Fig. 3.9). Neglecting gravity and capillary effects, they found that the average saturation behind the front ($\overline{S_{wf}}$) can be predicted by Buckley-Leverett (BL) theory for the 1D linear flow cases. It should be noted that the mobility ratio given in the horizontal axis of Fig. 3.9 is the mobility ratio defined by Eq.3.1.

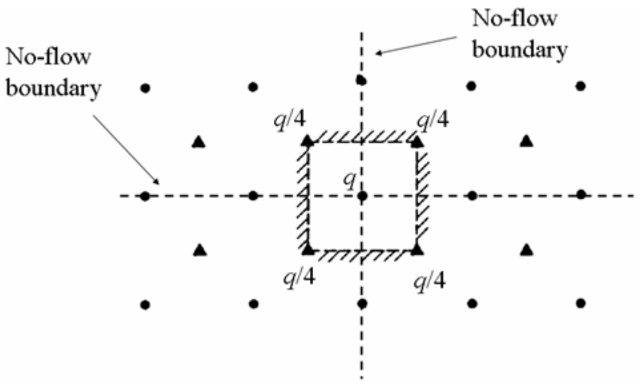

Ratio of producer to injector = 1 for a confined five-spot pattern

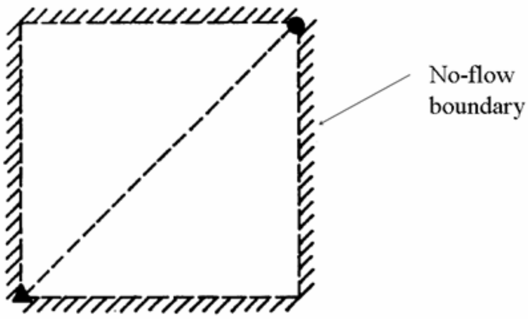

A quadrant of a five-spot pattern

Figure 3.8: Symmetry for a five-spot pattern; after Onur (2008).

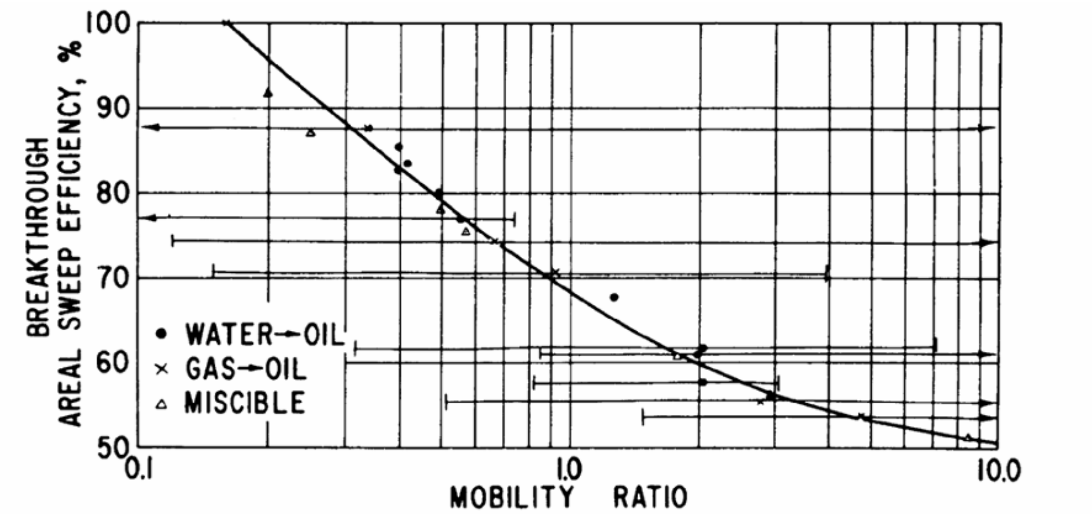

Figure 3.9: Craig-Geffen-Morse correlation for the areal sweep at BT as a function of mobility ratio, after Willhite (1986).

A simple analytical formula determining E_{Abt} is also given (Willhite, 1986) as:

$$E_{Abt} = 0.54602036 + \frac{0.03170817}{M} + \frac{0.30222997}{e^{M}} - 0.00509693\,M \quad \textbf{(3.4)}$$

We may need to account for several periods in the computations:

t=0 to t_{int}, time to interference

t_{int} to t_f, time to fill up

t_f to t_{bt}, time to BT

t_{bt} to t_{100}, time to $E_A = 1$

$t > t_{100}$

As we assume liquid filled reservoirs prior to waterflood, we will not consider the time to interference (t_{int}) and time to fill up (t_f). For such a case, it is sufficient to consider the following steps for prediction:

t=0 to t_{bt},

t_{bt} to t_{100}, time to $E_A = 1$

$t > t_{100}$

In each period given above, we specify a sequence of W_i, cumulative water injected given by:

$$W_i = Q_i V_p \tag{3.5}$$

Computations will require generating values of E_A and Q_i* corresponding to each value of W_i. Here, Q_i* is commonly referred to as the number of "contacted pore volumes of injected water'', though this terminology is not technically correct after t_{100}.

Up to time of breakthrough t_{bt}, Q_i* is given by

$$Q_i^* = \frac{W_i}{E_A V_p} \tag{3.6}$$

In Eqs. 3.4 and 3.5, V_p is the pore volume of the pattern in RB.

After determining S_{wf} and $\overline{S_{wf}}$ from f_w-S_w curve given, we will compute the mobility ratio M (Eq. 3.1) and then determine E_{Abt} from Fig. 3.9 or Eq. 3.4 using the computed value of M.

Using material balance, we can compute the cumulative water injected W_{ibt} at the time of BT from:

$$W_{ibt} = \frac{E_{Abt} V_p \left(\overline{S_{wf}} - S_{wi}\right)}{\left[1 - f_w(S_{wi})\right]} \tag{3.7}$$

Note that W_{ibt} is also equal to cumulative oil produced (N_{pbt}) up to t_{bt}. The Q_i* at the time of BT is computed from:

$$Q_{ibt}^* = \frac{W_{ibt}}{E_{Abt} V_p} = \frac{\left(\overline{S_{wf}} - S_{wi}\right)}{\left[1 - f_w(S_{wi})\right]} \tag{3.8}$$

For any time t, $t_{bt} < t \le t_{100}$, CGM gives the following correlation for the areal efficiency E_A:

$$E_A = E_{Abt} + 0.275 \ln\left(\frac{W_i}{W_{ibt}}\right) \tag{3.9}$$

If we specify a value of W_i, we can compute the corresponding value of E_A from Eq. 3.9. For time t=t_{100}, E_A =1 (and also E_A = 1 for all times t >t_{100}), At t=t_{100}, we can obtain the following equation from Eq. 3.9:

$$W_{i,100} = W_{ibt} \exp\left(\frac{1 - E_{Abt}}{0.275}\right) \tag{3.10}$$

which gives the value of cumulative water injected up to t_{100}. This is the W_i required to sweep the pattern area completely.

For any time after breakthrough, t>t_{bt}, the contacted pore volumes of water injected, Q_i* is defined implicitly by

$$\frac{dQ_i^*}{dW_i} = \frac{1}{E_A V_p} \tag{3.11}$$

Integrating Eq. 3.11 over time, it can be shown that

$$\frac{Q_i^*(t)}{Q_{ibt}^*} = 1 + a_1 e^{-a_1}\left[E_i(a_2) - E_i(a_1)\right] \tag{3.12}$$

where

$$a_1 = 3.65 E_{Abt} \tag{3.13}$$

$$a_2 = a_1 + \ln\left[\frac{W_i}{W_{ibt}}\right] \tag{3.14}$$

$$\begin{aligned} E_i(x) &= -\int_{-x}^{\infty} \frac{\exp(-u)}{u} du \\ &= 0.5772 + \ln(x) + \sum_{n=1}^{\infty} \frac{x^n}{n.n!} \end{aligned} \tag{3.15}$$

Then, for a given value of W_i such that W_{ibt}<W_i<$W_{i,100}$, we can calculate Q_i* from Eq. 3.12. Then using this value of Q_i*, we can compute S_{w2} and $\overline{S_{w2}}$ from the BL theory given in Chapter 3 as:

$$Q_i^*(t) = \frac{1}{\left(\frac{df_w}{dS_w}\right)_{S_{w2}}} \tag{3.16}$$

and

$$\overline{S_{w2}} = S_{w2} + \left[1 - f_w\left(S_{w2}\right)\right] Q_i^* \tag{3.17}$$

Recall from Chapter 2 that $\overline{S_{w2}}$ is the average water saturation in swept region (i.e., region contacted by injected water).

Then compute cumulative oil production from

$$N_p = \frac{E_A V_p \left(\overline{S_{w2}} - S_{wi}\right)}{B_o} \tag{3.18}$$

We repeat the computations for other values of W_i such that $W_{ibt}<W_i<W_{i,100}$ using Eqs. 3.12 through 3.18.

For $W_i>W_{i,100}$, E_A = 1, then we can integrate Eq. 3.11 to obtain

$$Q_i^* = Q_{i,100}^* + \frac{1}{V_p}\left(W_i - W_{i,100}\right) \tag{3.19}$$

Then specifying values of W_i such that $W_i>W_{i,100}$, we can compute Q_i* from Eq. 3.19, we compute S_{w2} and $\overline{S_{w2}}$ from the BL type equations (see Eqs. 3.17 and 3.18).

<u>Computations of WOR:</u> At the time of breakthrough, *WOR* is computed from

$$WOR = \frac{f_w\left(S_{wf}\right)/B_w}{\left[1 - f_w\left(S_{wf}\right)\right] / B_o} \tag{3.20}$$

After BT, unlike the 1-D linear case, we cannot use the preceding formula with S_{w2} to predict *WOR* times such that $t_{bt}<t<t_{100}$. *WOR* after BT is estimated by separating the displaced area into two distinct regions as shown in Fig. 3.10:

– A newly swept region (the region just swept by the injected water)

– Previously swept region containing all reservoir volume, where the water saturation is greater than S_{wf}.

As can be seen from Fig. 3.10, the oil is also displaced in the region “behind’’ the front. Performance in this region is estimated by assuming that all produced water comes from the previously swept zone, while oil is produced from both newly and previously swept zones. Hence, we can compute WOR after some time t_{bt} from:

$$WOR = \frac{B_o}{B_w} \frac{f_w(S_{w2})\left[1 - \dfrac{dN_{pu}}{dW_i}\right]}{\left(1 - f_w(S_{w2})\right)\left[1 - \dfrac{dN_{pu}}{dW_i}\right] + \dfrac{dN_{pu}}{dW_i}} \qquad \textbf{(3.21)}$$

where the incremental oil production with the cumulative water injected is computed from:

$$\frac{dN_{pu}}{dW_i} = \frac{W_{ibt}}{W_i} \frac{\left(S_{wf} - S_{wi}\right)}{\left(\overline{S}_{wf} - S_{wi}\right)} \frac{0.275}{E_{Abt}} \qquad \textbf{(3.22)}$$

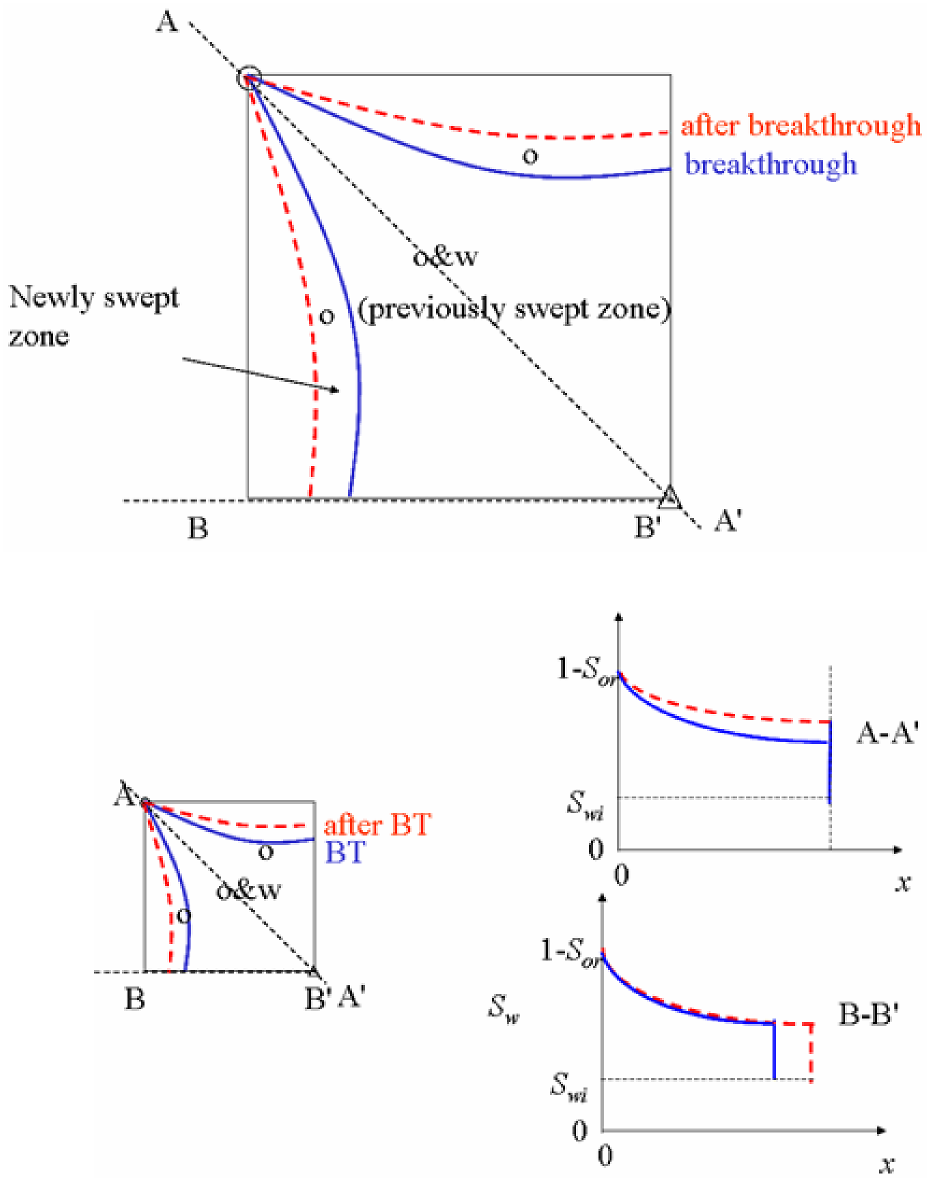

Figure 3.10: Schematic representation of swept regions for any time t such that $t_{bt}<t<t_{100}$, after Onur (2008).

To compute *WOR* for *Wi* such that $W_i>W_{i,100}$. First, we should note that Eq. 3.21 applies for $W_i > W_{i,100}$, but note that for $W_i > W_{i,100}$, $E_A=1$, i.e., no further oil can displaced by expanding the flood front. This means that

$$\frac{dN_{pu}}{dW_i}=0 \tag{3.23}$$

Using the preceding equation in Eq. 3.21 provides the equation to compute WOR for $W_i>W_{i,100}$ from:

$$WOR = \frac{B_o}{B_w} \frac{f_w(S_{w2})}{\left[1 - f_w(S_{w2})\right]} \quad \textbf{(3.24)}$$

<u>Computation of Cumulative Oil Produced:</u> The cumulative oil produced (i.e, oil produced by expanding the flood front) for W_i such that $W_{ibt}<W_i<W_{i,100}$ can be computed by the use of Eq. 3.22. Separating variables and integrating Eq. 3.22 from, W_{ibt} to W_i (where W_i less than $W_{i,100}$) gives

$$N_{pu} = N_{pbt} + 0.275 \frac{W_{ibt}}{E_{Abt}} \frac{\left(S_{wf} - S_{wi}\right)}{\left(\overline{S_{wf}} - S_{wi}\right)} \ln\left(\frac{W_i}{W_{ibt}}\right) \quad \textbf{(3.25)}$$

where N_{pbt} is the cumulative oil produced at the time of BT

3.2 Estimation of Injection Rates

The CGM model described in the previous section estimates water flood performance in a five-spot in terms of cumulative volume of water injected. When the injection rate is constant and known, oil displacement rates can be determined as a function of time (as we did in 1-D linear flow case). Otherwise, the CGM method does not provide information on the timing of production or the rates at which fluids can be injected or produced.

Many water floods operate under conditions where the pressure drop is known. We expect injection rate change with mobility ratio and E_A. So, what can we do? There is a correlation developed by Caudle and Witte (1959). Their correlation is based on the use of injection rate when the case mobility ratio is unity, E_A, and M. When the endpoint mobility ratio is one (i.e., M^*=1), the injection rate for a five-spot pattern can be calculated from:

$$i_b = \frac{3.541 \times 10^{-3} k_b k_{ro}^0 h}{\mu_o} \frac{\left(p_{inj} - p_{wf}\right)}{\left[\ln\left(\frac{d}{r_w}\right) + \frac{S_i + S_p}{2} - 0.619\right]} \quad \textbf{(3.26)}$$

where

d: is the distance from the injection well to the production well in ft.

r_w: is the effective wellbore radius in ft (see Fig. 3.11)

k_b : is the base permeability in md.,

S_i : is the skin factor at the injection well

S_p: is the skin factor at the production well

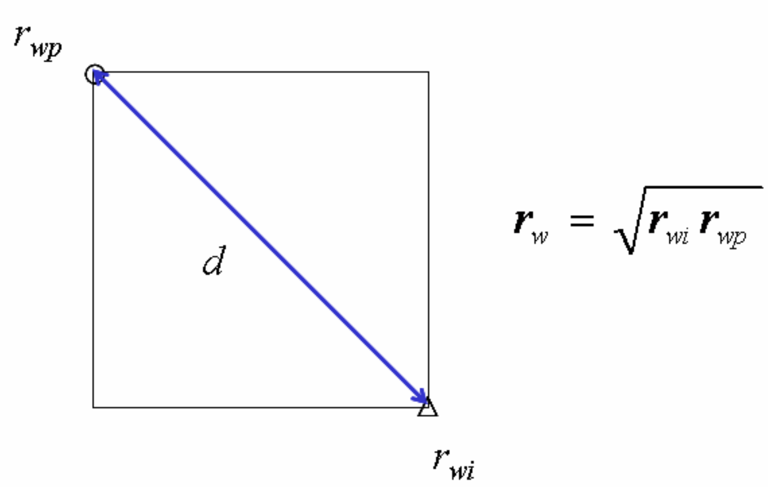

Figure 3.11: Effective wellbore radius.

The conductance ratio is define by

$$\gamma = \frac{i_w}{i_b} = \gamma(M, E_A) \tag{3.27}$$

which is the ratio of injection rate accounting for both mobility being different from unity and E_A to the base injection rate. Caudle and Witte developed the correlation shown in Fig. 3.12 to compute the injection rate, i_w. To use Fig. 3.12, for a given value of Δp and a given value of W_i (could be less or greater than W_{ibt}),

- Compute a base flow rate, i_b from Eq. 3.26
- Then compute mobility ratio from Eq. 3.1, if $W_i < W_{ibt}$. If $W_i > W_{ibt}$, the mobility ratio is computed from

$$M = \frac{(k_{rw})_{\overline{S_{w2}}}}{(k_{ro})_{S_{wi}}} \frac{\mu_o}{\mu_w} \tag{3.28}$$

- Then depending of the value of W_i, compute areal sweep efficiency, E_A from given equations previously.

– Using the values of E_A and the mobility ratio, determine (read) the conductance ratio from Fig. 3.12.

– Then compute i_w from

$$i_w = \gamma(M, E_A) \times i_b \tag{3.29}$$

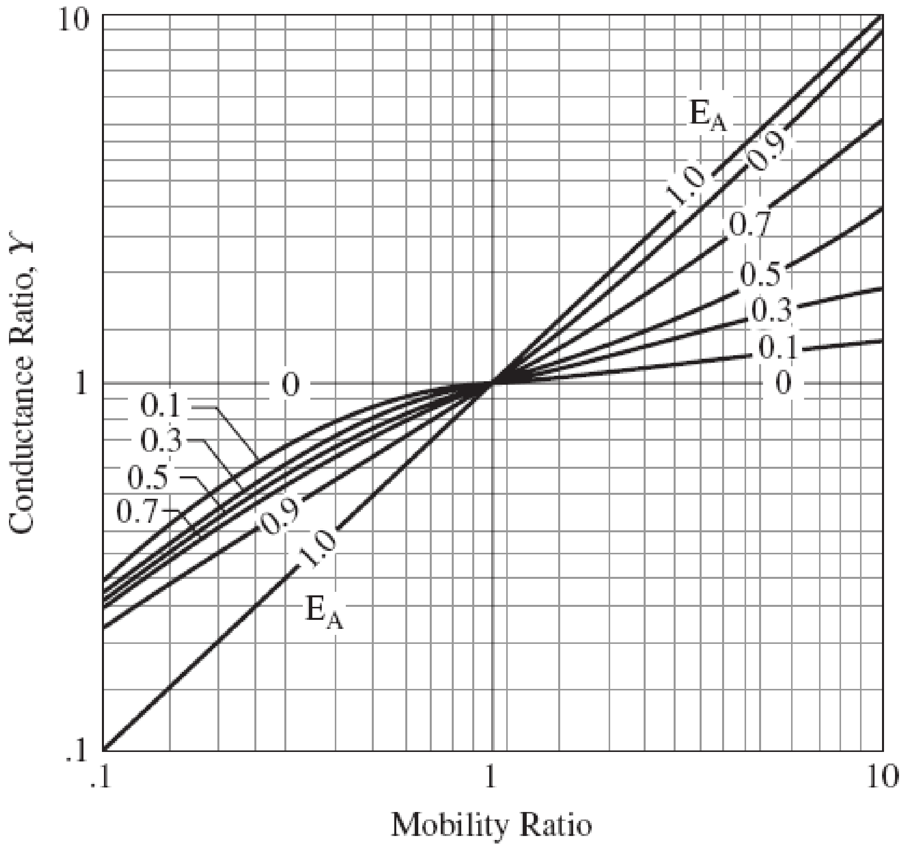

Figure 3.12: Caudle and Witte (1959) correlation for computing injection rate.

In the next chapter, we provide an example application for predicting the water flood performance based on the methodology presented here

4. EXAMPLE APPLICATIONS

In this chapter, we present four example applications to show the methodology provided in Chapters 2 and 3. First two examples (Example Applications 1 and 2) pertain to a case of 1D linear water flood performance predictions under constant-rate injection. In the first example, we consider experimental data for the f_w vs S_w curve, whereas in the second example we consider an analytical function for f_w vs. S_w curve. The third example (Example Application 3) pertains to a case of 1D linear water flood performance prediction under constant-pressure injection. The final example (Example Application 4) is for a 2D performance calculation for an areal five-spot pattern.

4.1 Example Application 1

Here, we consider a linear horizontal system with L=500 ft, A = 4000 ft^2, and porosity of 0.25, water is injected at a constant rate of 220 RB/D. Oil viscosity is 10 cp, and water viscosity is 1 cp. Using the Buckley-Leverett frontal advance theory given in Chapter 2, our objective is to calculate

(a) Cumulative oil production, time, pore volume water injected and oil production rate at water breakthrough.

(b) Cumulative oil production and water oil ratio after 2 years.

(c) Make a plot of S_w vs. x at t = 50 days

The relative permeability data are given in Table 4.1

Table 4.1: Relative permeability data.

S_w	0.30	0.335	0.37	0.409	0.440	0.475	0.51	0.545	0.58	0.615	0.65
k_{rw}	0	0.001	0.004	0.009	0.016	0.025	0.036	0.049	0.064	0.081	0.1
k_{ro}	1	0.729	0.512	0.343	0.216	0.125	0.064	0.027	0.008	0.001	0.0

(a) First, we need to construct the table values of f_w-S_w. Recall from Chapter 2, that f_w is to computed from

$$f_w = \frac{1}{1 + \frac{k_{ro}}{k_{rw}} \frac{\mu_w}{\mu_o}} \qquad \textbf{(4.1)}$$

Then, using these values in Eq. 4.1, we will compute f_w values. Note that the ratio of water viscosity to oil is 0.1. Table 4.2 gives the results. Fig. 4.1 shows a plot of f_w vs S_w. Note that for this problem, the initial water saturation, S_{wi} is equal to irreducible water saturation, S_{iw}; i.e., $S_{wi} = S_{iw}$, and $f_w(S_{wi})=f_w(S_{iw})=0$.

Table 4.2: k_{ro}/k_{rw}, f_w vs. S_w values.

S_w	k_{ro}/k_{rw}	f_w
0.3	Infinity	0
0.335	729	0.014
0.37	128	0.072
0.409	38.1	0.208
0.440	13.5	0.426
0.475	5.0	0.667
0.51	1.778	0.849
0.545	0.551	0.948
0.58	0.125	0.988
0.615	0.012	0.999
0.65	0.0	1.0

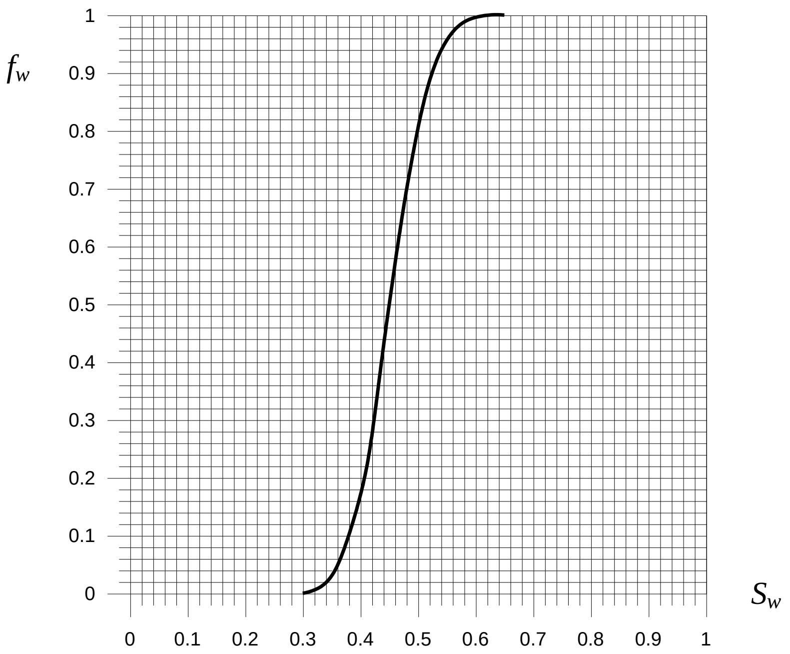

Figure 4.1: f_w-S_w curve.

Because f_w curve does not change rapidly with saturation, as can be seen in the scale used in Fig. 4.1, to be able to accurately determine the shock front saturation and hence the average saturation at the time of breakthrough, we will expand the saturation scale as shown in Fig.4.2.

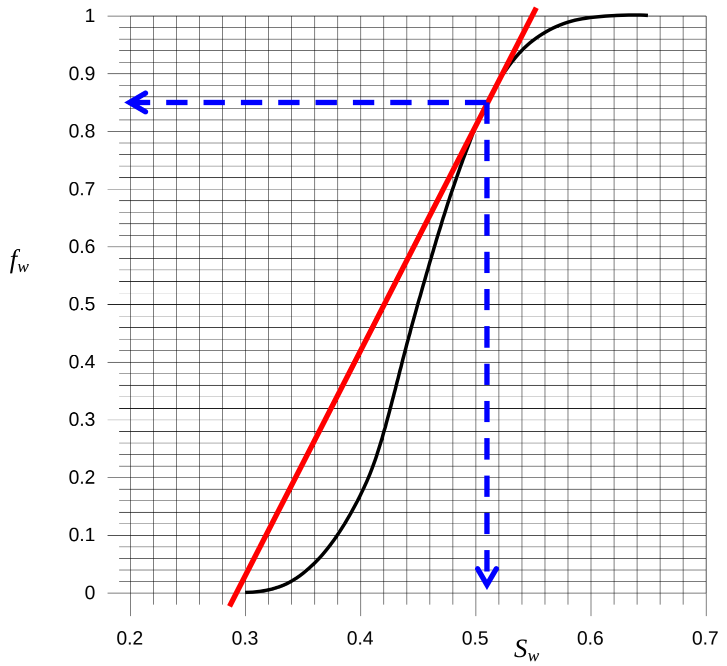

Figure 4.2: f_w-S_w curve using an expanded scale.

From the graph, we determined S_{wf}=0.51, $f_w(S_{wf})$ = 0.85, and $\overline{S_{wf}} = 0.547$, and the slope df_w/dS_w at S_{wf} is determined as

$$\left(\frac{df_w}{dS_w}\right)_{S_{wf}} = \frac{f_w(S_{wf}) - f_w(S_{wi})}{S_{wf} - S_{wi}} = \frac{0.85 - 0.0}{0.51 - 0.3} = 4.05$$
$$= \frac{1 - f_w(S_{wf})}{\overline{S_{wf}} - S_{wf}} \qquad \textbf{(4.2)}$$

Because injection rate, q_t, is constant for this problem, the time of BT, t_{bt}, can be computed from

$$t_{bt} = \frac{AL\phi}{5.615 q_t \left(\frac{df_w}{dS_w}\right)_{S_{wf}}} = \frac{4000 \times 500 \times 0.25}{5.615 \times 220 \times 4.05} = 100 \text{ days} \qquad \textbf{(4.3)}$$

The cumulative oil production at the time of breakthrough, $N_p(t_{bt})$ is computed as

$$N_p(t_{bt}) = \frac{AL\phi(\overline{S_{wf}} - S_{wi})}{5.615 B_o} = \frac{4000 \times 500 \times 0.25(0.547 - 0.3)}{5.615 \times 1.0} \qquad \textbf{(4.4)}$$

$$= 21{,}995 \text{ STB}$$

where we assumed B_o=1 RB/STB. Note that we could have simply used the formula given below to compute $N_p(t_{bt})$

$$N_p(t_{bt}) = \frac{q_t(1 - f_w(S_{wi}))t_{bt}}{B_o} = \frac{220 \times (1 - 0) \times 100}{1.0} \qquad \textbf{(4.5)}$$

$$= 22{,}000 \text{ STB}$$

Note that Eqs. 4.4 and 4.5 yield almost identical results, as expected. The difference is due to round off errors. Oil production rate at the time of breakthrough can also be simply computed dividing $N_p(t_{bt})$ by the time of breakthrough, i.e.,

$$q_o(t_{bt}) = \frac{N_p(t_{bt})}{t_{bt}} = \frac{22{,}000}{100} \text{ STB} = 220 \text{ STB/D} \qquad \textbf{(4.6)}$$

as expected. Because q_t is constant, and the water production at $x=L$ is considered zero at the onset of breakthrough, thus $q_o=q_t$.

Cumulative pore volumes of water injected up to t_{bt} is computed from

$$Q_i(t_{bt}) = \frac{5.615 q_t t_{bt}}{AL\phi} = \frac{5.615 \times 220 \times 100}{4000 \times 500 \times 0.25} = 0.247 \ (25\%) \qquad \textbf{(4.7)}$$

(b) The performance for t_2=730 days corresponds to performance after breakthrough. To find the cumulative oil production at this time, we will use the following equation:

$$N_p(t_2) = \frac{AL\phi\left(\overline{S_{w2}} - S_{wi}\right)}{5.615 B_o} \qquad \textbf{(4.8)}$$

where $\overline{S_{w2}}$ is the average water saturation in the reservoir at time t_2, or when the saturation S_{w2} reaches the production well, $x=L$. So, to compute the cumulative oil production from Eq. 4.8, we need to determine the value of $\overline{S_{w2}}$ and S_{w2}. The average saturation $\overline{S_{w2}}$ at time t_2 can be estimated graphically by drawing a tangent line to the f_w curve at S_{w2}. The slope of this line is $(df_w/dS_w)_{Sw2} = 1/Q_i(t_2)$, where $Q_i(t_2)$ is the cumulative pore volumes of water injected up to time t_2. The saturation value where this tangent line @ S_{w2} intersects the horizontal line $f_w = 1$ is $\overline{S_{w2}}$. The equation of this tangent line is then can be give as

$$1 = f_w\left(S_{w2}\right) + \left(\frac{df_w}{dS_w}\right)_{S_{w2}} \left(\overline{S_{w2}} - S_{w2}\right) \tag{4.9}$$

or

$$1 = f_w\left(S_{w2}\right) + \frac{1}{Q_i\left(t_2\right)} \left(\overline{S_{w2}} - S_{w2}\right) \tag{4.10}$$

The cumulative pore volumes of water injected up to t_2 is computed from

$$Q_i(t_2) = \frac{5.615 q_t t_2}{AL\phi} = \frac{5.615 \times 220 \times 730}{4000 \times 500 \times 0.25} = 1.804 \tag{4.11}$$

Rearranging Eq. 4.10 as

$$\left(\frac{df_w}{dS_w}\right)_{S_{w2}} = \frac{1}{Q_i(t_2)} = \frac{1 - f_w\left(S_{w2}\right)}{\overline{S_{w2}} - S_{w2}} = \frac{1}{1.804} = 0.554 \tag{4.12}$$

Now, we need to determine the values of $\overline{S_{w2}}$ and S_{w2} such that Eq. 4.12 is satisfied. This can be achieved by a trial and error procedure by determining a tangent line on the f_w curve that satisfies Eqs. 4.10 and 4.12. By a trial and error procedure, we determined $\overline{S_{w2}} = 0.605$, $S_{w2} = 0.59$, and $f_w(S_{w2}) = 0.992$. The tangent line drawn on the expanded f_w-S_w scale is shown in Fig. 4.3. Using these values in Eq. 4.8, we can compute the cumulative oil production at t_2 as

$$N_p(t_2) = \frac{AL\phi\left(\overline{S_{w2}} - S_{wi}\right)}{5.615 B_o} = \frac{4000 \times 500 \times 0.25\left(0.605 - 0.3\right)}{5.615 \times 1.0} = 27{,}159 \text{ STB} \tag{4.13}$$

The recovery factor at t_2 is then

$$RF(t_2) = \frac{N_p(t_2)}{OIIP} = \frac{N_p(t_2)}{\frac{AL\phi(1-S_{wi})}{5.615B_o}} = \frac{27159}{62333} = 0.436 \ \ (44\%) \tag{4.14}$$

The producing water oil ratio at t_2 (WOR) is computed from

$$\begin{aligned} WOR(t_2) &= \frac{q_w(t_2)}{q_o(t_2)} = \frac{f_w(S_{w2})}{B_w}\frac{B_o}{[1-f_w(S_{w2})]} \\ &= \frac{0.992}{1.0}\frac{1.0}{(1-0.992)} = 124 \text{ STB/STB} \end{aligned} \tag{4.15}$$

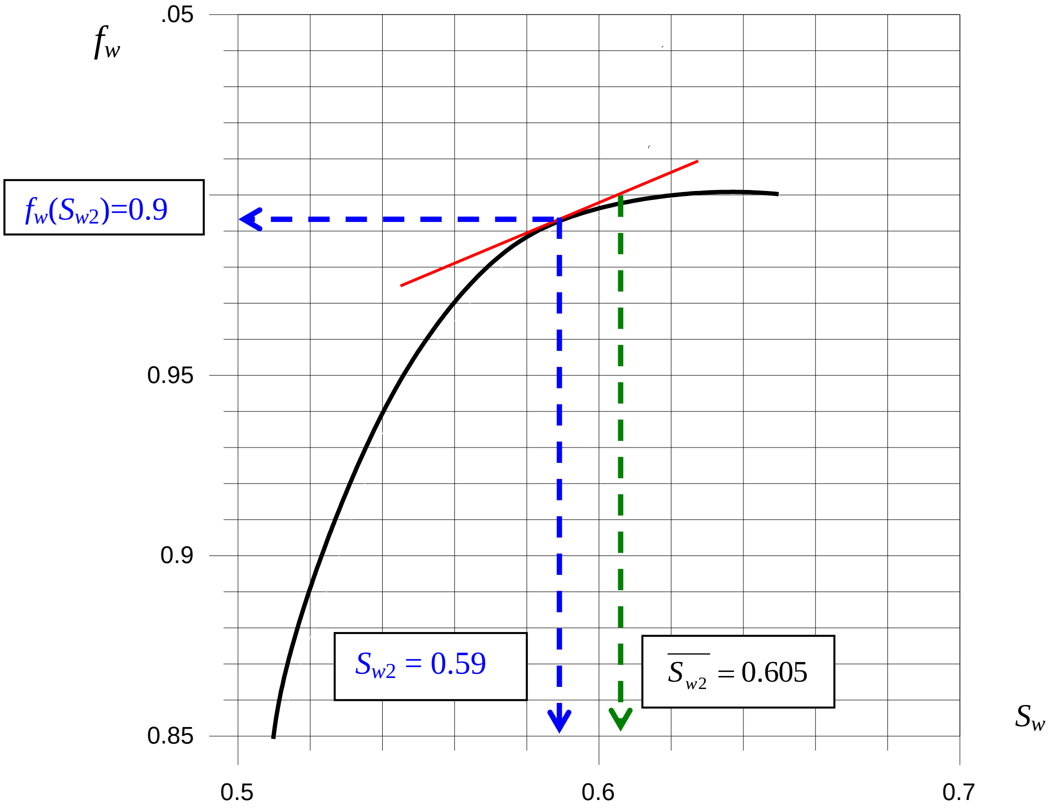

Figure 4.3: f_w-S_w curve using an expanded scale determine $\overline{S_{w2}}$ and S_{w2} values.

(c) Here, we are asked to compute the saturation profile in the reservoir at the time of 50 days. First, notice that t=50 days is a time before the time of breakthrough, i.e., t_{bt}=100 days. From Chapter 2, we know that the location of any saturation based on the B-L advance frontal theory is computed from:

$$x_{\hat{S}_w} = \frac{5.615 q_t t}{A\phi}\left(\frac{\partial f_w}{\partial S_w}\right)_{\hat{S}_w}, \quad for \ \ S_{wf} \le \hat{S}_w \le 1 - S_{or} \tag{4.16}$$

and

$$x_{\bar{S}_w} = \frac{5.615 q_t t}{A\phi}\left(\frac{\partial f_w}{\partial S_w}\right)_{S_{wf}} , \quad for\ S_{iw} \le \bar{S}_w < S_{wf} \qquad \textbf{(4.17)}$$

For the example considered, using the input data given and computed values of S_{wf} and $(\partial f_w / \partial S_w)_{S_{wf}}$, Eqs. 4.16 and 4.17 can be expressed as:

$$x_{\hat{S}_w} = \frac{5.615 \times 220 \times 50}{4000 \times 0.25}\left(\frac{\partial f_w}{\partial S_w}\right)_{\hat{S}_w} , \quad for\, 0.51 \le \hat{S}_w \le 0.65 \qquad \textbf{(4.18)}$$

and

$$\begin{aligned} x_{\hat{S}_w} &= \frac{5.615 \times 220 \times 50}{4000 \times 0.25} \times 4.05 \\ &= 250.15\ ft, \quad for\ \ 0.3 \le \hat{S}_w \le 0.51 \end{aligned} \qquad \textbf{(4.19)}$$

It is important to note that when Eqs. 4.17 and 4.18 are evaluated at $\hat{S}_w = S_{wf} = 0.51$, they will predict the location of the front at t = 50 days. So, the location of the shock front saturation S_{wf} for this example is at x_{Swf} = 250.15 ft. Based on the B-L theory, S_w = S_{iw} = 0.3 for all locations $x \ge x_{Swf}$ =250.15 ft.

To compute the locations of any saturation value $\hat{S}_w$ such that $0.51 \le \hat{S}_w \le 0.65$, we will use Eq. 4.18 by assuming arbitrary values of $\hat{S}_w$ in the interval $0.51 \le \hat{S}_w \le 0.65$. The assumed values of $\hat{S}_w$ are tabulated in Table 4.3. The values of $(\partial f_w / \partial S_w)_{\hat{S}_w}$ at an assumed water saturation value were computed by drawing a tangent line at this saturation value on f_w-S_w curve and then computing the slope of this tangent line. A graph of S_w vs. x at t=50 days is shown in Fig. 4.4.

Table 4.3: $\hat{S}_w$, $(\partial f_w / \partial S_w)_{\hat{S}_w}$ and $x_{\hat{S}_w}$ values.

$\hat{S}_w$	$(\partial f_w / \partial S_w)_{\hat{S}_w}$	$x_{\hat{S}_w}$ (computed from Eq. 4.18), ft
0.3	-	500
0.3	-	250.15
0.51	4.05	250.15
0.53	3.00	182.30
0.54	2.31	142.68
0.58	0.62	38.29
0.60	0.31	19.15
0.62	0.12	7.41
0.65	0.0	0

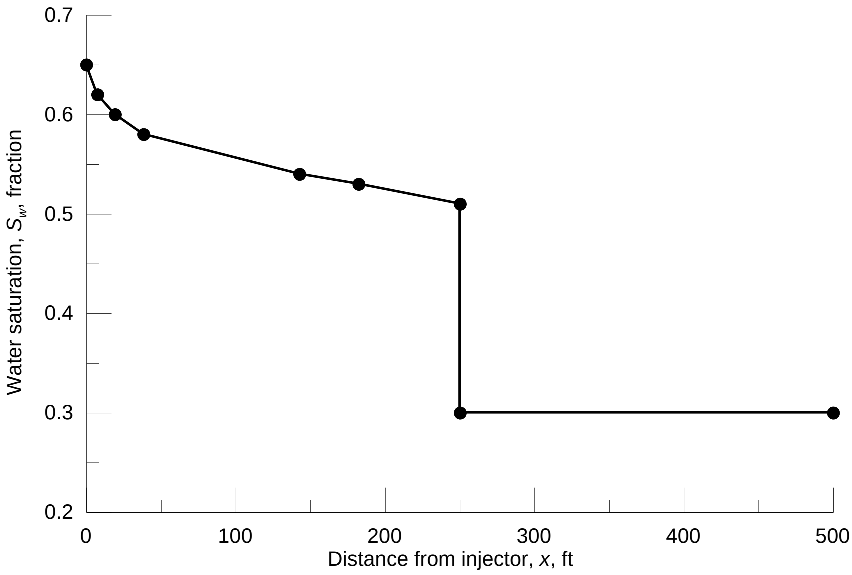

Figure 4.4: S_w vs. x at the time of t = 50 days

4.2 Example Application 2

In this example, we consider a linear horizontal system with L=500 ft, A=4000 ft^2, and porosity of 0.25, water is injected at a constant rate of 220 RB/D. The viscosity of oil (μ_o) is 2 cp. Further consider that we have the following functional (analytical) relationships for the relative permeability, fractional flow and derivative of fractional flow curves:

$$k_{ro} = k_{ro}^0 \left(1 - S_{wD}\right)^m \qquad \textbf{(4.20)}$$

and

$$k_{rw} = k_{rw}^0 \left(S_{wD}\right)^n \qquad \textbf{(4.21)}$$

where S_{wD} is given by

$$S_{wD} = \frac{S_w - S_{iw}}{1 - S_{or} - S_{iw}} \tag{4.22}$$

A formula based on Eqs. 4.20-4.22 for the f_w curve is given by

$$f_w = \frac{S_{wD}^n}{S_{wD}^n + A(1 - S_{wD})^m} \tag{4.23}$$

and the slope of f_w curve given by Eq. 1.4 is as follows

$$\frac{df_w}{dS_w} = \frac{AB\left[nS_{wD}^{n-1}(1 - S_{wD})^m + mS_{wD}^n(1 - S_{wD})^{m-1}\right]}{\left[S_{wD}^n + A(1 - S_{wD})^m\right]^2} \tag{4.24}$$

In Eqs. 4.23 and 4.24, A and B are given by

$$A = \frac{k_{ro}^0 \mu_w}{k_{rw}^0 \mu_o} \tag{4.25}$$

and

$$B = \frac{1}{1 - S_{or} - S_{iw}} \tag{4.26}$$

For the computation to be given, we will assume the values of S_{iw}=0.363, S_{or}=0.205, $k_{ro}^0 = 1.0$, and $k_{rw}^0 = 0.78$, n=m=2.

(a) We first calculate and graph f_w vs. S_w on the same plot for two different cases of flooding options. In the first option, we will assume that the injected water viscosity μ_w is 1 cp, and in the second option, μ_w is 5 cp and then discuss the results.

Figure 4.5 shows the graphs of f_w vs. S_w for the two options considered. As the f_w-S_w curve shifts to left for Option 2, Option 2 provides more favorable displacement. This is also verified by computing the end-point mobility ratios for each option from the well-known formula:

$M^* = \dfrac{k_{rw}^0 / \mu_w}{k_{ro}^0 / \mu_o}$, For option 1, M^*=1.56, while for option 2, M^*=0.312

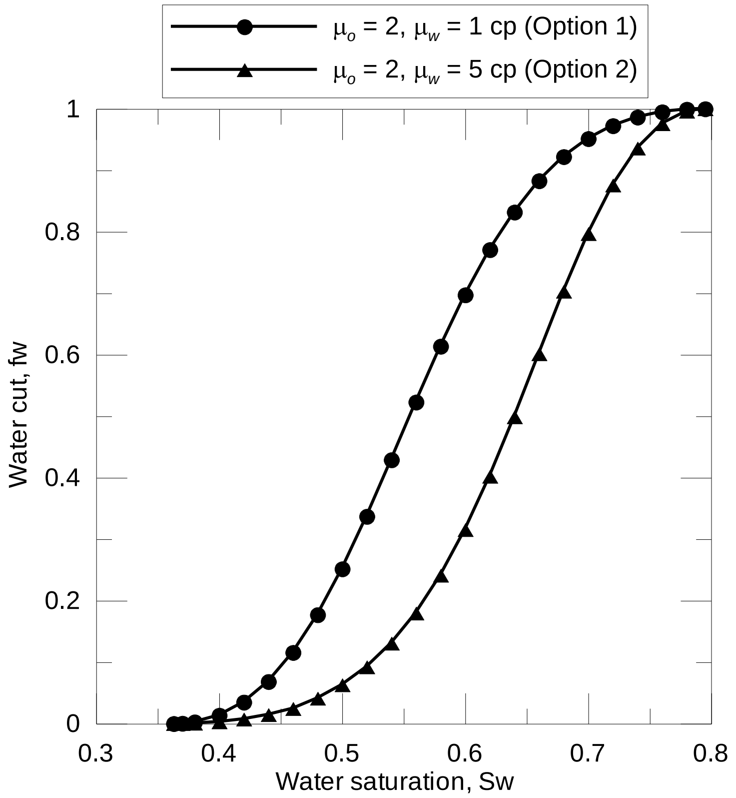

Figure 4.5: f_w vs. S_w for Options 1 and 2

(b) Now we calculate breakthrough times (BT) for Options 1 and 2 defined in Part a.

To compute BT for each option, we determine S_{wf} and the slope of the f_w at S_{wf} as described in Example Application 1, as shown in Fig. 4.6. For each option, these values are tabulated in Table 4.4.

Table 4.4: S_{wf} and other related values for Options 1 and 2

	S_{wf}	$f_w(S_{wf})$	$(df_w/dS_w)_{Swf}$	$\overline{S_{wf}}$
Option 1	0.63	0.803	3.01	0.695
Option 2	0.74	0.936	2.49	0.765

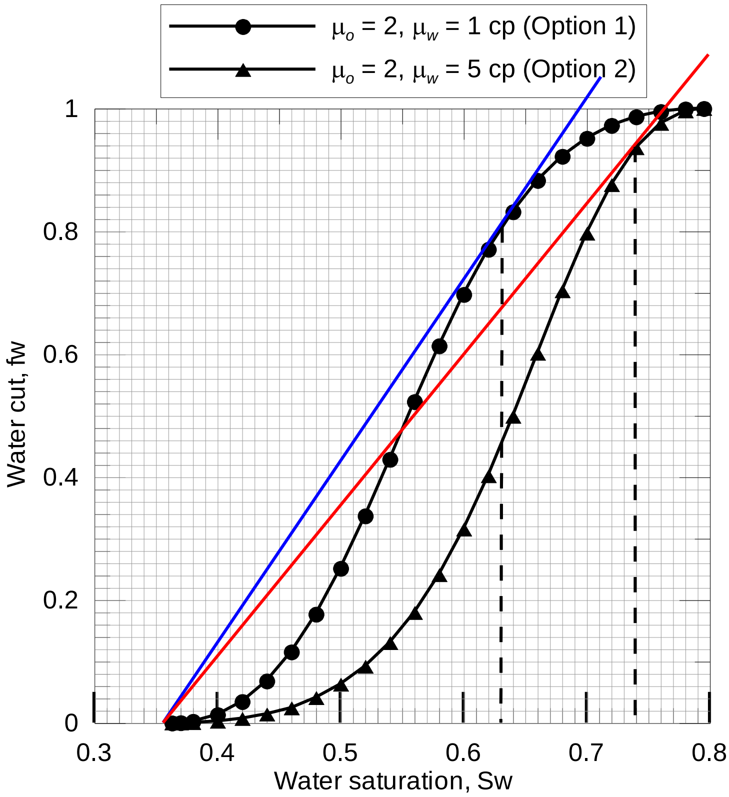

Figure 4.6: Determination of S_{wf} for Options 1 and 2.

Then, we can compute BTs for options from the following equation:

$$t_{bt} = \frac{AL\phi}{5.615 q_t \left(\frac{df_w}{dS_w} \right)_{S_{wf}}} \tag{4.27}$$

which yields t_{bt} = 131 days for Option 1, while for Option 2, t_{bt} = 163 days

(c) Next, we calculate and graph S_w vs. x for each option at t = 50, 100, t_{bt} (for each option), and 200 days. Note that the slopes required in Eq. 4.26 are simply to be computed from Eq. 4.24. The computed S_w vs. x profiles for Options 1 and 2 are tabulated in Tables 4.5 and 4.6, and the graphs of S_w-x are shown in Figs. 4.7 and 4.8.

Table 4.5: S_w versus x profiles at different times for Option 1.

S_w	x_{S_w} for t = 50 days	x_{S_w} for t = 100 days	x_{S_w} for t = 131 days	x_{S_w} for t = 200 days
0.363	500	500	500	NA
0.363	191.37	382.75	500	NA
0.37	191.37	382.75	500	NA
0.38	191.37	382.75	500	NA
0.4	191.37	382.75	500	NA
0.42	191.37	382.75	500	NA
0.44	191.37	382.75	500	NA
0.46	191.37	382.75	500	NA
0.5	191.37	382.75	500	NA
0.52	191.37	382.75	500	NA
0.54	191.37	382.75	500	NA
0.56	191.37	382.75	500	NA
0.58	191.37	382.75	500	NA
0.6	191.37	382.75	500	NA
0.63	191.37	382.75	500 (truncated)	NA
0.64	173.04	346.08	453.36	NA
0.66	137.46	274.91	360.13	500. (truncated)
0.68	105.03	210.05	275.17	420.1
0.7	76.88	153.76	201.42	307.52
0.72	53.33	106.66	139.71	213.32
0.74	34.17	68.35	89.54	136.70
0.76	18.95	37.89	49.64	75.78
0.78	7.06	14.13	18.51	28.26
0.795	0.0	0.0	0.0	0.0

Table 4.6: S_w versus x profiles at different times for Option 2.

S_w	x_{S_w} for t = 50 days	x_{S_w} for t = 100 days	x_{S_w} for t = 163 days	x_{S_w} for t = 200 days
0.363	500	500	500	NA
0.363	153.86	307.72	500	NA
0.37	153.86	307.72	500	NA
0.38	153.86	307.72	500	NA
0.4	153.86	307.72	500	NA
0.42	153.86	307.72	500	NA
0.44	153.86	307.72	500	NA
0.46	153.86	307.72	500	NA
0.5	153.86	307.72	500	NA
0.52	153.86	307.72	500	NA
0.54	153.86	307.72	500	NA
0.56	153.86	307.72	500	NA
0.58	153.86	307.72	500	NA
0.6	153.86	307.72	500	NA
0.63	153.86	307.72	500	NA
0.64	153.86	307.72	500	NA
0.66	153.86	307.72	500	NA
0.68	153.86	307.72	500	NA
0.7	153.86	307.72	500	NA
0.72	153.86	307.72	500	NA
0.74	153.86	307.72	500.	500. (Tranc.)
0.76	91.08	182.16	296.92	364.32
0.78	35.09	70.18	114.40	140.36
0.795	0.0	0.0	0.0	0.0

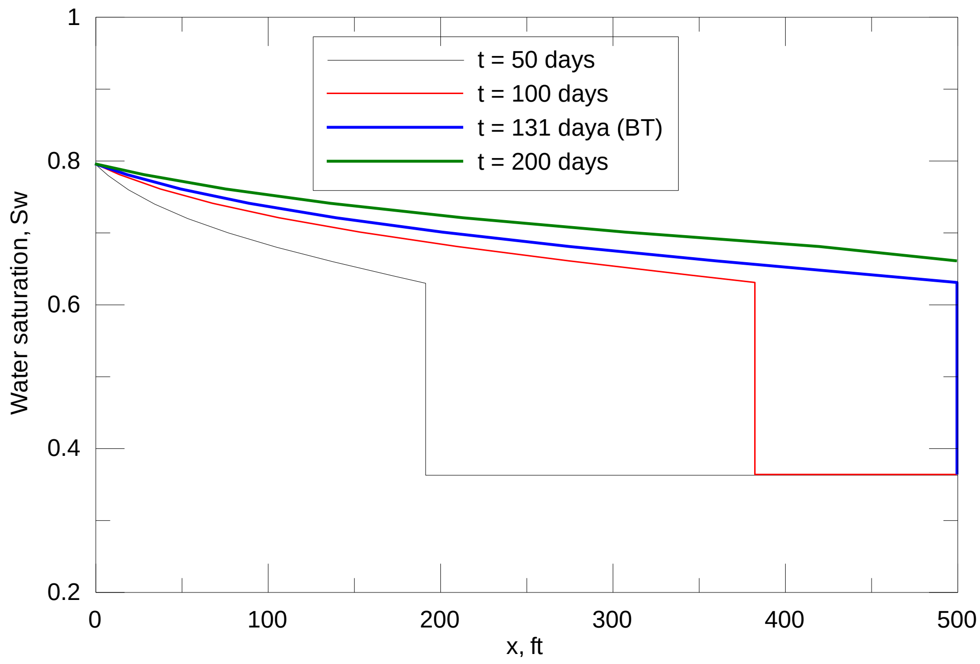

Figure 4.7: S_w vs. x profiles at different times for Option 1.

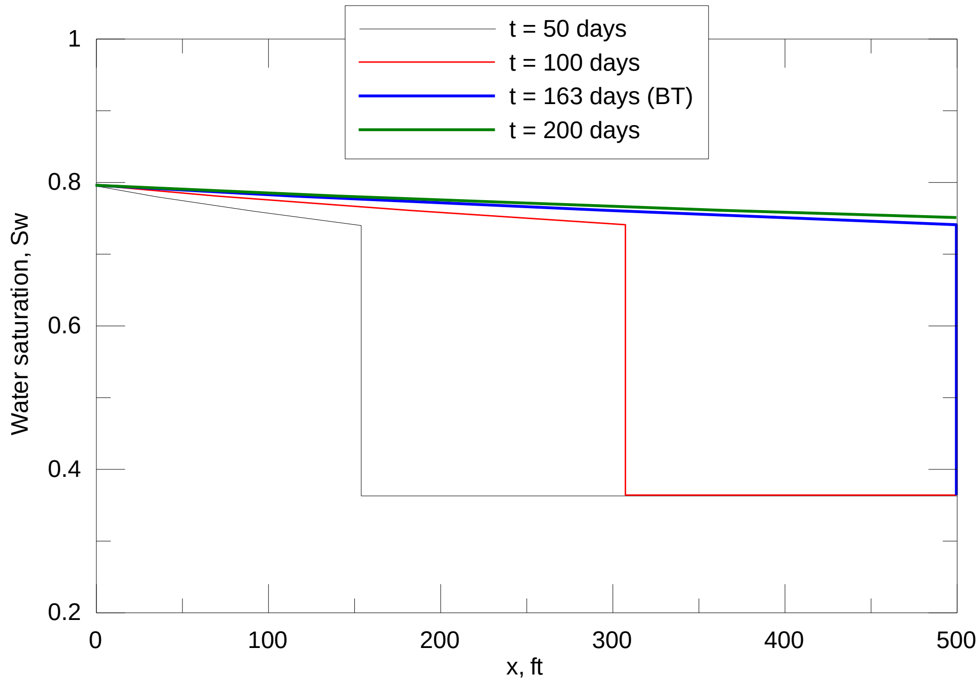

Figure 4.8: S_w vs. x profiles at different times for Option 2.

(d) Finally, we calculate and graph λ_t (total mobility) vs. x for each option at t=50, 100, t_{bt} (for each option), and 200 days. Note that to compute λ_t vs. x profiles, we will use the saturation values at computed values of x in Part c. Then, we will use the total mobility equation defined by

$$\lambda_t = \frac{k_{ro}}{\mu_o} + \frac{k_{rw}}{\mu_w} \quad \textbf{(4.28)}$$

which is a function of water saturation.

Tables 4.7-4.9 and Table A1 in Appendix - A present S_w and λ_t vs. x values for t=50, 100, 131 and 200 days for Option 1, respectively, while Tables A.2-A.5 in Appendix - A present S_w and λ_t vs. x values for t=50, 100, 163 and 200 days for Option 2, respectively. Fig. A.1 in Appendix - A shows λ_t vs. x profiles at four different time values for Option 1 (unfavorable case), and Fig. A.2 in Appendix - A shows λ_t vs. x profiles at four different time values for Option 2 (favorable case). Fig. A.2 in Appendix - A shows λ_t vs. S_w curves for both options.

Table 4.7: S_w and λ_t versus x profiles at t=50 days for Option 1.

S_w	λ_t, 1/cp	x_{S_w}, ft
0.363	0.5	500
0.363	0.5	191.37
0.37	0.5	191.37
0.38	0.5	191.37
0.4	0.5	191.37
0.42	0.5	191.37
0.44	0.5	191.37
0.46	0.5	191.37
0.48	0.5	191.37
0.5	0.5	191.37
0.52	0.5	191.37
0.54	0.5	191.37
0.56	0.5	191.37
0.58	0.5	191.37
0.6	0.5	191.37
0.63	0.371	191.37
0.64	0.385	173.04
0.66	0.418	137.46
0.68	0.455	105.03
0.7	0.498	76.88
0.72	0.548	53.33
0.74	0.602	34.17
0.76	0.662	18.95
0.78	0.727	7.06
0.795	0.78	0.0

Table 4.8: S_w and λ_t versus x profiles at t=100 days for Option 1.

S_w	λ_t , 1/cp	x_{Sw}, ft
0.363	0.5	500
0.363	0.5	382.75
0.37	0.5	382.75
0.38	0.5	382.75
0.4	0.5	382.75
0.42	0.5	382.75
0.44	0.5	382.75
0.46	0.5	382.75
0.48	0.5	382.75
0.5	0.5	382.75
0.52	0.5	382.75
0.54	0.5	382.75
0.56	0.5	382.75
0.58	0.5	382.75
0.6	0.5	382.75
0.63	0.371	382.75
0.64	0.385	346.08
0.66	0.418	274.91
0.68	0.455	210.05
0.7	0.498	153.76
0.72	0.548	106.66
0.74	0.602	68.35
0.76	0.662	37.89
0.78	0.727	14.13
0.795	0.78	0.0

Table 4.9: S_w and λ_t versus x profiles at t=131 (BT) days for Option 1.

S_w	λ_t , 1/cp	x_{Sw}, ft
0.363	0.5	500
0.363	0.5	500
0.37	0.5	500
0.38	0.5	500
0.4	0.5	500
0.42	0.5	500
0.44	0.5	500
0.46	0.5	500
0.48	0.5	500
0.5	0.5	500
0.52	0.5	500
0.54	0.5	500
0.56	0.5	500
0.58	0.5	500
0.6	0.5	500
0.63	0.371	500 (truncated)
0.64	0.385	453.36
0.66	0.418	360.13
0.68	0.455	275.17
0.7	0.498	201.42
0.72	0.548	139.71
0.74	0.602	89.54
0.76	0.662	49.64
0.78	0.727	18.51
0.795	0.78	0.0

4.3 Example Application 3

This example application illustrates the computation of water flood performance in a 1D linear system when the pressure difference between the injector and producer is constant. The pressure difference Δp is constant at value of 2000 psi. In this example, a long, narrow reservoir will be water flooded. The reservoir is 500 ft wide, 20 ft thick and 1000 ft long. Porosity of the reservoir is 0.206, and permeability is 23 md, water viscosity is 1.0 cp. For the purpose of comparison, we will consider two different cases of oil viscosity: **Case 1:** μ_o = 10 cp (unfavorable case), and **Case 2:** μ_o=1 cp (favorable case). We consider the same functional relationships for the relative permeabilities and the fractional flow curve as in Example Application 2 (see Eqs. 4.20-4.26). For the computation to be given, we will assume the same values of S_{iw} = 0.363, S_{or} = 0.205, $k_{ro}^0 = 1.0$, and $k_{rw}^0 = 0.78$, n = m = 2 for Example Application 2.

Case 1 μ_o = 10 cp (unfavorable case): First, we compute the value of the number of pore volumes injected up to breakthrough Q_{ibt} (i.e., $Q_i(t_{bt})$) from

$$Q_{ibt} = \frac{1}{\left(\dfrac{\partial f_w}{\partial S_w}\right)_{S_{wf}}} \tag{4.29}$$

To compute this we need to construct the fractional flow curve. Table 4.10 gives the values of S_w values (chosen), S_{wD}, and f_w values computed from Eqs. 4.20 through 4.26.

Table 4.10: S_w vs f_w.

S_w	S_{wD}	f_w
0.363	0	0
0.380	0.0394	0.0130
0.400	0.0856	0.0640
0.420	0.1319	0.1526
0.440	0.1782	0.2683
0.460	0.2245	0.3953
0.480	0.2708	0.5182
0.500	0.3171	0.6271
0.520	0.3634	0.7177
0.540	0.4097	0.7898
0.560	0.4560	0.8457
0.580	0.5023	0.8882
0.600	0.5486	0.9201
0.620	0.5949	0.9439
0.640	0.6412	0.9614
0.660	0.6875	0.9742
0.680	0.7338	0.9834
0.700	0.7801	0.9899
0.720	0.8264	0.9944
0.740	0.8727	0.9973
0.760	0.9190	0.9990
0.795	1.000	1.0000

Figure 4.9 shows the f_w vs S_w curve. Note that we determined S_{wf} = 0.51 and $f_w(S_{wf})$ = 0.68, and $\overline{S}_{wf} = 0.58$, and $\left(\frac{\partial f_w}{\partial S_w}\right)_{S_{wf}} = 4.5255$. Using the slope value in Eq. 4.29 gives:

$$Q_{ibt} = \frac{1}{\left(\frac{\partial f_w}{\partial S_w}\right)_{S_{wf}}} = \frac{1}{4.5255} = 0.221 \qquad \textbf{(4.30)}$$

Now, we will specify a sequence such that

$$0 = Q_{i,0} < Q_{i,1} < Q_{i,2} < \cdots < Q_{i,k-1} < Q_{i,k} = Q_{ibt} = 0.221 \qquad \textbf{(4.31)}$$

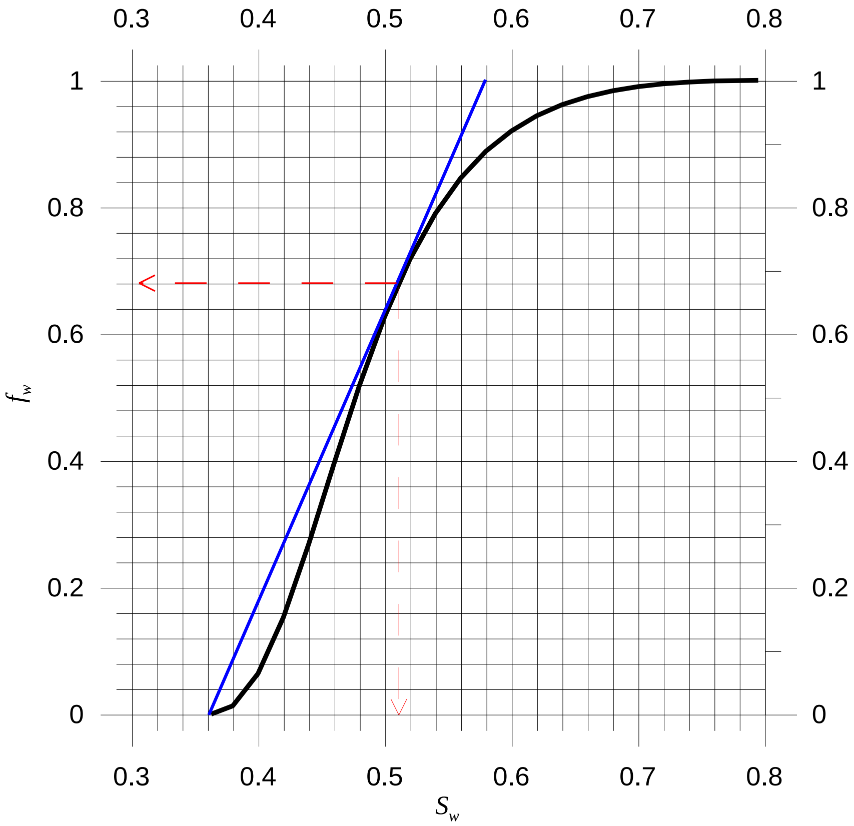

Figure 4.9: Fractional flow curve

where $Q_{i,l}$ = $Q_i(t_l)$, for l=0,…,k, and $t_k = t_{bt}$. It is important to note that we do not need to know the values of time to perform the calculations. To generate a sequence, we simply use five uniformly spaced values of Q_i's determined from

$$Q_{i,l} = Q_{i,l-1} + \frac{0.221}{5} = Q_{i,l-1} + \frac{0.221}{5} = Q_{i,l-1} + 0.0442 \quad \textbf{(4.32)}$$

for l=1,…,5, where $Q_{i,0}$ = 0. So, our specified values of Q_i's up to BT is as given in Table 4.11.

Table 4.11: Specified Q_i values up to BT.

Q_i
0.00
0.0442
0.0884
0.1326
0.1768
0.2210

Recall from Chapter 2 that q_t is given by

$$q_t(t) = \frac{1.127 \times 10^{-3} kA}{\mu_{app}} \frac{\Delta p}{L} \qquad \textbf{(4.33)}$$

where

$$\mu_{app}(t) = \frac{1}{L} \int_0^L \frac{1}{\lambda_t(x)} dx \qquad \textbf{(4.34)}$$

and

$$\lambda_t(x) = \frac{k_{ro}(S_w)}{\mu_o} + \frac{k_{rw}(S_w)}{\mu_w}, \text{ and } S_w = S_w(x,t) \qquad \textbf{(4.35)}$$

First, we will compute q_t at Q_i=0, or equivalently at $t = 0$, or equivalently $x_f = 0$. Note that at $t = 0$, the total mobility is

$$\lambda_t(x = 0) = \frac{k_{ro}(S_{wi})}{\mu_o} + \frac{k_{rw}(S_{wi})}{\mu_w} \qquad \textbf{(4.36)}$$

Because the initial water saturation is equal to irreducible water saturation, i.e., $S_{wi} = S_{iw}$, then the total mobility at time zero is simply the oil mobility at irreducible water saturation, and is constant for all x, i.e.,

$$\lambda_t(x = 0) = \frac{k_{ro}(S_{wi})}{\mu_o} = \text{constant} \qquad \textbf{(4.37)}$$

Using Eq. 4.37 in Eq. 4.34 and integrating the resulting equation gives

$$\mu_{app}(0) = \frac{1}{L} \int_0^L \frac{1}{\lambda_t(x)} dx = \frac{\mu_o}{Lk_{ro}(S_{iw})} \int_0^L dx = \frac{\mu_o}{k_{ro}(S_{iw})L} L = \frac{\mu_o}{k_{ro}(S_{iw})} \qquad \textbf{(4.38)}$$

Note that $k_{ro}(S_{iw})$ is the endpoint value of the oil relative permeability curve, i.e., $k_{ro}(S_{iw}) = k_{ro}^0 = 1.0$.

Now, using Eq. 4.38 in Eq. 4.33 and using the parameter values given in the resulting equation gives q_t at $t = 0$ as

$$q_t(0) = \frac{1.127*10^{-3} k k_{ro}(S_{iw}) A}{\mu_o}\frac{\Delta p}{L}$$
$$= \frac{1.127*10^{-3}*23*1.0*500*20}{10}\frac{2000}{1000} = 51.84 RB/D \tag{4.39}$$

The next step is to compute q_t for $Q_{i,1}$ = 0.0442. To achieve this, we need to find the location of the front for this value of Q_i and then generate the saturation profile in the reservoir. The location of front is computed from our general equation

$$x_{\hat{S}_w}(t) = LQ_i(t)\left(\frac{\partial f_w}{\partial S_w}\right)_{\hat{S}_w} \tag{4.40}$$

by setting $\hat{S}_w = S_{wf}$. Doing so, we compute

$$x_{f,1} = LQ_{i,1}\left(\frac{\partial f_w}{\partial S_w}\right)_{S_{wf}} = 1000 \times 0.0442 \times 4.5255 \approx 200\ ft \tag{4.40}$$

where the subsrcipt 1 in x_f is used to represent the location of front for $Q_{i,1}$.

Now, we compute the water saturation profile in the reservoir for the value of $Q_{i,1}$. We will specify several values of $\hat{S}_w$ such that $1 - S_{or} \le \hat{S}_w \le S_{wf}$, and use Eq. 4.40 to compute $x_{\hat{S}_w}$, the location of a given $\hat{S}_w$. Table 4.12 summarizes the results obtained for $Q_{i,1}$ = 0.0442. Because we determined S_w as a function of x, we can compute the total mobility using Eq. 4.35 and the relative permeability curves given (see Eqs. 4.21 and 4.22); i.e.,

$$k_{ro} = k_{ro}^0 (1 - S_{wD})^m \tag{4.41}$$

and

$$k_{rw} = k_{rw}^0 (S_{wD})^n \tag{4.42}$$

For instance, if we consider the saturation value of S_w = 0.51 (or S_{wD} = 0.3403) (note that this value is in fact the value of shock front saturation, S_{wf}) given in the first row of Table 4.12, then we can calculate relative permeabilites as

$$k_{ro}(S_{wf}) = k_{ro}^0(1 - S_{wD})^m = 1.0(1 - 0.3403)^2 = 0.4352 \quad \textbf{(4.43)}$$

and

$$k_{rw}(S_{wf}) = k_{rw}^0(S_{wD})^n = 0.78(0.3403)^2 = 0.0903 \quad \textbf{(4.44)}$$

Using these values and viscosity values in Eq. 4.36, we can compute the total mobility

$$\lambda_t(x = x_{f,1}) = \frac{k_{ro}(S_{wf})}{\mu_o} + \frac{k_{rw}(S_{wf})}{\mu_w} = \frac{0.4352}{10} + \frac{0.0903}{1} = 0.1338 \quad \textbf{(4.45)}$$

Similarly, we can compute total mobility for other values of S_w when $Q_{i,1}$ = 0.0442. The last column of Table 4.12 gives the computed values of the total mobility.

Table 4.12: Saturation and total mobility profile for $Q_{i,1}$ = 0.0442.

$\hat{S}_w$	S_{wD}	$\left(\frac{\partial f_w}{\partial S_w}\right)_{\hat{S}_w}$	$\frac{x_{\hat{S}_w}}{L}$	$x_{\hat{S}_w}$ *(ft)*	λ_t*, (1/cp)*
0.510	0.3403	4.5255	0.2000	200	0.1338
0.515	0.3519	4.2885	0.1896	189.6	0.1386
0.520	0.3634	4.0544	0.1792	179.2	0.1435
0.530	0.3866	3.6016	0.1592	159.2	0.1542
0.540	0.4097	3.1776	0.1404	140.5	0.1658
0.550	0.4328	2.7879	0.1232	123.3	0.1783
0.560	0.4560	2.4351	0.1076	107.6	0.1918
0.570	0.4792	2.1192	0.0937	93.7	0.2062
0.580	0.5023	1.8386	0.0813	81.3	0.2216
0.590	0.5255	1.5911	0.0703	70.3	0.2379
0.607	0.5648	1.2879	0.0569	56.9	0.2678
0.617	0.5879	1.0648	0.0471	47.1	0.2866
0.627	0.6111	0.9139	0.0404	40.4	0.3064
0.638	0.6366	0.7704	0.0341	34.1	0.3293
0.648	0.6597	0.6577	0.0291	29.1	0.3510
0.659	0.6851	0.5506	0.0243	24.3	0.3760
0.669	0.7083	0.4666	0.0206	20.6	0.3998
0.680	0.7338	0.3867	0.0171	17.1	0.4271
0.690	0.7569	0.3240	0.0143	14.3	0.4528
0.701	0.7824	0.2644	0.0117	11.7	0.4822
0.711	0.8056	0.2175	0.0096	9.6	0.5010
0.722	0.8310	0.1729	0.0076	7.6	0.5415
0.732	0.8542	0.1379	0.0061	6.1	0.5713
0.743	0.8796	0.1045	0.0046	4.6	0.6049
0.753	0.9023	0.0782	0.0035	3.5	0.6360
0.764	0.9282	0.0532	0.0024	2.4	0.6725
0.774	0.9513	0.0335	0.0015	1.5	0.7061
0.785	0.9769	0.0147	0.0006	0.65	0.7444
0.795	1.0000	0.0000	0.0000	0.00	0.7800

Figure 4.10 shows the computed saturation and total mobility profiles for $Q_{i,1}$ = 0.0442. Note that to obtain saturation and total mobility profiles shown in the Figure 4.10 for saturation values less than S_{wf}, we simply used the shock front concept, which says that we should set all saturation values less than S_{wf} to the irreducible water saturation, S_{iw} = 0.363 after $x_f \geq 200$ ft, and that total mobility is equal to oil mobility at S_{iw}, i.e.,

$$\lambda_t(x > 200\, ft) = \frac{k_{ro}(S_{iw})}{\mu_o} + \frac{k_{rw}(S_{iw})}{\mu_w} = \frac{k_{ro}(S_{iw})}{\mu_o} = \frac{1}{10} = 0.1\, cp \qquad \textbf{(4.46)}$$

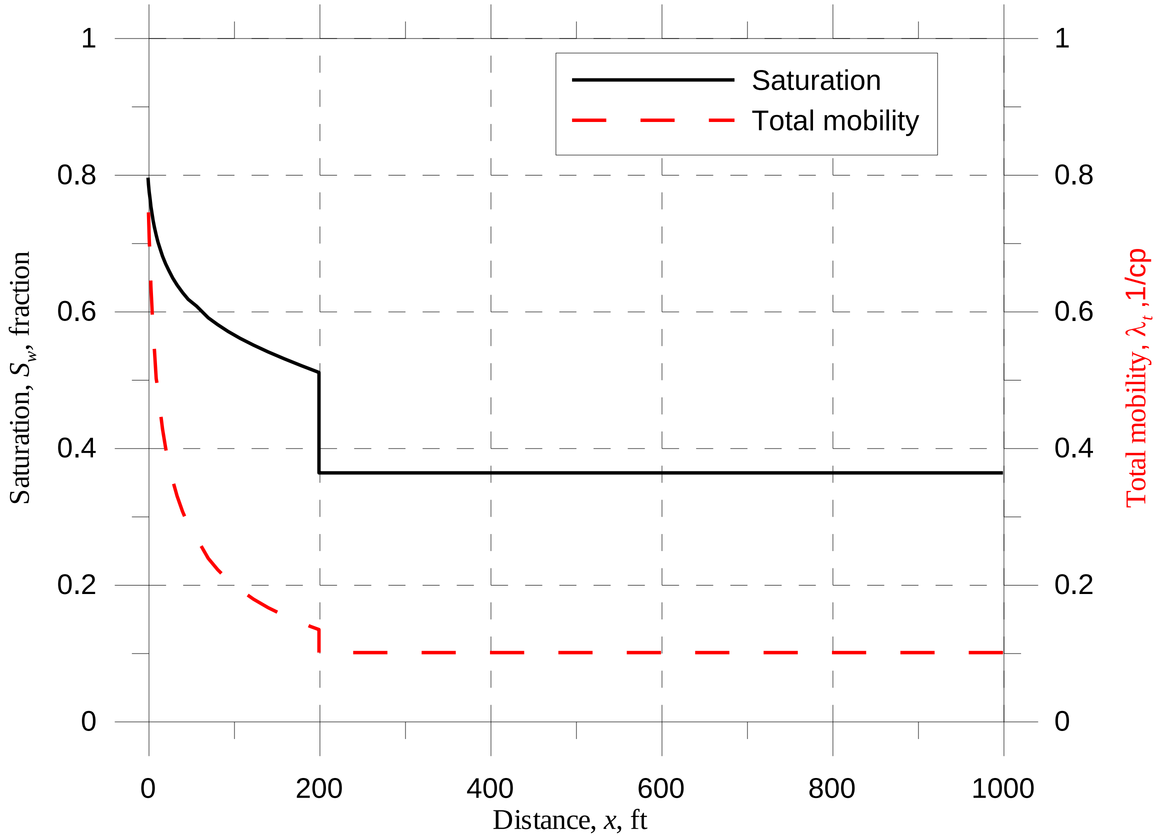

Figure 4.10: Saturation and total mobility profiles for $Q_{i,1}$ = 0.0442

Next, we integrate the inverse of total mobility profile obtained for $Q_{i,1}$ = 0.0442 with respect to x to obtain the apparent viscosity for $Q_{i,1}$ = 0.0442. As stated in Chapter 2, we have to use a numerical integration scheme to compute the apparent viscosity (Eq. 4.34). For its common use and simplicity, we will use the (composite) trapezoidal rule of integration. Before applying this rule to Eq. 4.34, first we note that before BT , Eq. 4.47 can be rewritten as

$$\mu_{app}(t) = \frac{1}{L}\left[\int_0^{x_f} \frac{1}{\lambda_t(x)} dx + \int_x^L \frac{1}{\lambda_t(x)} dx\right]$$
$$= \frac{1}{L}\left[\int_0^{x_f(t)} \frac{1}{\lambda_t(x)} dx + \int_{x_{f(t)}}^L \frac{1}{\lambda_t(x)} dx\right] \qquad \textbf{(4.47)}$$
$$= \frac{1}{L}\left[\int_0^{x_f(t)} \frac{1}{\lambda_t(x)} dx + \frac{1}{\lambda_o^0}(L - x_f)\right]$$

where the second integral follows from that fact that for $x \geq x_f$, the total mobility is equal to endpoint oil mobility, i.e., $\lambda_t(x \geq x_f) = \frac{k_{ro}(S_{iw})}{\mu_o} + \frac{k_{rw}(S_{iw})}{\mu_w} = \frac{k_{ro}(S_{iw})}{\mu_o} = \lambda_o^0$. Eq. 4.47 holds for all values of Q_i less than Q_{ibt}. Now, we can apply trapezoidal rule to the first integral in Eq. 4.47 to obtain

$$\mu_{app}(t) = \frac{1}{L}\left[\int_0^{x_f} \frac{1}{\lambda_t(x)} dx\right]$$
$$= \frac{1}{2L}\sum_{j=1}^{r}\left[\frac{1}{\lambda_t(x_j)} + \frac{1}{\lambda_t(x_{j-1})}\right](x_j - x_{j-1}) + \frac{1}{\lambda_o^0 L}(L - x_f) \qquad \textbf{(4.48)}$$

where $x_0 = 0$, and $x_r = x_f$. Using the total mobility profile given in Table 4.12 and the total mobility value $\lambda_t(x \geq 200\ ft) = \lambda_o^0 = 0.1$ in Eq. 4.48, (note from Table 4.12, that r =28 when we apply Eq. 4.48) gives

$$\mu_{app}(Q_{i,1} = 0.0442) = 0.9718 + \frac{1}{0.1}\frac{(1000 - 200)}{1000} = 8.9718\ cp \qquad \textbf{(4.49)}$$

Then, we compute q_t for $Q_{i,1} = 0.0442$ as

$$q_t(Q_{i,1} = 0.0442) = \frac{1.127 * 10^{-3} kA}{\mu_{app}(Q_{i,1})}\frac{\Delta p}{L}$$
$$= \frac{1.127 * 10^{-3} * 23 * 500 * 20}{8.9718}\frac{2000}{1000} = 57.78 bbl/D \qquad \textbf{(4.50)}$$

The cumulative oil production N_p (in bbl) can be computed from

$$N_p = V_p\left[\bar{S}_w(Q_i) - S_{wi}\right] \qquad \textbf{(4.51)}$$

where $\bar{S}_w(Q_i)$ is the average saturation in the reservoir when the number of cumulative pore volumes of water injected is Q_i, and is computed from

$$\bar{S}_w(Q_i) = S_{wi} + \left[1 - f_w(S_{wi})\right]Q_i \qquad \textbf{(4.52)}$$

If Q_i is less than or equal to Q_{ibt}. in Eq. 4.51, V_p is the total pore volume in bbl, i.e.,

$$V_p = \frac{\phi AL}{5.615} \qquad \textbf{(4.53)}$$

For our problem, $S_{wi} = S_{iw}$, so in Eq. 4.52, $f_w(S_{wi})$=0, thus, the average saturation at $Q_{i,1}$ = 0.0442 is computed from Eq. 4.52 as

$$\bar{S}_w(Q_i) = S_{wi} + \left[1 - f_w(S_{wi})\right]Q_i = 0.363 + [1 - 0] \times 0.0442 \approx 0.407 \qquad \textbf{(4.54)}$$

The total pore volume V_p is

$$V_p = \frac{\phi AL}{5.615} = \frac{0.206 \times 500 \times 20 \times 1000}{5.615} = 366{,}874 \text{ bbl} \qquad \textbf{(4.55)}$$

Using the values of average saturation and pore volume in Eq. 4.51, the cumulative oil production in bbl is

$$N_p = V_p\left[\bar{S}_w(Q_i) - S_{wi}\right] = 366{,}877 \times \left[0.407 - 0.363\right] = 16{,}142 \text{ bbl} \qquad \textbf{(4.56)}$$

$N_p(PV)$ given is the cumulative oil produced divided by the total pore volume, i.e., the cumulative pore volumes of oil produced. Note that it is a fraction and defined by

$$N_p(PV) = \frac{N_p}{V_p} \qquad \textbf{(4.57)}$$

Up to BT, $N_p(PV)$ should be equal to cumulative pore volumes of water injected, i.e.,

$$N_p(PV) = \frac{N_p}{V_p} = Q_i(t) \qquad \textbf{(4.58)}$$

So, for $Q_{i,1}$ = 0.0442, the value of $N_p(PV)$ = 0.0442.

If $Q_i<Q_{ibt}$, the oil and water productions, q_o and q_w, at the production end is computed from

$$q_o(Q_i) = [1 - f_w(S_{wi})]q_t(Q_i) \tag{4.59}$$

and

$$q_w(Q_i) = f_w(S_{wi})q_t(Q_i) \tag{4.60}$$

If $Q_i = Q_{ibt}$, then the oil and water productions are computed from

$$q_o(Q_i) = [1 - f_w(S_{wf})]q_t(Q_i) \tag{4.61}$$

and

$$q_w(Q_i) = f_w(S_{wf})q_t(Q_i) \tag{4.62}$$

For our problem $S_{wi} = S_{iw}$, and for $Q_{i,1}$ = 0.0442, we use Eqs. 4.59 and 4.60 with $f_w(S_{wi})$ = 0 to compute oil and water productions:

$$q_o(Q_{i,1}) = [1 - f_w(S_{wi})]q_t(Q_{i,1}) = (1-0)\times 57.78 = 57.78 \text{ bbl} \tag{4.63}$$

and

$$q_w(Q_{i,1}) = f_w(S_{wi})q_t(Q_{i,1}) = 0 \times 57.78 = 0 \text{ bbl} \tag{4.64}$$

Then, for $Q_{i,1}$ = 0.0442, WOR is

$$WOR(Q_{i,1}) = \frac{q_w}{q_o} = \frac{0}{57.78} = 0 \tag{4.65}$$

We perform similar calculations for other specified values of Q_i given in Table 4.11. Tables 4.13 through 4.16 gives the saturation and total mobility profiles for Q_i=0.0884, 0.1326, 0.1768, and 0.2210, respectively.

Table 4.13: Saturation and total mobility profiles for $Q_{i,2}$ = 0.0884.

$\hat{S}_w$	S_{wD}	$\left(\frac{\partial f_w}{\partial S_w}\right)_{\hat{S}_w}$	$\frac{x_{\hat{S}_w}}{L}$	$x_{\hat{S}_w}$ (ft)	λ_t, (1/cp)
0.510	0.3403	4.5255	0.4000	400	0.1338
0.515	0.3519	4.2885	0.3791	379.1	0.1386
0.520	0.3634	4.0544	0.3584	358.4	0.1435
0.530	0.3866	3.6016	0.3184	318.4	0.1542
0.540	0.4097	3.1776	0.2809	280.9	0.1658
0.550	0.4328	2.7879	0.2465	246.5	0.1783
0.560	0.4560	2.4351	0.2153	215.3	0.1918
0.570	0.4792	2.1192	0.1873	187.3	0.2062
0.580	0.5023	1.8386	0.1625	162.5	0.2216
0.590	0.5255	1.5911	0.1407	140.7	0.2379
0.607	0.5648	1.2879	0.1139	113.9	0.2678
0.617	0.5879	1.0648	0.0941	94.1	0.2866
0.627	0.6111	0.9139	0.0808	80.8	0.3064
0.638	0.6366	0.7704	0.0681	68.1	0.3293
0.648	0.6597	0.6577	0.0581	58.1	0.3510
0.659	0.6851	0.5506	0.0487	48.7	0.3760
0.669	0.7083	0.4666	0.0412	41.2	0.3998
0.680	0.7338	0.3867	0.0342	34.2	0.4271
0.690	0.7569	0.3240	0.0286	28.6	0.4528
0.701	0.7824	0.2644	0.0234	23.4	0.4822
0.711	0.8056	0.2175	0.0192	19.2	0.5010
0.722	0.8310	0.1729	0.0153	15.3	0.5415
0.732	0.8542	0.1379	0.0122	12.2	0.5713
0.743	0.8796	0.1045	0.0092	9.2	0.6049
0.753	0.9023	0.0782	0.0069	6.9	0.6360
0.764	0.9282	0.0532	0.0047	4.7	0.6725
0.774	0.9513	0.0335	0.0030	3	0.7061
0.785	0.9769	0.0147	0.0013	1.3	0.7444
0.795	1.0000	0.0000	0	0	0.7800

Table 4.14: S_w and λ_t versus x profiles at t = 200 days for Option 2.

$\hat{S}_w$	S_{wD}	$\left(\frac{\partial f_w}{\partial S_w}\right)_{\hat{S}_w}$	$\frac{x_{\hat{S}_w}}{L}$	$x_{\hat{S}_w}$ (ft)	λ_t, (1/cp)
0.510	0.3403	4.5255	0.6000	600	0.1338
0.515	0.3519	4.2885	0.5687	568.7	0.1386
0.520	0.3634	4.0544	0.5376	537.6	0.1435
0.530	0.3866	3.6016	0.4776	477.6	0.1542
0.540	0.4097	3.1776	0.4213	421.3	0.1658
0.550	0.4328	2.7879	0.3697	369.7	0.1783
0.560	0.4560	2.4351	0.3229	322.9	0.1918
0.570	0.4792	2.1192	0.2810	281	0.2062
0.580	0.5023	1.8386	0.2438	243.8	0.2216
0.590	0.5255	1.5911	0.2110	211	0.2379
0.607	0.5648	1.2879	0.1708	170.8	0.2678
0.617	0.5879	1.0648	0.1412	141.2	0.2866
0.627	0.6111	0.9139	0.1212	121.2	0.3064
0.638	0.6366	0.7704	0.1022	102.2	0.3293
0.648	0.6597	0.6577	0.0872	87.2	0.3510
0.659	0.6851	0.5506	0.0730	73	0.3760
0.669	0.7083	0.4666	0.0619	61.9	0.3998

Table 4.14: (contd) S_w and λ_t versus x profiles at t = 200 days for Option 2.

0.680	0.7338	0.3867	0.0513	51.3	0.4271
0.690	0.7569	0.3240	0.0430	43	0.4528
0.701	0.7824	0.2644	0.0351	35.1	0.4822
0.711	0.8056	0.2175	0.0288	28.8	0.5010
0.722	0.8310	0.1729	0.0229	22.9	0.5415
0.732	0.8542	0.1379	0.0183	18.3	0.5713
0.743	0.8796	0.1045	0.0139	13.9	0.6049
0.753	0.9023	0.0782	0.0104	10.4	0.6360
0.764	0.9282	0.0532	0.0071	7.1	0.6725
0.774	0.9513	0.0335	0.0044	4.4	0.7061
0.785	0.9769	0.0147	0.0019	1.9	0.7444
0.795	1.0000	0.0000	0	0	0.7800

Table 4.15: Saturation and total mobility profiles for $Q_{i,4}$ = 0.1768.

$\hat{S}_w$	S_{wD}	$\left(\frac{\partial f_w}{\partial S_w}\right)_{\hat{S}_w}$	$\frac{x_{\hat{S}_w}}{L}$	$x_{\hat{S}_w}$ (ft)	λ_t, (1/cp)
0.510	0.3403	4.5255	0.8000	800.0	0.1338
0.515	0.3519	4.2885	0.7582	758.2	0.1386
0.520	0.3634	4.0544	0.7168	716.8	0.1435
0.530	0.3866	3.6016	0.6368	636.8	0.1542
0.540	0.4097	3.1776	0.5618	561.8	0.1658
0.550	0.4328	2.7879	0.4929	492.9	0.1783
0.560	0.4560	2.4351	0.4305	430.5	0.1918
0.570	0.4792	2.1192	0.3747	374.7	0.2062
0.580	0.5023	1.8386	0.3251	325.1	0.2216
0.590	0.5255	1.5911	0.2813	281.3	0.2379
0.607	0.5648	1.2879	0.2277	227.7	0.2678
0.617	0.5879	1.0648	0.1883	188.3	0.2866
0.627	0.6111	0.9139	0.1616	161.6	0.3064
0.638	0.6366	0.7704	0.1362	136.2	0.3293
0.648	0.6597	0.6577	0.1163	116.3	0.3510
0.659	0.6851	0.5506	0.0973	97.3	0.3760
0.669	0.7083	0.4666	0.0825	82.5	0.3998
0.680	0.7338	0.3867	0.0684	68.4	0.4271
0.690	0.7569	0.3240	0.0573	57.3	0.4528
0.701	0.7824	0.2644	0.0467	46.7	0.4822
0.711	0.8056	0.2175	0.0385	38.5	0.5010
0.722	0.8310	0.1729	0.0306	30.6	0.5415
0.732	0.8542	0.1379	0.0244	24.4	0.5713
0.743	0.8796	0.1045	0.0185	18.5	0.6049
0.753	0.9023	0.0782	0.0138	13.8	0.6360
0.764	0.9282	0.0532	0.0094	9.4	0.6725
0.774	0.9513	0.0335	0.0059	5.9	0.7061
0.785	0.9769	0.0147	0.0026	2.6	0.7444
0.795	1.0000	0.0000	0	0	0.7800

Table 4.16: Saturation and total mobility profiles for $Q_{i,5}$ = 0.2210.

$\hat{S}_w$	S_{wD}	$\left(\frac{\partial f_w}{\partial S_w}\right)_{\hat{S}_w}$	$\frac{x_{\hat{S}_w}}{L}$	$x_{\hat{S}_w}$ (ft)	λ_t, (1/cp)
0.510	0.3403	4.5255	1.000	1000	0.1338
0.515	0.3519	4.2885	0.9478	947.8	0.1386
0.520	0.3634	4.0544	0.8960	896	0.1435
0.530	0.3866	3.6016	0.7960	796	0.1542
0.540	0.4097	3.1776	0.7022	702.2	0.1658
0.550	0.4328	2.7879	0.6161	616.1	0.1783
0.560	0.4560	2.4351	0.5382	538.2	0.1918
0.570	0.4792	2.1192	0.4683	468.3	0.2062
0.580	0.5023	1.8386	0.4063	406.3	0.2216
0.590	0.5255	1.5911	0.3516	351.6	0.2379
0.607	0.5648	1.2879	0.2846	284.6	0.2678
0.617	0.5879	1.0648	0.2353	235.3	0.2866
0.627	0.6111	0.9139	0.2020	202	0.3064
0.638	0.6366	0.7704	0.1703	170.3	0.3293
0.648	0.6597	0.6577	0.1454	145.4	0.3510
0.659	0.6851	0.5506	0.1219	121.9	0.3760
0.669	0.7083	0.4666	0.1031	103.1	0.3998
0.680	0.7338	0.3867	0.0855	85.5	0.4271
0.690	0.7569	0.3240	0.0716	71.6	0.4528
0.701	0.7824	0.2644	0.0584	58.4	0.4822
0.711	0.8056	0.2175	0.0481	48.1	0.5010
0.722	0.8310	0.1729	0.0382	38.2	0.5415
0.732	0.8542	0.1379	0.0305	30.5	0.5713
0.743	0.8796	0.1045	0.0231	23.1	0.6049
0.753	0.9023	0.0782	0.0173	17.3	0.6360
0.764	0.9282	0.0532	0.0118	11.8	0.6725
0.774	0.9513	0.0335	0.0074	7.4	0.7061
0.785	0.9769	0.0147	0.0032	3.2	0.7444
0.795	1.0000	0.0000	0	0	0.7800

Performance After Breakthrough: To predict performance after breakthrough, as we mentioned in Chapter 2, we specify a set of S_{w2} values at x=L, which is greater than S_{wf}, as

$$0.51 = S_{wf} = S_w(t_k = t_{bt}) < S_{w2}(t_{k+1}) < \cdots \tag{4.66}$$

Somewhat arbitrarily, we specify a sequence of S_w given in the first column of Table 4.17. Then, for each value of S_w, we compute the cumulative pore volumes of water injected from

$$Q_i(t_{k+j}) = \frac{1}{\left(\frac{\partial f_w}{\partial S_w}\right)_{Sw2(t_{k+j})}} \tag{4.67}$$

The second column of Table 4.17 gives the computed values of Q_i from Eq. 4.67 Note that for each value of S_w, the slope of fractional flow curve in Eq. 4.67 is computed from Eq. 4.24.

Table 4.17: A sequence of S_{w2} for performance computations after BT.

S_{w2}	Q_i
0.510	0.221
0.530	0.278
0.550	0.359
0.570	0.472
0.607	0.776
0.638	1.298
0.669	2.143
0.690	3.086
0.722	5.784

The next step is to compute the saturation and total mobility profiles in the reservoir for each specified value of saturation S_{w2} at $x = L$ (see first column of Table 4.17). The saturation profile is computed by the use of the following equation:

$$x_{\hat{S}_w}(t) = LQ_i(t)\left(\frac{\partial f_w}{\partial S_w}\right)_{\hat{S}_w} \qquad \textbf{(4.68)}$$

by using a sequence of water saturation starting from the specified value of S_w (x=L) to 1-S_{or}. For instance, let's compute the saturation profile for S_{w2} (x=L) = 0.53 and Q_i=0.278 (see second row of Table 4.17). We generate a sequence of S_w in increasing order from 0.53 to 1-S_{or}, and then apply Eq. 4.68 for each value of S_w in the sequence. Table 4.18 summarizes the results obtained.

Table 4.18: Saturation and total mobility profiles for $Q_{i,5}$=0.278 and S_{w2}(x=L)=0.53.

$\hat{S}_w$	S_{wD}	$\left(\frac{\partial f_w}{\partial S_w}\right)_{\hat{S}_w}$	$\frac{x_{\hat{S}_w}}{L}$	$x_{\hat{S}_w}$ (ft)	λ_t, (1/cp)
0.530	0.3866	3.6016	1.0000	1000	0.1542
0.540	0.4097	3.1776	0.8834	883.4	0.1658
0.550	0.4328	2.7879	0.7750	775	0.1783
0.560	0.4560	2.4351	0.6770	677	0.1918
0.570	0.4792	2.1192	0.5891	589.1	0.2062
0.580	0.5023	1.8386	0.5111	511.1	0.2216
0.590	0.5255	1.5911	0.4423	442.3	0.2379
0.607	0.5648	1.2879	0.3580	358	0.2678
0.617	0.5879	1.0648	0.2960	296	0.2866
0.627	0.6111	0.9139	0.2541	254.1	0.3064
0.638	0.6366	0.7704	0.2142	214.2	0.3293
0.648	0.6597	0.6577	0.1828	182.8	0.3510
0.659	0.6851	0.5506	0.1531	153.1	0.3760

Table 4.18: (contd) Saturation and total mobility profiles for $Q_{i,5}$=0.278 and $S_{w2}(x=L)$=0.53.

0.669	0.7083	0.4666	0.1297	129.7	0.3998
0.680	0.7338	0.3867	0.1075	107.5	0.4271
0.690	0.7569	0.3240	0.0901	90.1	0.4528
0.701	0.7824	0.2644	0.0735	73.5	0.4822
0.711	0.8056	0.2175	0.0605	60.5	0.5010
0.722	0.8310	0.1729	0.0481	48.1	0.5415
0.732	0.8542	0.1379	0.0383	38.3	0.5713
0.743	0.8796	0.1045	0.0291	29.1	0.6049
0.753	0.9023	0.0782	0.0217	21.7	0.6360
0.764	0.9282	0.0532	0.0148	14.8	0.6725
0.774	0.9513	0.0335	0.0093	9.3	0.7061
0.785	0.9769	0.0147	0.0041	4.1	0.7444
0.795	1.0000	0.0000	0	0	0.7800

Once we computed saturation profile, we generate the total mobility profile using Eq. 4.68 (see last column of Table 4.18). Then, we compute the apparent viscosity after BT from Eq. 4.34 using the trapezoidal rule: i.e.,

$$\mu_{app}(t) = \frac{1}{L}\int_0^L \frac{1}{\lambda_t(x)}dx = \frac{1}{2L}\sum_{j=1}\left(\frac{1}{\lambda_{t,j}} + \frac{1}{\lambda_{t,j-1}}\right)\left(x_j - x_{j-1}\right) \quad \textbf{(4.69)}$$

Then the injection rate is computed from Eq. 4.33. For instance, the computed apparent viscosity and injection rate for the case where for S_{w2} (x=L) = 0.53 and Q_i = 0.278 are

$$\mu_{app}(Qi = 0.278) = 4.314 \text{ cp} \quad \textbf{(4.70)}$$

and

$$\begin{aligned} q_t(Q_{i,1} = 0.0442) &= \frac{1.127*10^{-3}kA}{\mu_{app}(Q_{i,1})}\frac{\Delta p}{L} \\ &= \frac{1.127*10^{-3}*23*500*20}{4.314}\frac{2000}{1000} = 57.78 bbl/D \end{aligned} \quad \textbf{(4.71)}$$

Next, we compute the average saturation in the reservoir when the water saturation at x=L is $S_{w2}(t_{k+j})$ from

$$\bar{S}_w(Q_i) = S_{w2}(t_{k+j}) + \left[1 - f_w(S_{w2})\right]Q_i(t_{k+j}) \quad \textbf{(4.72)}$$

For instance, the average saturation in the reservoir for $S_{w2}(x=L)$=0.53 and Q_i=0.278, and $f_w(0.53)$=0.7560, is computed as

$$\bar{S}_w(Q_i) = S_{w2}(t_{k+j}) + [1 - f_w(S_{w2})]Q_i(t_{k+j})$$
$$= 0.53 + [1 - 0.7560] * 0.278 = 0.598 \qquad \textbf{(4.73)}$$

The cumulative oil production after BT is computed by the use of Eq. 4.73, and $N_p(PV)$ after BT is computed by the use of Eq. 4.74. For instance, the cumulative oil production N_p and N_p(PV) for the case where S_{w2} (x=L) = 0.53 and Q_i = 0.278 are computed as

$$N_p = V_p[\bar{S}_w(Q_i) - S_{wi}] = 366{,}877 \times [0.598 - 0.363] = 86{,}216 \text{ bbl} \qquad \textbf{(4.74)}$$

and

$$N_p(PV) = \frac{N_p}{V_p} = \frac{86{,}216}{366{,}877} = 0.235 \qquad \textbf{(4.75)}$$

The oil and water production rates after BT are computed from are computed from

$$q_o(Q_i) = [1 - f_w(S_{w2})]q_t(Q_i) \qquad \textbf{(4.76)}$$

and

$$q_w(Q_i) = f_w(S_{w2})q_t(Q_i) \qquad \textbf{(4.77)}$$

WOR after BT (assuming $B_o = B_w = 1$) is simply computed from

$$WOR = \frac{q_w}{q_o} = \frac{Eq.\,4.76}{Eq.\,4.77} \qquad \textbf{(4.78)}$$

For instance, the oil and water production rates and *WOR* for the case where S_{w2} (x=L) = 0.53 and Q_i = 0.278 are computed as

$$q_o(Q_i) = [1 - f_w(S_{w2})]q_t(Q_i) = [1 - 0.7560] \times 120.2 = 29.3 \text{ bbl/D} \qquad \textbf{(4.79)}$$

$$q_w(Q_i) = f_w(S_{w2})q_t(Q_i) = 0.7560 \times 102.2 = 90.9 \text{ bbl/D} \qquad \textbf{(4.80)}$$

and

$$WOR = \frac{q_w}{q_o} = \frac{90.9}{29.3} = 3.1 \quad \textbf{(4.81)}$$

We perform similar calculations for other specified values of Q_i given in Table 4.17. Tables 4.19-4.21 and Tables B1-B4 in Appendix B give the saturation and total mobility profiles for Q_i =0.359, 0.472, 0.776, 1.298, 2.143, 3.086, and 5.784, respectively.

Table 4.19: Saturation and total mobility profiles for $Q_{i,6}$ = 0.359 and $S_{w2}(x=L)$=0.55.

$\hat{S}_w$	S_{wD}	$\left(\frac{\partial f_w}{\partial S_w}\right)_{\hat{S}_w}$	$\frac{x_{\hat{S}_w}}{L}$	$x_{\hat{S}_w}$ (ft)	λ_t, (1/cp)
0.550	0.4328	2.7879	1.0000	1000	0.1783
0.560	0.4560	2.4351	0.8742	874.2	0.1918
0.570	0.4792	2.1192	0.7608	760.8	0.2062
0.580	0.5023	1.8386	0.6601	660.1	0.2216
0.590	0.5255	1.5911	0.5712	571.2	0.2379
0.607	0.5648	1.2879	0.4624	462.4	0.2678
0.617	0.5879	1.0648	0.3823	382.3	0.2866
0.627	0.6111	0.9139	0.3281	328.1	0.3064
0.638	0.6366	0.7704	0.2766	276.6	0.3293
0.648	0.6597	0.6577	0.2361	236.1	0.3510
0.659	0.6851	0.5506	0.1977	197.7	0.3760
0.669	0.7083	0.4666	0.1675	167.5	0.3998
0.680	0.7338	0.3867	0.1388	138.8	0.4271
0.690	0.7569	0.3240	0.1163	116.3	0.4528
0.701	0.7824	0.2644	0.0949	94.9	0.4822
0.711	0.8056	0.2175	0.0781	78.1	0.5010
0.722	0.8310	0.1729	0.0621	62.1	0.5415
0.732	0.8542	0.1379	0.0495	49.5	0.5713
0.743	0.8796	0.1045	0.0375	37.5	0.6049
0.753	0.9023	0.0782	0.0281	28.1	0.6360
0.764	0.9282	0.0532	0.0191	19.1	0.6725
0.774	0.9513	0.0335	0.0121	12.1	0.7061
0.785	0.9769	0.0147	0.0053	5.3	0.7444
0.795	1.0000	0.0000	0	0	0.7800

Table 4.20: Saturation and total mobility profiles for $Q_{i,7}$=0.472 and $S_{w2}(x=L)$=0.570.

$\hat{S}_w$	S_{wD}	$\left(\frac{\partial f_w}{\partial S_w}\right)_{\hat{S}_w}$	$\frac{x_{\hat{S}_w}}{L}$	$x_{\hat{S}_w}$ (ft)	λ_t, (1/cp)
0.570	0.4792	2.1192	1.0000	1000	0.2062
0.580	0.5023	1.8386	0.8678	867.8	0.2216
0.590	0.5255	1.5911	0.7510	751	0.2379
0.607	0.5648	1.2879	0.6079	607.9	0.2678
0.617	0.5879	1.0648	0.5026	502.6	0.2866
0.627	0.6111	0.9139	0.4314	431.4	0.3064
0.638	0.6366	0.7704	0.3636	363.6	0.3293
0.648	0.6597	0.6577	0.3104	310.4	0.3510
0.659	0.6851	0.5506	0.2599	259.9	0.3760

Table 4.20: (contd) Saturation and total mobility profiles for $Q_{i,7}$=0.472 and $S_{w2}(x=L)$=0.570.

0.669	0.7083	0.4666	0.2202	220.2	0.3998
0.680	0.7338	0.3867	0.1825	182.5	0.4271
0.690	0.7569	0.3240	0.1529	152.9	0.4528
0.701	0.7824	0.2644	0.1248	124.8	0.4822
0.711	0.8056	0.2175	0.1027	102.7	0.5010
0.722	0.8310	0.1729	0.0816	81.6	0.5415
0.732	0.8542	0.1379	0.0651	65.1	0.5713
0.743	0.8796	0.1045	0.0493	49.3	0.6049
0.753	0.9023	0.0782	0.0369	36.9	0.6360
0.764	0.9282	0.0532	0.0251	25.1	0.6725
0.774	0.9513	0.0335	0.0158	15.8	0.7061
0.785	0.9769	0.0147	0.0069	6.9	0.7444
0.795	1.0000	0.0000	0	0	0.7800

Table 4.21: Saturation and total mobility profiles for $Q_{i,8}$ = 0.776 and $S_{w2}(x=L)$ = 0.607.

$\hat{S}_w$	S_{wD}	$\left(\frac{\partial f_w}{\partial S_w}\right)_{\hat{S}_w}$	$\frac{x_{\hat{S}_w}}{L}$	$x_{\hat{S}_w}$ (ft)	λ_t, (1/cp)
0.607	0.5648	1.2879	1.0000	1000	0.2678
0.617	0.5879	1.0648	0.8268	826.8	0.2866
0.627	0.6111	0.9139	0.7096	709.6	0.3064
0.638	0.6366	0.7704	0.5982	598.2	0.3293
0.648	0.6597	0.6577	0.5107	510.7	0.3510
0.659	0.6851	0.5506	0.4275	427.5	0.3760
0.669	0.7083	0.4666	0.3623	362.3	0.3998
0.680	0.7338	0.3867	0.3003	300.3	0.4271
0.690	0.7569	0.3240	0.2516	251.6	0.4528
0.701	0.7824	0.2644	0.2053	205.3	0.4822
0.711	0.8056	0.2175	0.1689	168.9	0.5010
0.722	0.8310	0.1729	0.1342	134.2	0.5415
0.732	0.8542	0.1379	0.1071	107.1	0.5713
0.743	0.8796	0.1045	0.0811	81.1	0.6049
0.753	0.9023	0.0782	0.0607	60.7	0.6360
0.764	0.9282	0.0532	0.0413	41.3	0.6725
0.774	0.9513	0.0335	0.0260	26	0.7061
0.785	0.9769	0.0147	0.0114	11.4	0.7444
0.795	1.0000	0.0000	0	0	0.7800

Table 4.22 presents the results for Q_i, μ_{app}, q_t, q_o, q_w, WOR, N_p, and $N_p(PV)$ up to breakthrough as well as after breakthrough.

Table 4.22: Results for Performance Parameters for μ_o = 10 cp.

Q_i	μ_{app}, cp	S_w	q_t, bbl/D	q_o, bbl/D	q_w, bbl/D	**WOR**	N_p, bbl	$N_p(PV)$
0.000	10.0	0.363	51.84	51.84	0.00	0.00	0.0	0.0
0.044	8.972	0.407	57.78	57.78	0.00	0.00	16,142	0.044
0.088	7.944	0.451	65.26	65.26	0.00	0.00	32,284	0.088
0.133	6.916	0.496	74.96	74.96	0.00	0.00	48,426	0.133
0.177	5.887	0.539	88.06	88.06	0.00	0.00	64,568	0.177
0.221(BT)	4.859	0.584	106.7	34.14	72.6	2.13	79,612	0.217
0.278	4.314	0.598	120.2	29.30	90.9	3.10	86,216	0.235
0.359	3.809	0.615	136.1	24.55	111.55	4.54	92,453	0.252
0.472	3.362	0.632	154.2	20.28	133.92	6.60	98,690	0.269
0.776	2.741	0.662	189.1	13.37	175.76	13.15	109,646	0.299
1.298	2.288	0.690	226.6	9.09	217.50	23.94	119,969	0.327
2.143	1.970	0.715	263.2	5.61	257.55	45.91	129,011	0.352
3.086	1.799	0.731	288.2	3.83	284.34	74.19	135,027	0.368
5.784	1.586	0.753	326.9	1.73	325.17	187.7	142,956	0.390

Case 2: μ_o = 1 cp (favorable case): We will repeat the similar calculations as in Case 1 for this favorable case.

Table 4.23 gives the values of S_w values (arbitrarily chosen), S_{wD}, and f_w values computed from Eqs. 4.20 through 4.24.

Table 4.23: S_w vs f_w for μ_o = 1 cp.

S_w	S_{wD}	f_w
0.363	0	0
0.380	0.0394	0.0013
0.400	0.0856	0.0068
0.420	0.1319	0.0177
0.440	0.1782	0.0354
0.460	0.2245	0.0614
0.480	0.2708	0.0971
0.500	0.3171	0.1440
0.520	0.3634	0.2027
0.540	0.4097	0.2731
0.560	0.4560	0.3540
0.580	0.5023	0.4427
0.600	0.5486	0.5353
0.620	0.5949	0.6272
0.640	0.6412	0.7136
0.660	0.6875	0.7906
0.680	0.7338	0.8556
0.700	0.7801	0.9075
0.720	0.8264	0.9465
0.740	0.8727	0.9734
0.760	0.9190	0.9901
0.795	1.000	1

Figure 4.11 shows the f_w vs S_w curve for the case where oil viscosity is 1 cp. Note that we determined S_{wf} =0.68 and $f_w(S_{wf})$=0.86, and $\overline{S}_{wf} = 0.73$. The slope of

fractional flow curve at S_{wf} is calculated from Eq.4.24, and is equal to $\left(\frac{\partial f_w}{\partial S_w}\right)_{S_{wf}} = 2.9276$.

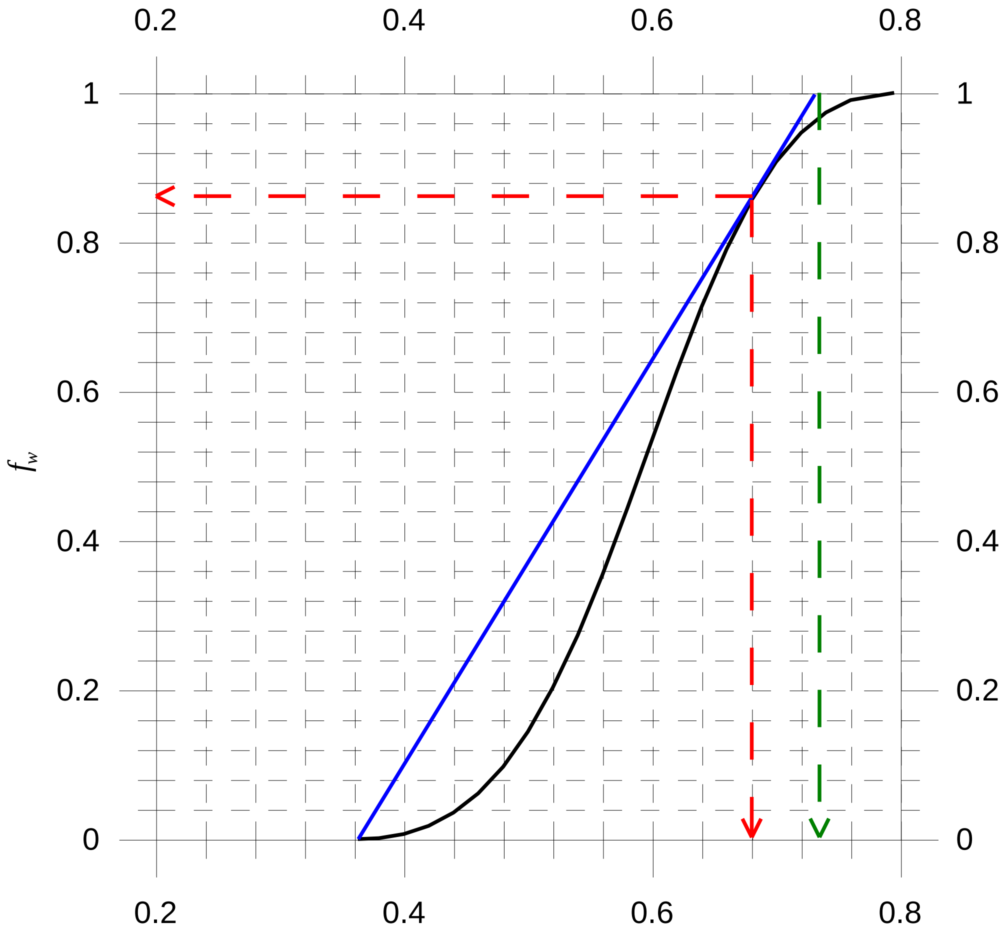

Figure 4.11: Fractional flow curve for μ_o=1 cp.

First, we compute the value of the number of pore volumes of water injected up to breakthrough Q_{ibt} (i.e., $Q_i(t_{bt})$) from

$$Q_{ibt} = \frac{1}{\left(\frac{\partial f_w}{\partial S_w}\right)_{S_{wf}}} = \frac{1}{2.9276} = 0.3416 \tag{4.82}$$

Now, we will specify a sequence such that

$$0 = Q_{i,0} < Q_{i,1} < Q_{i,2} < \cdots < Q_{i,k-1} < Q_{i,k} = Q_{ibt} = 0.3416 \tag{4.83}$$

To generate a sequence, we simply use five uniformly spaced values of Q_i's determined from

$$Q_{i,l} = Q_{i,l-1} + \frac{0.3416}{5} = Q_{i,l-1} + \frac{0.3416}{5} = Q_{i,l-1} + 0.0683 \quad \textbf{(4.84)}$$

for l=1,…,5, where $Q_{i,0}$ = 0. So, my specified values of Q_i's up to BT is given in Table 4.24.

Table 4.24: Specified Q_i values up to BT.

Qi
0.00
0.0683
0.1366
0.2049
0.2732
0.3416

Injection rate at t =0 is

$$\begin{aligned} q_t(0) &= \frac{1.127 * 10^{-3} kA}{\mu_{app}(Q_{i,1})} \frac{\Delta p}{L} \\ &= \frac{1.127 * 10^{-3} * 23 * 500 * 20}{1} \frac{2000}{1000} = 518.4 bbl/D \end{aligned} \quad \textbf{(4.85)}$$

and the apparent viscosity at t = 0 is $\mu_{app}(0)$ = 1 cp. Table 4.25 gives the specified values of S_w, the slope values computed from Eq. 4.24 for the specified values of S_w, the values of $\frac{x_{\hat{S}_w}}{L}$ and $x_{\hat{S}_w}$ computed for $Q_{i,1}$ = 0.0683. Tables 4.25 through 4.29 give the results for other specified values of Q_i given in Table 4.24.

Table 4.25: Saturation and total mobility profiles for $Q_{i,1}$ = 0.0683.

$\hat{S}_w$	S_{wD}	$\left(\frac{\partial f_w}{\partial S_w}\right)_{\hat{S}_w}$	$\frac{x_{\hat{S}_w}}{L}$	$x_{\hat{S}_w}$ (ft)	λ_t, (1/cp)
0.680	0.7338	2.9276	0.2000	200.0	0.4909
0.690	0.7569	2.5956	0.1773	177.3	0.5060
0.701	0.7824	2.2320	0.1524	152.4	0.5248
0.711	0.8056	1.9110	0.1305	130.5	0.5440
0.722	0.8310	1.5764	0.1077	107.7	0.5672
0.732	0.8542	1.2903	0.0881	88.1	0.5904
0.743	0.8796	1.0014	0.0684	68.4	0.6180
0.753	0.9023	0.7662	0.0523	52.3	0.6446
0.764	0.9282	0.5248	0.0358	35.8	0.6772
0.774	0.9513	0.3335	0.0228	22.8	0.7082
0.785	0.9769	0.1469	0.0100	10.0	0.7449
0.795	1.0000	0	0	0	0.78

Table 4.26: Saturation and total mobility profiles for $Q_{i,2}$ = 0.1366.

$\hat{S}_w$	S_{wD}	$\left(\frac{\partial f_w}{\partial S_w}\right)_{\hat{S}_w}$	$\frac{x_{\hat{S}_w}}{L}$	$x_{\hat{S}_w}$ (ft)	λ_t, (1/cp)
0.680	0.7338	2.9276	0.4000	400.0	0.4909
0.690	0.7569	2.5956	0.3546	354.6	0.5060
0.701	0.7824	2.2320	0.3049	304.9	0.5248
0.711	0.8056	1.9110	0.2610	261.0	0.5440
0.722	0.8310	1.5764	0.2153	215.3	0.5672
0.732	0.8542	1.2903	0.1763	176.3	0.5904
0.743	0.8796	1.0014	0.1368	136.8	0.6180
0.753	0.9023	0.7662	0.1047	104.7	0.6446
0.764	0.9282	0.5248	0.0717	71.7	0.6772
0.774	0.9513	0.3335	0.0456	45.6	0.7082
0.785	0.9769	0.1469	0.0201	20.1	0.7449
0.795	1.0000	0	0	0	0.78

Table 4.27: Saturation and total mobility profiles for $Q_{i,3}$ = 0.2049.

$\hat{S}_w$	S_{wD}	$\left(\frac{\partial f_w}{\partial S_w}\right)_{\hat{S}_w}$	$\frac{x_{\hat{S}_w}}{L}$	$x_{\hat{S}_w}$ (ft)	λ_t, (1/cp)
0.680	0.7338	2.9276	0.6000	600.0	0.4909
0.690	0.7569	2.5956	0.5318	531.8	0.5060
0.701	0.7824	2.2320	0.4573	457.3	0.5248
0.711	0.8056	1.9110	0.3916	391.6	0.5440
0.722	0.8310	1.5764	0.3230	323.0	0.5672
0.732	0.8542	1.2903	0.2644	264.4	0.5904
0.743	0.8796	1.0014	0.2052	205.2	0.6180
0.753	0.9023	0.7662	0.1570	157.0	0.6446
0.764	0.9282	0.5248	0.1075	107.5	0.6772
0.774	0.9513	0.3335	0.0683	68.3	0.7082
0.785	0.9769	0.1469	0.0301	30.1	0.7449
0.795	1.0000	0	0	0	0.78

Table 4.28: Saturation and total mobility profiles for $Q_{i,4}$ = 0.2732.

$\hat{S}_w$	S_{wD}	$\left(\frac{\partial f_w}{\partial S_w}\right)_{\hat{S}_w}$	$\frac{x_{\hat{S}_w}}{L}$	$x_{\hat{S}_w}$ (ft)	λ_t, (1/cp)
0.680	0.7338	2.9276	0.8000	800.0	0.4909
0.690	0.7569	2.5956	0.7091	709.1	0.5060
0.701	0.7824	2.2320	0.6100	610.0	0.5248
0.711	0.8056	1.9110	0.5221	522.1	0.5440
0.722	0.8310	1.5764	0.4307	430.7	0.5672
0.732	0.8542	1.2903	0.3525	352.5	0.5904
0.743	0.8796	1.0014	0.2736	273.6	0.6180
0.753	0.9023	0.7662	0.2093	209.3	0.6446
0.764	0.9282	0.5248	0.1434	143.4	0.6772
0.774	0.9513	0.3335	0.0911	91.1	0.7082
0.785	0.9769	0.1469	0.0401	40.1	0.7449
0.795	1.0000	0	0	0	0.78

Table 4.29: Saturation and total mobility profiles for $Q_{i,5} = 0.3416$.

$\hat{S}_w$	S_{wD}	$\left(\dfrac{\partial f_w}{\partial S_w}\right)_{\hat{S}_w}$	$\dfrac{x_{\hat{S}_w}}{L}$	$x_{\hat{S}_w}$ (ft)	λ_t, (1/cp)
0.680	0.7338	2.9276	1.0000	1000.0	0.4909
0.690	0.7569	2.5956	0.8867	886.7	0.5060
0.701	0.7824	2.2320	0.7625	762.5	0.5248
0.711	0.8056	1.9110	0.6528	652.8	0.5440
0.722	0.8310	1.5764	0.5385	538.5	0.5672
0.732	0.8542	1.2903	0.4408	440.8	0.5904
0.743	0.8796	1.0014	0.3421	342.1	0.6180
0.753	0.9023	0.7662	0.2617	261.7	0.6446
0.764	0.9282	0.5248	0.1793	179.3	0.6772
0.774	0.9513	0.3335	0.1139	113.9	0.7082
0.785	0.9769	0.1469	0.0502	50.2	0.7449
0.795	1.0000	0	0	0	0.78

<u>Performance After Breakthrough:</u> Somewhat arbitrarily, we specify a sequence of S_w as given in the first column of Table 4.30. Then, for each value of S_w, we compute the cumulative pore volumes of water injected from

$$Q_i(t_{k+j}) = \frac{1}{\left(\dfrac{\partial f_w}{\partial S_w}\right)_{Sw2(t_{k+j})}} \tag{4.86}$$

The second column of Table 4.30 gives the computed values of Q_i from the preceding equation.

Table 4.30: A sequence of S_{w2} for performance computations after BT for $\mu_o = 1$ cp.

S_{w2}	Q_i
0.690	0.385
0.711	0.523
0.732	0.776
0.753	1.305
0.774	2.999

Table 4.31 gives the values of water cut that will be needed in computations.

Table 4.31: Saturation and water cut values.

$\hat{S}_w$	S_{wD}	f_w
0.680	0.7338	0.8556
0.690	0.7569	0.8832
0.701	0.7824	0.9098
0.711	0.8056	0.9305
0.722	0.8310	0.9496
0.732	0.8542	0.9640
0.743	0.8796	0.9765
0.753	0.9023	0.9852
0.764	0.9282	0.9924
0.774	0.9513	0.9967
0.785	0.9769	0.9993
0.795	1.0000	1

Tables 4.32 through 4.36 give the saturation and total mobility profiles for each value of Q_i given in Table 4.30.

Table 4.32: Saturation and total mobility profiles for $Q_{i,6}$ = 0.385.

$\hat{S}_w$	S_{wD}	$\left(\frac{\partial f_w}{\partial S_w}\right)_{\hat{S}_w}$	$\frac{x_{\hat{S}_w}}{L}$	$x_{\hat{S}_w}$ (ft)	λ_t, (1/cp)
0.690	0.7569	2.5956	0.1000	1000.0	0.5060
0.701	0.7824	2.2320	0.8593	859.3	0.5248
0.711	0.8056	1.9110	0.7357	735.7	0.5440
0.722	0.8310	1.5764	0.6069	606.9	0.5672
0.732	0.8542	1.2903	0.4968	496.8	0.5904
0.743	0.8796	1.0014	0.3855	385.5	0.6180
0.753	0.9023	0.7662	0.2950	295.0	0.6446
0.764	0.9282	0.5248	0.2020	202.0	0.6772
0.774	0.9513	0.3335	0.1284	128.4	0.7082
0.785	0.9769	0.1469	0.0566	56.6	0.7449
0.795	1.0000	0	0	0	0.78

Table 4.33: Saturation and total mobility profiles for $Q_{i,7}$ = 0.523.

$\hat{S}_w$	S_{wD}	$\left(\frac{\partial f_w}{\partial S_w}\right)_{\hat{S}_w}$	$\frac{x_{\hat{S}_w}}{L}$	$x_{\hat{S}_w}$ (ft)	λ_t, (1/cp)
0.711	0.8056	1.9110	0.1000	1000	0.5440
0.722	0.8310	1.5764	0.8245	824.5	0.5672
0.732	0.8542	1.2903	0.6748	674.8	0.5904
0.743	0.8796	1.0014	0.5237	523.7	0.6180
0.753	0.9023	0.7662	0.4007	400.7	0.6446
0.764	0.9282	0.5248	0.2745	274.5	0.6772
0.774	0.9513	0.3335	0.1744	174.4	0.7082
0.785	0.9769	0.1469	0.0768	76.8	0.7449
0.795	1.0000	0	0	0	0.78

Table 4.34: Saturation and total mobility profiles for $Q_{i,8}$ = 0.776.

$\hat{S}_w$	S_{wD}	$\left(\frac{\partial f_w}{\partial S_w}\right)_{\hat{S}_w}$	$\frac{x_{\hat{S}_w}}{L}$	$x_{\hat{S}_w}$ (ft)	λ_t, (1/cp)
0.732	0.8542	1.2903	0.1000	1000.0	0.5904
0.743	0.8796	1.0014	0.7761	776.1	0.6180
0.753	0.9023	0.7662	0.5938	593.8	0.6446
0.764	0.9282	0.5248	0.4067	406.7	0.6772
0.774	0.9513	0.3335	0.2585	258.5	0.7082
0.785	0.9769	0.1469	0.1139	113.9	0.7449
0.795	1.0000	0	0	0	0.78

Table 4.35: Saturation and total mobility profiles for $Q_{i,9}$ = 1.305.

$\hat{S}_w$	S_{wD}	$\left(\frac{\partial f_w}{\partial S_w}\right)_{\hat{S}_w}$	$\frac{x_{\hat{S}_w}}{L}$	$x_{\hat{S}_w}$ (ft)	λ_t, (1/cp)
0.753	0.9023	0.7662	1.0000	1000.0	0.6446
0.764	0.9282	0.5248	0.6849	684.9	0.6772
0.774	0.9513	0.3335	0.4353	435.3	0.7082
0.785	0.9769	0.1469	0.1917	191.7	0.7449
0.795	1.0000	0	0	0	0.78

Table 4.36: Saturation and total mobility profiles for $Q_{i,10}$ = 2.999.

$\hat{S}_w$	S_{wD}	$\left(\frac{\partial f_w}{\partial S_w}\right)_{\hat{S}_w}$	$\frac{x_{\hat{S}_w}}{L}$	$x_{\hat{S}_w}$ (ft)	λ_t, (1/cp)
0.774	0.9513	0.3335	1.0000	1000	0.7082
0.785	0.9769	0.1469	0.4405	440.5	0.7449
0.795	1.0000	0	0	0.0	0.78

Table 4.37 summarizes the results for performance parameters for the case where oil viscosity is 1 cp.

Table 4.37: Results for Performance Parameters for μ_o = 1 cp.

Q_i	μ_{app}, cp	S_w	q_t, bbl/D	q_o, bbl/D	q_w, bbl/D	WOR	N_p, bbl	$N_p(PV)$
0.000	1.0	0.363	518.4	518.4	0.00	0.00	0.0	0.0
0.068	1.142	0.431	453.8	453.8	0.00	0.00	25,058	0.068
0.137	1.285	0.500	403.5	403.5	0.00	0.00	50,116	0.137
0.205	1.427	0.568	363.2	363.2	0.00	0.00	75,174	0.205
0.273	1.570	0.636	330.3	330.3	0.00	0.00	100,232	0.273
0.342 (BT)	1.712	0.729	302.8	43.7	259.1	5.92	134,644	0.367
0.385	1.675	0.734	309.5	36.2	273.3	7.55	136,467	0.372
0.523	1.591	0.747	325.8	22.6	303.2	13.4	141,016	0.384
0.776	1.506	0.760	344.2	12.4	331.8	26.9	145,627	0.397
1.305	1.425	0.772	363.8	5.4	358.4	66.6	150,168	0.409
2.999	1.349	0.784	384.3	1.3	383.0	294.6	154,417	0.421

Discussion of Results: For the unfavorable case (μ_o = 10 cp), because water behind the front flows more easily than oil ahead of front (i.e., the injected water has less resistance to flow), the injection rate increases. After breakthrough, preferential flow path is for water, so injection rate continues to increase.

For the favorable case (μ_o = 1 cp), oil ahead of the front moves easily than water behind the front. As the amount of water injected increases, injection rate (q_t) decreases. After breakthrough, water can flow easily from injector to producer, so injection rate increases.

Also, it is worth to note from Fig. 4.13 that injection rates for the favorable case is higher than the unfavorable case. This means that there is less resistance to flow in the favorable case. Note also that the BT for the unfavorable case occurs earlier than that for the favorable case, and that cumulative production for the favorable case is quite high compared to that of unfavorable case. Most importantly, to have the same amount of cumulative production, the favorable case requires significantly more volumes of water injected. By inspecting Fig. 4.14, we see that to produce 140,000 bbl of oil, in the favorable case, we only need to inject 0.5 PV of water, while to produce the same amount in the unfavorable case, we need to inject 4.7 PV of water. Clearly, these results indicate that the greater the oil viscosity is the less efficient the water flood is.

Figure 4.12 shows graphs of apparent viscosity vs. Q_i for μ_o=1 and 10 cp.

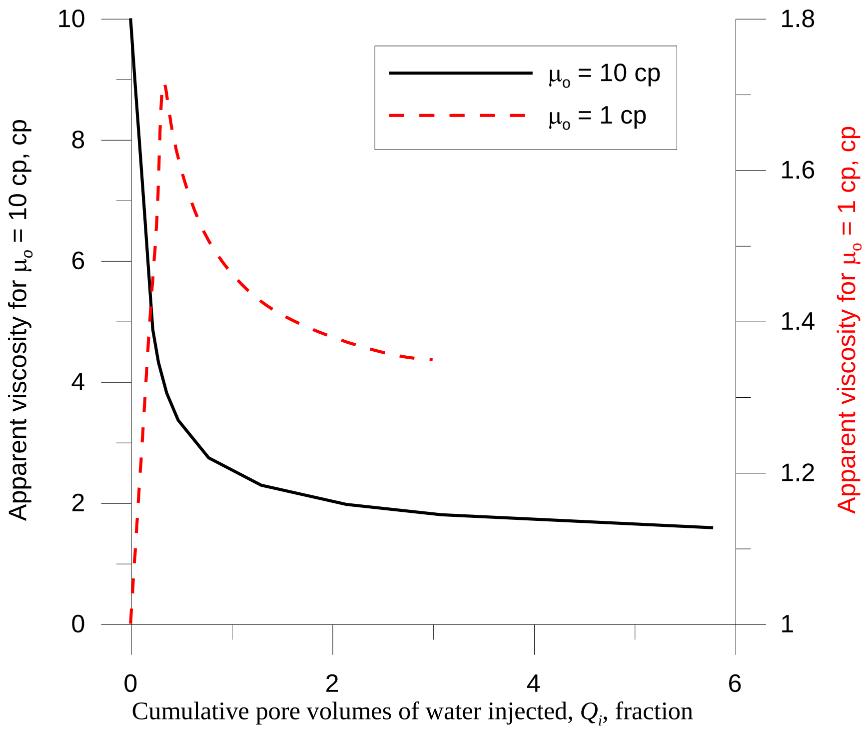

Figure 4.12: Fractional apparent viscosity vs. Q_i for μ_o = 1 and 10 cp.

Figure 4.13 shows graphs of injection rate (q_t) vs. Q_i for μ_o=1 and 10 cp.

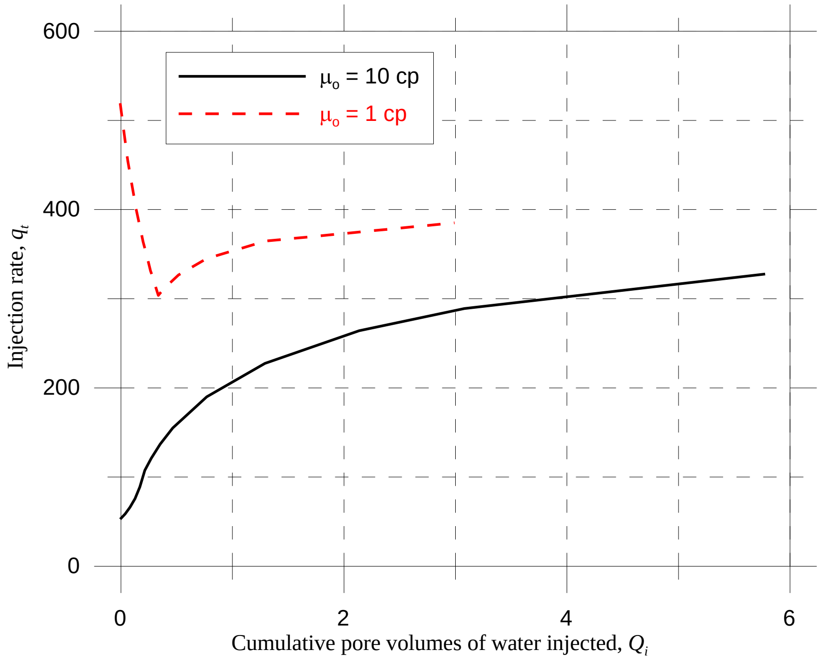

Figure 4.13: q_t vs. Q_i for μ_o=1 and 10 cp.

Figure 4.14 shows graphs cumulative oil production in bbl (N_p) vs. Q_i for μ_o = 1 and 10 cp.

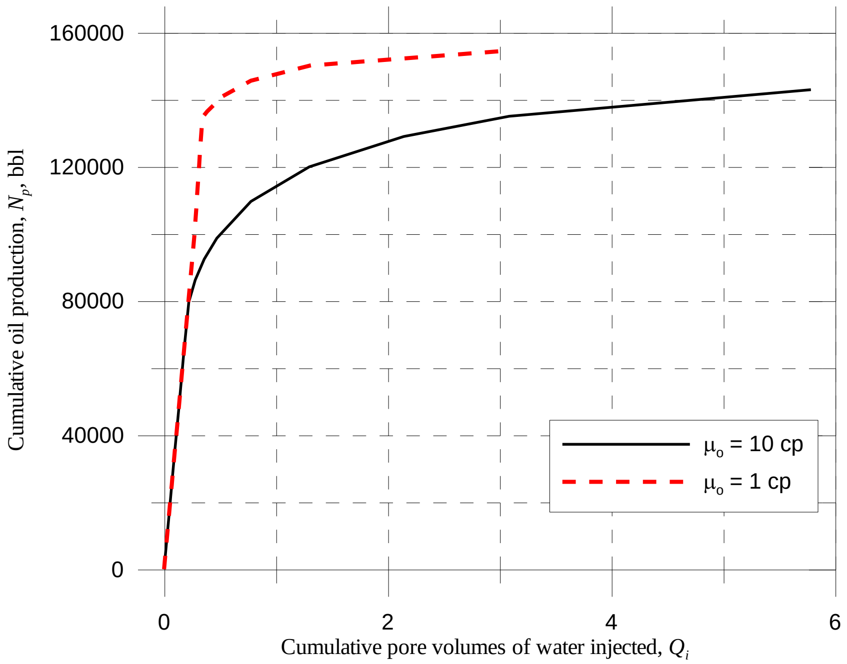

Figure 4.14: N_p vs. Q_i for μ_o = 1 and 10 cp.

4.4 Example Application 4

In the final example application we consider waterflood performance in a five-spot pattern with 10 acre. The pressure drop between an injector and a producer will be maintained at a constant pressure drop of 2000 psia. The oil and water formation volume factors B_o = 1.2 RB/STB and B_w = 1.0 RB/STB. Viscosities of the oil and water are μ_o = 10 cp, and μ_w = 1 cp. Porosity of the reservoir is 0.206, and permeability is 23 md and formation thickness is 20 ft The initial and irreducible oil saturations are given by S_{oi}=0.637, and S_{or}= 0.205.

Prepare a table as shown in Table 4.38 given below which will include all columns filled with the correct number**.** We have computed the breakthrough time to be t_{bt} = 977 days based on the equations given previously.

Table 4.38: Experimental data.

Time (days)	W_i (RB)	Q_i*	***M***	E_A	i_w	S_{w2}	$\overline{S}_{w2}$	N_p	***WOR***
	30,000								
977 (=t_{bt})									
	89,991								
				1.0					
	293,284								

The oil and relative permeability curves will be computed from analytical expressions given below

$$k_{ro} = k_{ro}^0 (1 - S_{wD})^m \tag{4.87}$$

and

$$k_{rw} = k_{rw}^0 (S_{wD})^n \tag{4.88}$$

where S_{wD} is given by

$$S_{wD} = \frac{S_w - S_{iw}}{1 - S_{or} - S_{iw}} \tag{4.89}$$

A formula based on Eqs 4.87-4.89 for the f_w curve is given by

$$f_w = \frac{S_{wD}^n}{S_{wD}^n + A(1 - S_{wD})^m} \tag{4.90}$$

The relative permeability data generated from above equations and the fractional flow curve are shown in Figs. 4.18 and 4.19, respectively.

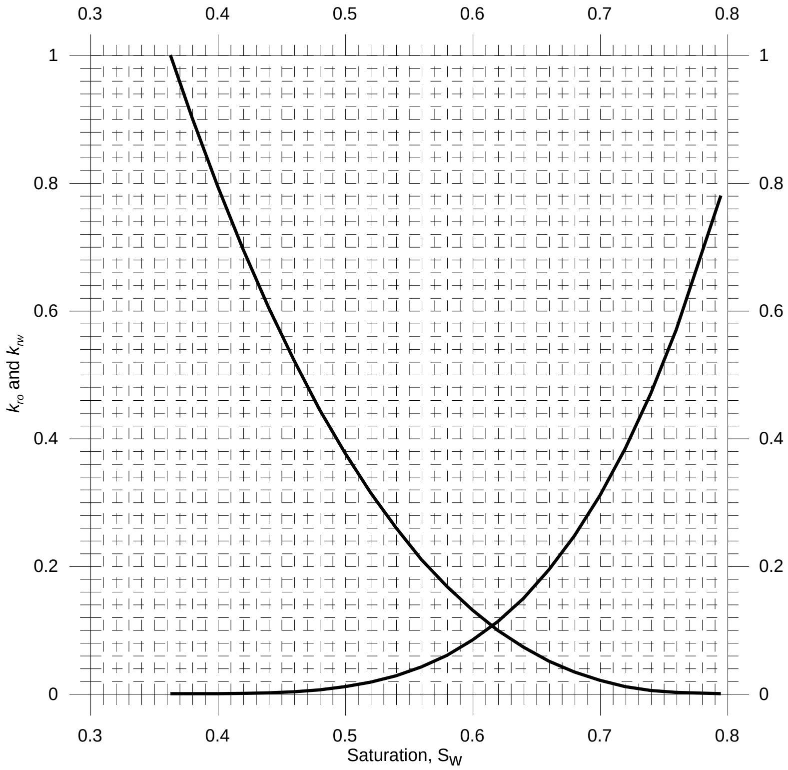

Figure 4.15: Relative permeability data.

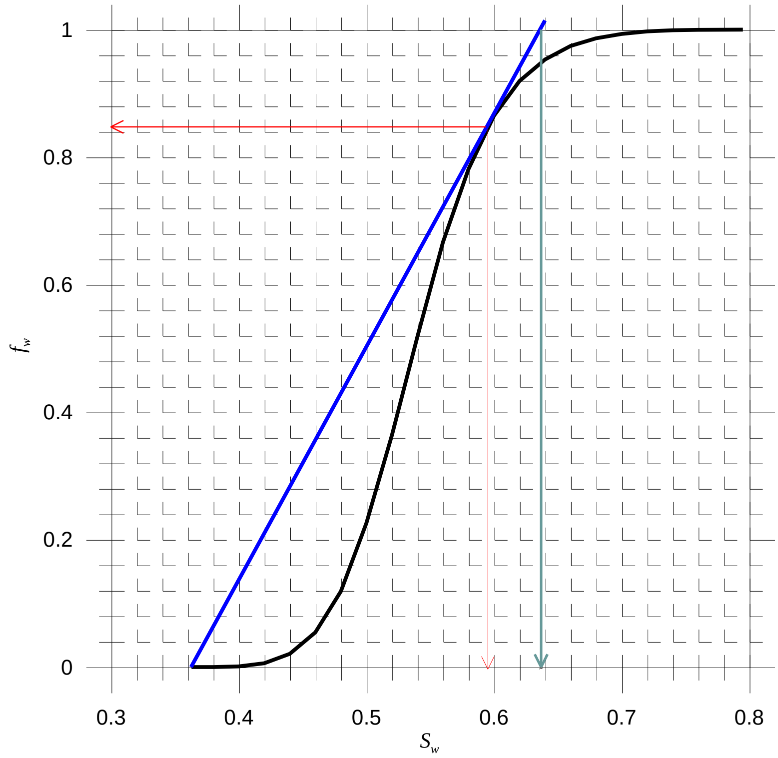

Figure 4.16: Fractional flow curve with tangent drawn to find S_{wf}.

The slope of the fractional flow curve, i.e., df_w/dS_w, as a function of S_w is shown in Fig. 4.17.

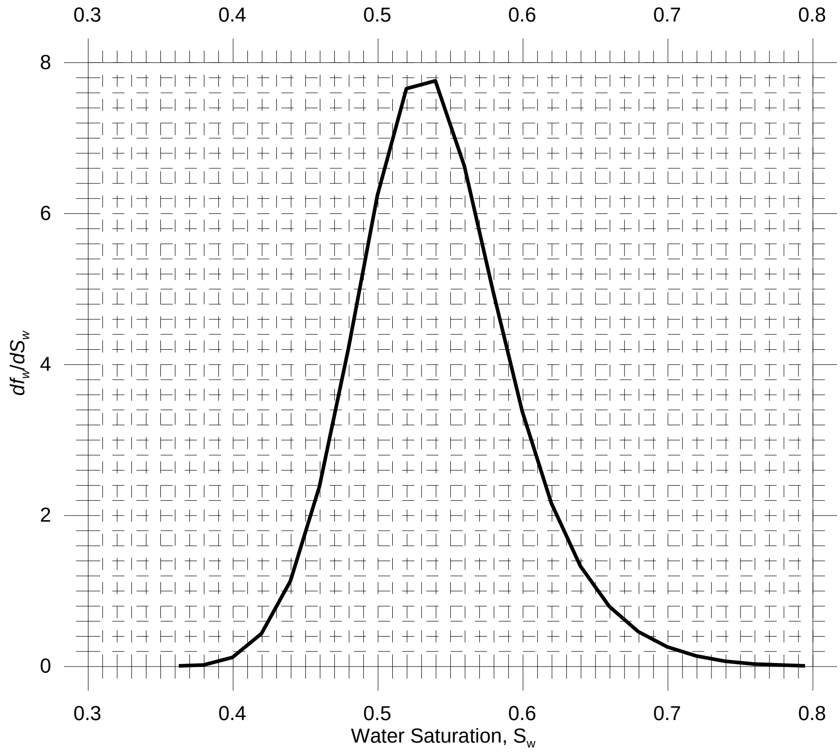

Figure 4.17: The slope of the fractional flow curve as a function of S_w.

From the graphs above, we determined $\overline{S_{wf}} = 0.637$, $k_{rw}(\overline{S_{wf}}) = 0.143$, $S_{wf} = 0.596$, $f_w(S_{wf}) = 0.851$ and $\frac{df_w}{dS_w}(S_{wf}) = 3.652$.

Then, we determine the mobility ratio up to breakthrough and the other parameters such as V_p, E_{Abt}, W_{ibt}, and $W_{i,100}$ using the appropriate formula given in the chapter 3.

$$M = \frac{\mu_o}{\mu_w}\frac{(k_{rw})_{\bar{S}_{wf}}}{(k_{ro})_{S_{wi}}} = \frac{10}{1}\frac{0.143}{1} = 1.43 \quad \textbf{(4.91)}$$

Pore volume is comptuted from

$$V_p = \frac{Ah\phi}{5.615} = \frac{10 \times 43{,}560 \times 20 \times 0.206}{5.615} \approx 319{,}621\ RB \quad \textbf{(4.92)}$$

Areal sweep efficiency determing is given by below equation:

$$
\begin{aligned}
E_{Abt} &= 0.54602036 + \frac{0.03170817}{M} + \frac{0.30222997}{e^{M}} - 0.00509693\,M \\
&= 0.54602036 + \frac{0.03170817}{1.43} + \frac{0.30222997}{e^{1.43}} - 0.00509693 \times 1.43 \\
&= 0.633
\end{aligned} \qquad \textbf{(4.93)}
$$

Water injected at breakthrough W_{ib}:

$$
W_{ibt} = 319{,}621 \times 0.633 \frac{[0.637 - 0.363]}{[1-0]} = 55{,}436\ RB \qquad \textbf{(4.94)}
$$

For time $t{=}t_{100}$

$$
\begin{aligned}
W_{i,100} &= W_{ibt} \exp\left(\frac{1 - E_{Abt}}{0.275}\right) \\
&= 55{,}436 \exp\left(\frac{1 - 0.633}{0.275}\right) \\
&= 210{,}560\ \ RB
\end{aligned} \qquad \textbf{(4.95)}
$$

The base injection rate which will be needed in the computation of injection rates is computed from

$$
\begin{aligned}
i_b &= \frac{3.541 \times 10^{-3} k_b k_{ro}^{0} h}{\mu_o} \frac{\left(p_{inj} - p_{wf}\right)}{\left[\ln\left(\dfrac{d}{r_w}\right) + \dfrac{S_i + S_p}{2} - 0.619\right]} \\
&= \frac{3.541 \times 10^{-3} \times 23 \times 1 \times 20}{10} \frac{(2000)}{\left[\ln\left(\dfrac{466.7}{0.5}\right) + \dfrac{0+0}{2} - 0.619\right]} \\
&= 52.4 \text{ RB/D}
\end{aligned} \qquad \textbf{(4.96)}
$$

Computations for the first row of table Now, we fill the first row of Table 4.38. Mobility is M = 1.43 as W_i = 30,000 RB is less than W_{ibt} In addition, $S_{w2} = S_{wf}$ =0.596 and $\overline{S_{w2}} = \overline{S_{wf}} = 0.637$. Because we have irreducible water saturation in the reservoir at t = 0, we should have no water production up to breakthrough. So, WOR = 0, when W_i = 30,000 RB. Next, we compute the areal sweep efficiency, E_A, when W_i = 30,000 RB. It is computed from

$$E_A = \frac{W_i}{V_p}\frac{\left[1 - f_w\left(S_{wi}\right)\right]}{\left[\overline{S}_{wf} - S_{wi}\right]} = \frac{30{,}000 \times [1-0]}{319{,}621 \times [0.637 - 0.363]} \approx 0.343 \qquad \textbf{(4.97)}$$

The number of contacted pore volumes of injected water is computed by using the formula given below

$$Q_i^* = \frac{W_i}{E_A V_p} = \frac{30{,}000}{0.342 \times 319{,}621} = 0.274 \qquad \textbf{(4.98)}$$

Next, we compute the injection rate by using Fig. 3.12. Using M = 1.43 and E_A = 0.342, we determined the conductance ratio as γ = 1.1 from Fig. 3.12. Then, the injection rate, i_w is

$$i_w = \gamma\, i_b = 1.1 \times 52.4 = 57.6\ RB/D \qquad \textbf{(4.99)}$$

Now, we compute the cumulative oil produced from

$$\begin{aligned} N_p &= \frac{E_A V_p \left(\overline{S_{wf}} - S_{wi}\right)}{B_o} \\ &= \frac{0.342 \times 319{,}621(0.637 - 0.363)}{1.2} = 24{,}959\ STB \end{aligned} \qquad \textbf{(4.100)}$$

<u>Computations for the second row of table 4.38 (i.e., computations at the breakthrough).</u> The cumulative volume of water injected at BT is W_{ibt} and was computed previously as W_{ibt} =55,436 RB. The value of Q_i^* is the same for all W_i's such that $W_i \le W_{ibt}$. So, Q_i^* = 0.274 for W_{ibt}. In addition, $S_{w2} = S_{wf}$ =0.596 and $\overline{S_{w2}} = \overline{S_{wf}} = 0.637$. The areal sweep efficiency, E_{Abt}, was computed as E_{Abt} = 0.633. So, using M = 1.43 and E_{Abt} = 0.633, we determine the conductance ratio from Fig. 3.12. We determined it as γ = 1.2. So, the injection rate is 1.2x52.4=62.9 RB/D. The cumulative oil production at BT is computed as

$$\begin{aligned} N_p &= \frac{E_A V_p \left(\overline{S_{wf}} - S_{wi}\right)}{B_o} \\ &= \frac{0.633 \times 319{,}621(0.637 - 0.363)}{1.2} = 46{,}196\ STB \end{aligned} \qquad \textbf{(4.101)}$$

The *WOR* ratio at the breakthrough is computed from

$$WOR = \frac{B_o}{B_w} \frac{f_w(S_{wf})\left[1 - \dfrac{dN_{pu}}{dW_i}\right]}{f_o(S_{wf})\left[1 - \dfrac{dN_{pu}}{dW_i}\right] + \dfrac{dN_{pu}}{dW_i}} \tag{4.102}$$

where $\dfrac{dN_{pu}}{dW_i}$ is computed from

$$\frac{dN_{pu}}{dW_i} = \frac{W_{ibt}}{W_i} \frac{\left(S_{wf} - S_{wi}\right)}{\left(\overline{S_{wf}} - S_{wi}\right)} \frac{0.275}{E_{Abt}} \tag{4.103}$$

When applying Eq. 4.103 at BT, we take W_i in Eq. 4.103 to be equal to W_{ibt}. So, Eq. 4.103 at BT gives

$$\begin{aligned} \frac{dN_{pu}}{dW_i} &= \frac{W_{ibt}}{W_{ibt}} \frac{\left(S_{wf} - S_{wi}\right)0.275}{(S_{wf} - S_{wi})E_{Abt}} = \frac{\left(S_{wf} - S_{wi}\right)0.275}{(S_{wf} - S_{wi})E_{Abt}} \\ &= \frac{\left(0.596 - 0.363\right)}{\left(0.596 - 0.363\right)} \frac{0.275}{0.633} = 0.369 \end{aligned} \tag{4.104}$$

By using this value in the *WOR* equation, we compute *WOR* as

$$\begin{aligned} WOR &= \frac{B_o}{B_w} \frac{f_w(S_{wf})\left[1 - \dfrac{dN_{pu}}{dW_i}\right]}{f_o(S_{wf})\left[1 - \dfrac{dN_{pu}}{dW_i}\right] + \dfrac{dN_{pu}}{dW_i}} \\ &= \frac{1.2}{1.0}\left(\frac{0.851[1 - 0.369]}{0.149[1 - 0.369] + 0.369}\right) = 1.67\ STB/STB \end{aligned} \tag{4.105}$$

<u>Computations for the third row of Table 4.38</u> The performance computation for this row is carried out by considering the fact that the value of W_i (=89,991) specified is between W_{ibt} and $W_{i,100}$.

The areal sweep efficiency is computed from

$$E_A = E_{Abt} + 0.275 \ln\left(\frac{W_i}{W_{ibt}}\right) \tag{4.106}$$

which gives

$$E_A = 0.633 + 0.275\ln\left(\frac{89991}{54,436}\right) = 0.771 \tag{4.107}$$

We compute Q_i^* from

$$\frac{Q_i^*(t)}{Q_{ibt}^*} = 1 + a_1 e^{-a_1}\left[E_i(a_2) - E_i(a_1)\right] \tag{4.108}$$

$$a_1 = 3.65 E_{Abt} \tag{4.109}$$

and

$$a_2 = a_1 + \ln\left[\frac{W_i}{W_{ibt}}\right] \tag{4.110}$$

Performing the calculations, we obtain

$$a_1 = 3.65 E_{Abt} = 3.65 \times 0.633 = 2.31 \tag{4.111}$$

$$a_2 = a_1 + \ln\left[\frac{W_i}{W_{ibt}}\right] = 2.31 + \ln\left(\frac{89,991}{54,436}\right) = 2.81 \tag{4.112}$$

Solving simultaneously above Eqs gives:

$$\begin{aligned} E_i(a_2) &= E_i(2.81) = 8.738 \\ E_i(a_1) &= E_i(2.31) = 6.198 \end{aligned} \tag{4.113}$$

Then,

$$\frac{Q_i^*(t)}{Q_{ibt}^*} = 1 + a_1 e^{-a_1}\left[E_i(a_2) - E_i(a_1)\right]$$

$$= \frac{30{,}000 \times [1-0]}{319{,}621 \times [0.637 - 0.363]} \approx 0.343 \qquad \textbf{(4.114)}$$

which yields to

$$Q_i^*(t) = 1.582 Q_{ibt}^* = 1.582 \times 0.274 = 0.433 \qquad \textbf{(4.115)}$$

Now, we can determine S_{w2} after we compute the slope of fractional curve at Q_i^*, i.e.,

$$Q_i^*(t) = \frac{1}{\left(\frac{df_w}{dS_w}\right)_{S_{w2}}} \qquad \textbf{(4.116)}$$

which can be rearranged to obtain

$$\left(\frac{df_w}{dS_w}\right)_{S_{w2}} = \frac{1}{Q_i^*(t)} = \frac{1}{0.433} = 2.309 \qquad \textbf{(4.117)}$$

Now, we can determine the value of S_{w2}, which will give the slope of 2.309. For this purpose, we can do graphical interpolation based on the slope curve shown in Fig. 4.17. The determination of S_{w2} is shown in Fig. 4.18. Note that S_{w2} = 0.62

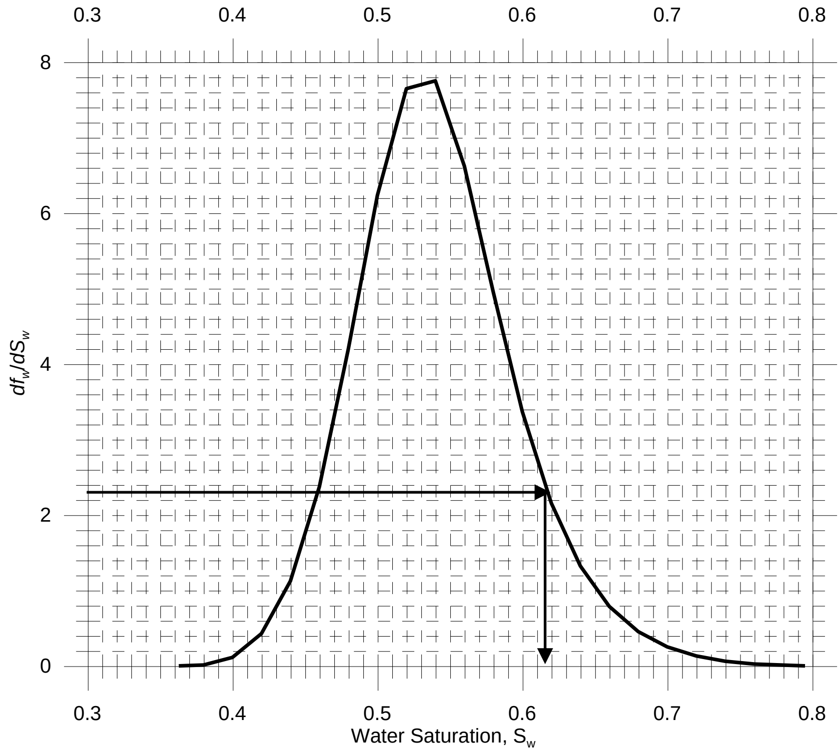

Figure 4.18: Determination of S_{w2}.

The value of average saturation in the reservoir is computed from

$$\overline{S_{w2}} = S_{w2} + [1 - f_w(S_{w2})] Q_i^* \quad \textbf{(4.118)}$$

which requires we determine $f_w(S_{w2})$. From Fig. 4.16, we determined $f_w(S_{w2}) = 0.92$. Then,

$$\overline{S_{w2}} = 0.62 + [1 - 0.92]\, 0.433 = 0.655 \quad \textbf{(4.119)}$$

At this stage, we can compute the cumulative oil production from

$$\begin{aligned} N_p &= \frac{E_A V_p \left(\overline{S_{w2}} - S_{wi}\right)}{B_o} \\ &= \frac{0.771 \times 319{,}621(0.655 - 0.363)}{1.2} = 59{,}964\ STB \end{aligned} \quad \textbf{(4.120)}$$

Next, we compute M from

$$M = \frac{\mu_o}{\mu_w} \frac{(k_{rw})_{\bar{S}_{w2}}}{(k_{ro})_{S_{wi}}} \quad \textbf{(4.121)}$$

which requires that we first determine the value of water relative permeability at $\overline{S_{w2}}$. We determined its value from Fig. 4.15 as $\left(k_{rw}\right)_{\overline{S_{w2}}} = \left(k_{rw}\right)_{0.655} = 0.182$. Then,

$$M = \frac{\mu_o}{\mu_w}\frac{\left(k_{rw}\right)_{\bar{S}_{w2}}}{\left(k_{ro}\right)_{S_{wi}}} = \frac{10}{1}\frac{0.182}{1} = 1.82 \qquad \textbf{(4.122)}$$

Next, we compute the injection rate by using Fig. 3.12. Using M = 1.82 and E_A = 0.771, w determined the conductance ratio as γ = 1.5 from Fig. 3.12. Then, the injection rate, i_w is

$$i_w = \gamma i_b = 1.5 \times 52.4 = 78.6\ RB/D \qquad \textbf{(4.123)}$$

The *WOR* is computed from

$$WOR = \frac{B_o}{B_w}\frac{f_w(S_{w2})\left[1-\dfrac{dN_{pu}}{dW_i}\right]}{f_o(S_{w2})\left[1-\dfrac{dN_{pu}}{dW_i}\right]+\dfrac{dN_{pu}}{dW_i}} \qquad \textbf{(4.124)}$$

where $\dfrac{dN_{pu}}{dW_i}$ is computed from

$$\frac{dN_{pu}}{dW_i} = \frac{W_{ibt}}{W_i}\frac{\left(S_{wf} - S_{wi}\right)}{\left(\overline{S_{wf}} - S_{wi}\right)}\frac{0.275}{E_{Abt}} \qquad \textbf{(4.124)}$$

Then,

$$\begin{aligned}\frac{dN_{pu}}{dW_i} &= \frac{W_{ibt}}{W_i}\frac{\left(S_{wf} - S_{wi}\right)}{\left(\overline{S_{wf}} - S_{wi}\right)}\frac{0.275}{E_{Abt}} \\ &= \frac{55{,}436}{89991}\frac{\left(0.596 - 0.363\right)}{\left(0.637 - 0.363\right)}\frac{0.275}{0.633} = 0.228\end{aligned} \qquad \textbf{(4.125)}$$

and

$$WOR = \frac{B_o}{B_w} \frac{f_w(S_{w2})\left[1-\frac{dN_{pu}}{dW_i}\right]}{f_o(S_{w2})\left[1-\frac{dN_{pu}}{dW_i}\right]+\frac{dN_{pu}}{dW_i}} \tag{4.126}$$

$$= \frac{1.2}{1} \frac{0.92\times[1-0.228]}{[1-0.92][1-0.228]+0.228} = 2.94 STB/STB$$

<u>Computations for the fourth row of Table 4.38</u>. The computations for this row are carried out by the same equations used for the computations for the third row. Here, $E_A = 1$, i.e., we are on the onset of 100% sweep.

We compute $Q^*_{i,100}$ from

$$\frac{Q^*_{i,100}(t)}{Q^*_{ibt}} = 1 + a_1 e^{-a_1}\left[E_i(a_2) - E_i(a_1)\right] \tag{4.127}$$

$$a_1 = 3.65 E_{Abt} \tag{4.128}$$

and

$$a_2 = a_1 + \ln\left[\frac{W_{i,100}}{W_{ibt}}\right] \tag{4.129}$$

Performing the calculations, we obtain

$$a_1 = 3.65 E_{Abt} = 3.65 \times 0.633 = 2.31 \tag{4.130}$$

$$a_2 = a_1 + \ln\left[\frac{W_{i,100}}{W_{ibt}}\right] = 2.31 + \ln\left(\frac{210{,}560}{54{,}436}\right) = 3.66 \tag{4.131}$$

Solving simultaneously above Eqs gives:

$$\begin{aligned} E_i(a_2) &= E_i(3.66) = 15.530 \\ E_i(a_1) &= E_i(2.31) = 6.198 \end{aligned} \tag{4.132}$$

Then,

$$\frac{Q^*_{i,100}}{Q^*_{ibt}} = 1 + a_1 e^{-a_1}\left[E_i(a_2) - E_i(a_1)\right]$$
$$= 1 + 2.31e^{-2.31}[15.530 - 6.198] = 3.140 \qquad \textbf{(4.133)}$$

which yields to

$$Q^*_{i,100}(t) = 3.140 Q^*_{ibt} = 3.140 \times 0.274 = 0.860 \qquad \textbf{(4.134)}$$

Now, we can determine S_{w2} after we compute the slope of fractional curve at $Qi*$, i.e.,

$$Q^*_{i,100}(t) = \frac{1}{\left(\frac{df_w}{dS_w}\right)_{S_{w2}}} \qquad \textbf{(4.135)}$$

which can be rearranged to obtain

$$\left(\frac{df_w}{dS_w}\right)_{S_{w2}} = \frac{1}{Q^*_{i,100}(t)} = \frac{1}{0.860} = 1.16 \qquad \textbf{(4.136)}$$

Now, we can determine the value of S_{w2}, which will give the slope of 1.16. We can do a graphical interpolation based on the slope curve shown in Fig. 4.20. The determination of S_{w2} is shown in Fig. 4.22. Note that S_{w2} = 0.648

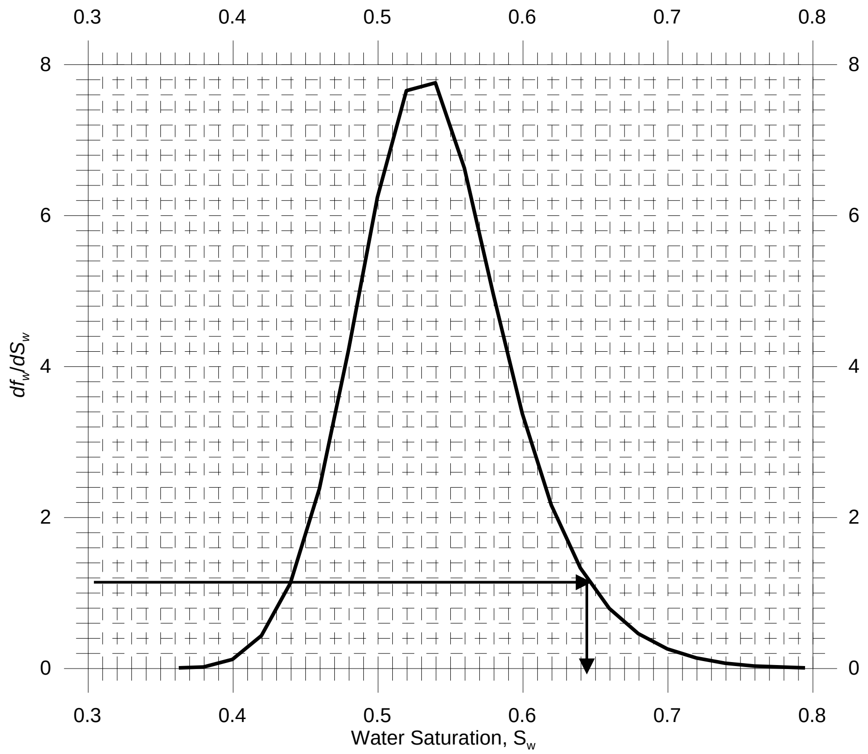

Figure 4.19: Determination of S_{w2}.

The value of average saturation in the reservoir is computed from

$$\overline{S_{w2}} = S_{w2} + \left[1 - f_w\left(S_{w2}\right)\right] Q_i^* \quad \textbf{(4.137)}$$

which requires we determine $f_w(S_{w2})$. From Fig. 4.16, we determined $f_w(S_{w2}) = 0.96$. Then,

$$\overline{S_{w2}} = 0.648 + \left[1 - 0.96\right] 0.860 = 0.682 \quad \textbf{(4.138)}$$

At this stage, we can compute the cumulative oil production from

$$\begin{aligned} N_p &= \frac{E_A V_p \left(\overline{S_{w2}} - S_{wi}\right)}{B_o} \\ &= \frac{1 \times 319{,}621\left(0.682 - 0.363\right)}{1.2} = 85{,}072\ STB \end{aligned} \quad \textbf{(4.139)}$$

Next, we compute M from

$$M = \frac{\mu_o}{\mu_w} \frac{\left(k_{rw}\right)_{\bar{S}_{w2}}}{\left(k_{ro}\right)_{S_{wi}}} \quad \textbf{(4.140)}$$

which requires that we first determine the value of water relative permeability at $\overline{S_{w2}}$. We determined its value from Fig. 4.15 as $(k_{rw})_{\overline{S_{w2}}} = (k_{rw})_{0.682} = 0.252$. Then,

$$M = \frac{\mu_o}{\mu_w}\frac{(k_{rw})_{\bar{S}_{w2}}}{(k_{ro})_{S_{wi}}} = \frac{10}{1}\frac{0.252}{1} = 2.5 \qquad \textbf{(4.141)}$$

Next, we compute the injection rate by using Fig. 3.12. Using M = 2.5 and E_A = 1, we determined the conductance ratio as γ = 2.52 from Fig. 3.12. Then, the injection rate, i_w is

$$i_w = \gamma\, i_b = 2.5 \times 52.4 = 132.3 \text{ RB/D} \qquad \textbf{(4.142)}$$

Because E_A = 1, then WOR is computed from

$$WOR = \frac{B_o}{B_w}\frac{f_w(S_{w2})}{f_o(S_{w2})} = \frac{1.2}{1.0}\frac{0.96}{[1-0.96]} = 28.8 STB/STB \qquad \textbf{(4.143)}$$

<u>Computations for the last row of Table 4.38</u>. The computations for this row are carried out by considering the fact that $W_i > W_{i,100}$ and E_A = 1

We compute Q_i^*, from

$$\begin{aligned} Q_i^* &= Q_{i,100}^* + \frac{1}{V_p}\left(W_i - W_{i,100}\right) \\ &= 0.860 + \frac{1}{319{,}621}\left(293{,}284 - 210{,}560\right) = 1.119 \end{aligned} \qquad \textbf{(4.144)}$$

Now, we can determine S_{w2} after we compute the slope of fractional curve at Q_i^*,i.e.,

$$Q_i^*(t) = \frac{1}{\left(\dfrac{df_w}{dS_w}\right)_{S_{w2}}} \qquad \textbf{(4.145)}$$

which can be rearranged to obtain

$$\left(\frac{df_w}{dS_w}\right)_{S_{w2}} = \frac{1}{Q_i^*(t)} = \frac{1}{1.119} = 0.894 \qquad \textbf{(4.146)}$$

Now, we can determine the value of S_{w2}, which will give the slope of 0.894. We can do a graphical interpolation based on the slope curve shown in Fig. 4.17. The determination of S_{w2} is shown in Fig. 4.20. Note that S_{w2} = 0.657

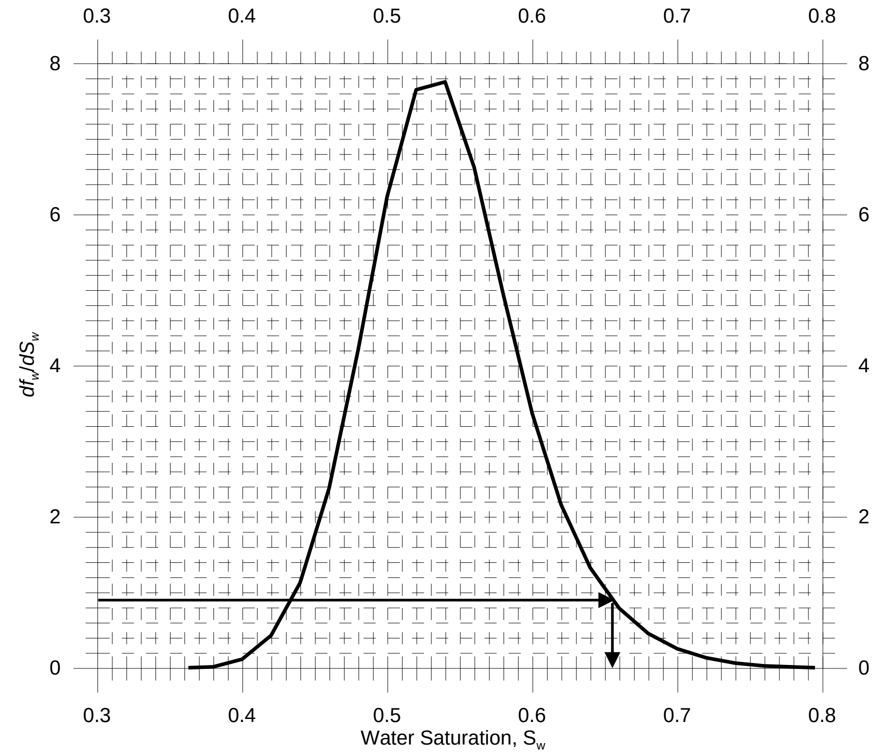

Figure 4.20: The slope determination of S_{w2}.

The value of average saturation in the reservoir is computed from

$$\overline{S_{w2}} = S_{w2} + \left[1 - f_w\left(S_{w2}\right)\right] Q_i^* \qquad \textbf{(4.147)}$$

which requires we determine $f_w(S_{w2})$. From Fig. 4.16, we determined $f_w(S_{w2}=0.657)$ = 0.97. Then,

$$\overline{S_{w2}} = 0.657 + \left[1 - 0.97\right]1.119 = 0.690 \qquad \textbf{(4.148)}$$

At this stage, we can compute the cumulative oil production from

$$\begin{aligned} N_p &= \frac{E_A V_p \left(\overline{S_{w2}} - S_{wi}\right)}{B_o} \\ &= \frac{1 \times 319{,}621\left(0.690 - 0.363\right)}{1.2} = 87{,}097 \ STB \end{aligned} \qquad \textbf{(4.149)}$$

Next, we compute M from

$$M = \frac{\mu_o}{\mu_w}\frac{(k_{rw})_{\bar{S}_{w2}}}{(k_{ro})_{S_{wi}}} \quad \textbf{(4.150)}$$

which requires that we first determine the value of water relative permeability at $\overline{S_{w2}}$. We determined its value from Fig. 4.15 as $(k_{rw})_{\overline{S_{w2}}} = (k_{rw})_{0.690} = 0.277$. Then,

$$M = \frac{\mu_o}{\mu_w}\frac{(k_{rw})_{\bar{S}_{w2}}}{(k_{ro})_{S_{wi}}} = \frac{10}{1}\frac{0.277}{1} = 2.77 \quad \textbf{(4.151)}$$

Next, we compute the injection rate by using Fig. 3.12 of chapter 3. Using M = 2.77 and E_A = 1, we determined the conductance ratio as γ = 2.77 from Fig. 3.12. Then, the injection rate, i_w is

$$i_w = \gamma i_b = 2.77 \times 52.4 = 145.1\, RB/D \quad \textbf{(4.152)}$$

Because E_A = 1, then WOR is computed from

$$WOR = \frac{B_o}{B_w}\frac{f_w(S_{w2})}{f_o(S_{w2})} = \frac{1.2}{1.0}\frac{0.97}{[1-0.97]} = 38.8 STB/STB \quad \textbf{(4.153)}$$

Finally, we compute the time values by using the cumulative volume of injected water and injection rates. To do these calculations, recall that we use the trapezoidal rule of integration. Simply, Let ΔW_i be incremental cumulative volume of injected water and $i_{w,ave}$ be the arithmetic average of two consecutive injection rates, and Δt be the incremental time. Then,

$$\Delta W_i = i_{w,ave}\Delta t \quad \textbf{(4.153)}$$

where

$$\Delta W_i = W_i(t_{j+1}) - W_i(t_j) \quad \textbf{(4.154)}$$

$$i_{w,ave} = \frac{i_w(t_{j+1}) + i_w(t_j)}{2} \quad \textbf{(4.155)}$$

and

$$\Delta t = t_{j+1} - t_j \tag{4.156}$$

Now, we apply the above formulas to determine the time values in the first column of Table 4.38. Because the time of breakthrough is given, then using the above equations, we can compute the time for W_i = 30,000 as

$$\Delta t = \frac{\Delta W_i}{i_{w,ave}} = \frac{55{,}436 - 30{,}000}{\left[\dfrac{57.6 + 62.9}{2}\right]} = 422.2\,days \tag{4.157}$$

$$t = t_{bt} - \Delta t = 977 - 422.2 = 554 \textit{ days} \text{ at } W_i\text{=30,000 } RB \tag{4.158}$$

The time for the third row is calculated similarly, i.e.,

$$\Delta t = \frac{\Delta W_i}{i_{w,ave}} = \frac{89{,}991 - 55{,}436}{\left[\dfrac{78.6 + 62.9}{2}\right]} = 488\,days \tag{4.159}$$

$$t = t_{bt} + \Delta t = 977 + 488 \approx 1465 \textit{ days} \text{ at } W_i\text{=89,991 } RB \tag{4.160}$$

The time for the fourth row is

$$\Delta t = \frac{\Delta W_i}{i_{w,ave}} = \frac{210{,}560 - 89{,}991}{\left[\dfrac{78.6 + 132.3}{2}\right]} = 1143\,days \tag{4.161}$$

$$t = t_{Wi=89,991} + \Delta t = 1465 + 1143 \approx 2608 \textit{ days} \text{ at } W_i\text{=210,560 } RB \tag{4.162}$$

The time for the last row is

$$\Delta t = \frac{\Delta W_i}{i_{w,ave}} = \frac{293{,}284 - 210{,}560}{\left[\dfrac{145.1 + 132.3}{2}\right]} = 596\,days \tag{4.163}$$

$$t = t_{Wi=210,560} + \Delta t = 2608 + 596 \approx 3204 \textit{ days} \text{ at } W_i\text{=293,284 } RB \tag{4.164}$$

All results are summarized in Table 4.39.

Table 4.39: Displacement performance of five-spot pattern.

Time (days)	W_i (RB)	Q_i^*	***M***	E_A	i_w	S_{w2}	$\overline{S_{w2}}$	N_p	***WOR***
554	30,000	0.274	1.43	0.342	57.6	0.596	0.637	24,959	0.00
977 (= t_{bt})	55,436	0.274	1.43	0.633	62.9	0.596	0.637	46,196	1.67
1465	89,991	0.433	1.82	0.771	78.6	0.620	0.655	59,964	2.94
2608	210,560	0.860	2.52	1.0	132.3	0.648	0.682	85,072	28.8
3204	293,284	1.119	2.77	1.0	145.1	0.657	0.690	87,097	38.8

5. CONCLUSIONS AND RECOMENDATIONS

The main purpose of this research was to predict reservoir displacement process in 1D linear and areal waterflooding performance under constant rate injection and constant pressure injection. Consequently, using the Buckley-Leverett model, we showed how water saturation profile in between the injector and the producer, cumulative oil production, pore volume water injected, and oil production rate can be predicted before and after water breakthrough. These parameters can help us in forecasting both technological and economical risks. These points were illustrated by four example applications given in Chapter 4.

As a result of the example applications considered, we can state the following conlusions:

- Waterflooding performance is greatly affected by the mobility ratio. Favorable case always provides better performance compared to unfavorable case regardless of the production mode at the injector and producer.
- When considering the effect of mobility ratio for the constant pressure at injection and production wells, it is observed that, although favorable mobility ratio causes earlier breakthrough than does unfavorable ratio, favorable mobility ratio provides higher oil production.
- Under constant-pressure injection mode, for the unfavorable case, water behind the front flows more easily than oil ahead of front (i.e., the injected water has less resistance to flow), the injection rate increases. After breakthrough, preferential flow path is for water, so injection rate continues to increase.
- Under constant-pressure injection mode, for the favorable case, oil ahead of the front moves easily than water behind the front. As the amount of water injected increases, injection rate (q_t) decreases. After breakthrough, water can flow easily from injector to producer, so injection rate increases.
- It was shown that injection rates (under constant-pressure injection mode) for the favorable case is higher than the unfavorable case. This means that there

is less resistance to flow in the favorable case. In addition, it was shown that the BT for the unfavorable case occurs earlier than that for the favorable case, and that cumulative production for the favorable case is quite high compared to that of unfavorable case. Most importantly, to have the same amount of cumulative production, the favorable case requires significantly more volumes of water injected.

- The example applications showed that the greater the oil viscosity is the less efficient the water flood is.
- Based on the Buckley-Leverett theory and its assumptions, the absolute permeability has no effect on water saturation profiles, water oil ratio, and oil production, but it does affect the flowing bottom-hole pressures of the injector and producer. The higher the permeability the better is the performance of the flowing bottom-hole pressures at the injector and producer.
- In low permeability reservoirs, care should be given to the fracturing pressure of the reservoir, as injection of water for low permeability reservoirs increases injection bottom-hole pressure significantly.

The following recommendations are given:

- In this work, we assumed steady-state conditions, incompressible flow and ignored gravity and capillary pressure effects, it is recommended that the waterflooding performance for more general cases including transient, compressible flow and capillary and gravity effects be studied in a future work.
- Note that in our work, we have assumed 100% sweep efficiency in the vertical direction. This may not be realistic for multilayer systems showing different rock properties in the vertical direction. Hence, the extension of the Buckley-Leverrett theory should be considered for multilayered systems where the effect of vertical displacement on the performance of waterflood for such systems could be studied.
- In this work, only uniform porosity and permeability cases were considered. It is recommended that in a future work, the effect of heterogeneous porosity and permeability fields on waterflooding be investigated, but such an

investigation will require the use of a numerical simulation model considering simultaneous flow of oil and water.

REFERENCES

Buckley, S.E. and Leverett, M.C., 1942. Mechanism of Fluid Displacement in Sands, Trans., AIME 146, 107-116.

Craft, B.C. and Hawkins, M., 1991. Applied Reservoir Engineering, 2nd edition, Prentice-Hall Inc., Englewood Cliffs, New Jersey.

Craig. F.F. Jr., 1993, The Reservoir Engineering Aspect of Waterflooding, SPE Monograph, Volume 3.

Craig, F.F.Jr., Geffen, T.M., and Morse, R.A., 1955. Oil Recovery Performance of Pattern Gas or Water Injection Opertations from Model Tests. J. Pet. Tech. (January) 7-15.

Dake, L.P., 1978. Fundamentals of Reservoir Engineering, Elsevier Science B.V, Amsterdam, the Netherlands.

Dandekar, A.Y., 2006. Petroleum Reservoir Rock and Fluid Properties, Taylor & Francis Group, 204-246.

Dykstra, H., Parsons R.L., 1950. The Prediction of Oil Recovery by Waterfloding. Secondary Recovery of Oil in the USA 2nd edition, API, New York.

Kleppe J., 2009. Reservoir Recovery Techniques, NTNU, *Course Notes*, Trondheim, Norway.

Onur, M., 2008. Enhanced Oil Recovery, ITU, *Course Notes*, Istanbul, Turkey.

Pande, K.K and at all, 1987, Frontal Advance Theory for Flow in Heterogeneous Porous Media, This paper was prepared for presentation at the SPE California Regional Meeting held in Ventura California, April 8-10, SPE 16344, Society of Petroleum Engineers, Inc.

Satter, A., Igbal, G.M., and Buchwalter, J.L., 2008. Practical Enhanced Reservoir Engineering, PennWell Corporation, Tulsa, Oklahoma.

Tarek, A.H., 2001 Reservoir Engineering Handbook 2nd edition Butterworth-Heinemann Publications, USA.

Willhite G.P., 1986 Waterflooding, SPE, Richardson, Texas, USA.

APPENDICES

APPENDIX A.

Table A.1: S_w and λ_t versus x profiles at t = 200 days for Option 1.

S_w	λ_t , 1/cp	x_{S_w} , ft
0.363	0.5	NA
0.363	0.5	NA
0.37	0.5	NA
0.38	0.5	NA
0.4	0.5	NA
0.42	0.5	NA
0.44	0.5	NA
0.46	0.5	NA
0.48	0.5	NA
0.5	0.5	NA
0.52	0.5	NA
0.54	0.5	NA
0.56	0.5	NA
0.58	0.5	NA
0.6	0.5	NA
0.63	0.371	NA
0.64	0.385	NA
0.66	0.418	500. (truncated)
0.68	0.455	420.1
0.7	0.498	307.52
0.72	0.548	213.32
0.74	0.602	136.70
0.76	0.662	75.78
0.78	0.727	28.26
0.795	0.78	0.0

Table A.2: S_w and λ_t versus x profiles at t = 50 days for Option 2.

S_w	λ_t , 1/cp	x_{S_w} , ft
0.363	0.5	500
0.363	0.5	153.86
0.37	0.484	153.86
0.38	0.462	153.86
0.4	0.419	153.86
0.42	0.379	153.86
0.44	0.343	153.86

Table A.2: (contd) S_w and λ_t versus x profiles at t = 50 days for Option 2.

0.46	0.309	153.86
0.48	0.277	153.86
0.5	0.249	153.86
0.52	0.223	153.86
0.54	0.200	153.86
0.56	0.180	153.86
0.58	0.163	153.86
0.6	0.149	153.86
0.63	0.133	153.86
0.64	0.129	153.86
0.66	0.123	153.86
0.68	0.119	153.86
0.7	0.119	153.86
0.72	0.122	153.86
0.74	0.127	153.86
0.76	0.135	91.08
0.78	0.146	35.09
0.795	0.156	0.0

Table A.3: S_w and λ_t versus x profiles at t = 100 days for Option 2.

S_w	λ_t, 1/cp	x_{S_w}, ft
0.363	0.5	500
0.363	0.5	307.72
0.37	0.484	307.72
0.38	0.462	307.72
0.4	0.419	307.72
0.42	0.379	307.72
0.44	0.343	307.72
0.46	0.309	307.72
0.48	0.277	307.72
0.5	0.249	307.72
0.52	0.223	307.72
0.54	0.200	307.72
0.56	0.180	307.72
0.58	0.163	307.72
0.6	0.149	307.72
0.63	0.133	307.72
0.64	0.129	307.72
0.66	0.123	307.72
0.68	0.119	307.72
0.7	0.119	307.72
0.72	0.122	307.72
0.74	0.127	307.72
0.76	0.135	182.16
0.78	0.146	70.18
0.795	0.156	0.0

Table A.4: S_w and λ_t versus x profiles at t = 163 days (BT) for Option 2.

S_w	λ_t, 1/cp	x_{S_w}, ft
0.363	0.5	500
0.363	0.5	500
0.37	0.484	500
0.38	0.462	500
0.4	0.419	500
0.42	0.379	500
0.44	0.343	500
0.46	0.309	500
0.48	0.277	500
0.5	0.249	500
0.52	0.223	500
0.54	0.200	500
0.56	0.180	500
0.58	0.163	500
0.6	0.149	500
0.63	0.133	500
0.64	0.129	500
0.66	0.123	500
0.68	0.119	500
0.7	0.119	500
0.72	0.122	500
0.74	0.127	500.
0.76	0.135	296.92
0.78	0.146	114.40
0.795	0.156	0.0

Table A.5: S_w and λ_t versus x profiles at t = 200 days for Option 2.

S_w	λ_t, 1/cp	x_{S_w}, ft
0.363	0.5	NA
0.363	0.5	NA
0.37	0.484	NA
0.38	0.462	NA
0.4	0.419	NA
0.42	0.379	NA
0.44	0.343	NA
0.46	0.309	NA
0.48	0.277	NA
0.5	0.249	NA
0.52	0.223	NA
0.54	0.200	NA
0.56	0.180	NA
0.58	0.163	NA
0.6	0.149	NA
0.63	0.133	NA
0.64	0.129	NA

Table A.5: (contd) S_w and λ_t versus x profiles at t = 200 days for Option 2.

0.66	0.123	NA
0.68	0.119	NA
0.7	0.119	NA
0.72	0.122	NA
0.74	0.127	500.
0.76	0.135	364.32
0.78	0.146	140.36
0.795	0.156	0.0

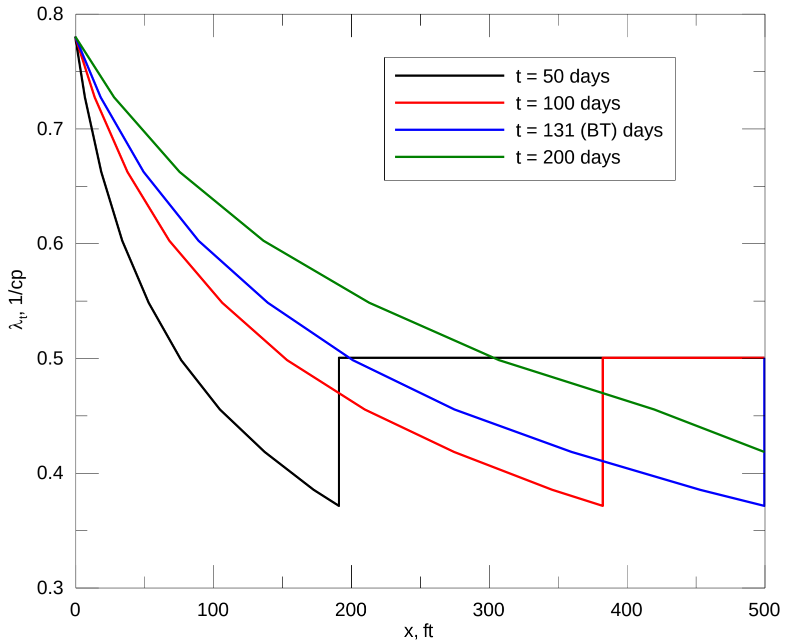

Figure A.1: λ_t vs. x profiles at different times for Option 1.

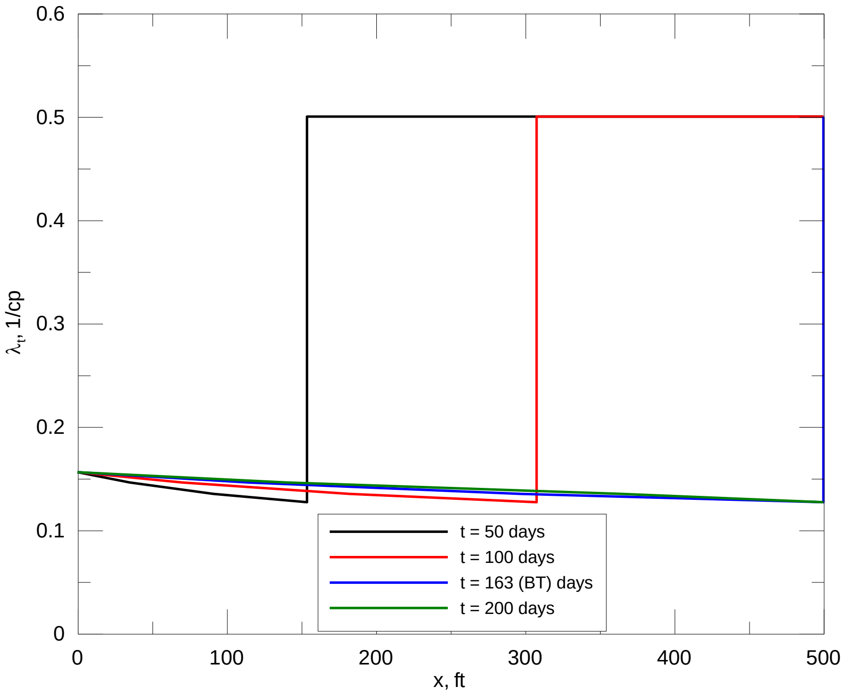

Figure A.2: λ_t vs. x profiles at different times for Option 2.

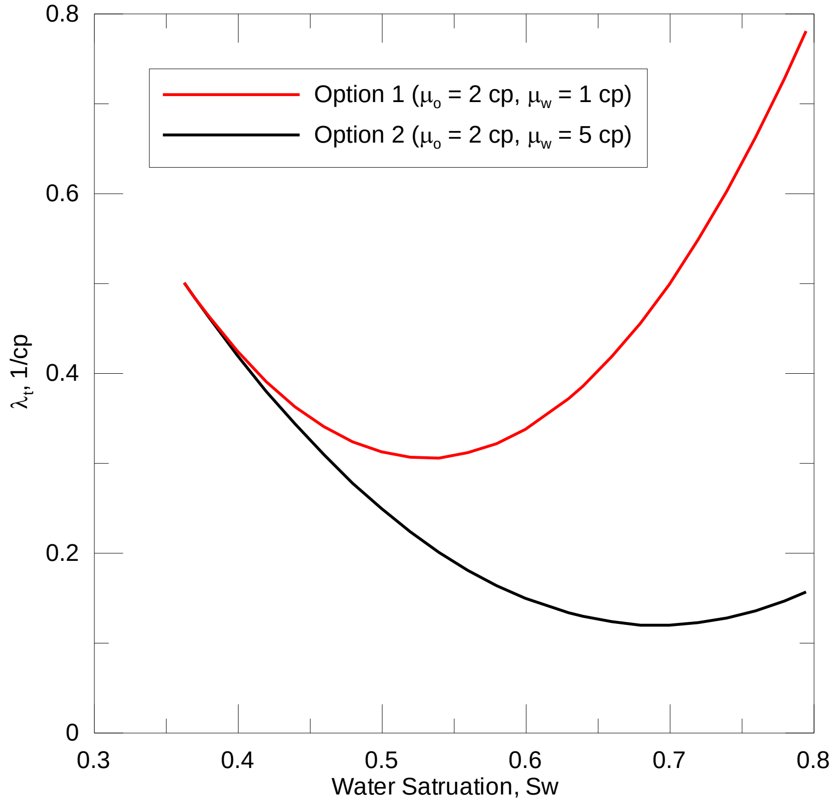

Figure A.3: λ_t vs. S_w profiles for Options 1 & 2.

APPENDIX B.

Table B.1: Saturation and total mobility profiles for $Q_{i,9}$=1.298 and $S_{w2}(x=L)$ =0.638.

$\hat{S}_w$	S_{wD}	$\left(\frac{\partial f_w}{\partial S_w}\right)_{\hat{S}_w}$	$\frac{x_{\hat{S}_w}}{L}$	$x_{\hat{S}_w}$ (ft)	λ_t, (1/cp)
0.638	0.6366	0.7704	1.0000	1000	0.3293
0.648	0.6597	0.6577	0.8537	853.7	0.3510
0.659	0.6851	0.5506	0.7147	714.7	0.3760
0.669	0.7083	0.4666	0.6056	605.6	0.3998
0.680	0.7338	0.3867	0.5019	501.9	0.4271
0.690	0.7569	0.3240	0.4206	420.6	0.4528
0.701	0.7824	0.2644	0.3432	343.2	0.4822
0.711	0.8056	0.2175	0.2823	282.3	0.5010
0.722	0.8310	0.1729	0.2244	224.4	0.5415
0.732	0.8542	0.1379	0.1790	179	0.5713
0.743	0.8796	0.1045	0.1356	135.6	0.6049
0.753	0.9023	0.0782	0.1015	101.5	0.6360
0.764	0.9282	0.0532	0.0691	69.1	0.6725
0.774	0.9513	0.0335	0.0435	43.5	0.7061
0.785	0.9769	0.0147	0.0191	19.1	0.7444
0.795	1.0000	0.0000	0	0	0.7800

Table B.2: Saturation and total mobility profiles for $Q_{i,10}$=2.143 and $S_{w2}(x=L)$=0.669.

$\hat{S}_w$	S_{wD}	$\left(\frac{\partial f_w}{\partial S_w}\right)_{\hat{S}_w}$	$\frac{x_{\hat{S}_w}}{L}$	$x_{\hat{S}_w}$ (ft)	λ_t, (1/cp)
0.669	0.7083	0.4666	1.0000	1000	0.3998
0.680	0.7338	0.3867	0.8287	828.7	0.4271
0.690	0.7569	0.3240	0.6943	694.3	0.4528
0.701	0.7824	0.2644	0.5666	566.6	0.4822
0.711	0.8056	0.2175	0.4661	466.1	0.5010
0.722	0.8310	0.1729	0.3705	370.5	0.5415
0.732	0.8542	0.1379	0.2955	295.5	0.5713
0.743	0.8796	0.1045	0.2239	223.9	0.6049
0.753	0.9023	0.0782	0.1676	167.6	0.6360
0.764	0.9282	0.0532	0.1140	114	0.6725
0.774	0.9513	0.0335	0.0718	71.8	0.7061
0.785	0.9769	0.0147	0.0315	31.5	0.7444
0.795	1.0000	0.0000	0	0	0.7800

Table B.3: Saturation and total mobility profiles for $Q_{i,11}$=3.086 and $S_{w2}(x=L)$=0.690.

$\hat{S}_w$	S_{wD}	$\left(\frac{\partial f_w}{\partial S_w}\right)_{\hat{S}_w}$	$\frac{x_{\hat{S}_w}}{L}$	$x_{\hat{S}_w}$ (ft)	λ_t, (1/cp)
0.690	0.7569	0.3240	1.0000	1000.0	0.4528
0.701	0.7824	0.2644	0.8159	815.9	0.4822
0.711	0.8056	0.2175	0.6712	671.2	0.5010
0.722	0.8310	0.1729	0.5336	533.6	0.5415
0.732	0.8542	0.1379	0.4256	425.6	0.5713
0.743	0.8796	0.1045	0.3225	322.5	0.6049
0.753	0.9023	0.0782	0.2413	241.3	0.6360
0.764	0.9282	0.0532	0.1642	164.2	0.6725
0.774	0.9513	0.0335	0.1034	103.4	0.7061
0.785	0.9769	0.0147	0.0454	45.4	0.7444
0.795	1.0000	0.0000	0	0	0.7800

Table B.4: Saturation and total mobility profiles for $Q_{i,12}$=5.784 and $S_{w2}(x=L)$=0.722.

$\hat{S}_w$	S_{wD}	$\left(\frac{\partial f_w}{\partial S_w}\right)_{\hat{S}_w}$	$\frac{x_{\hat{S}_w}}{L}$	$x_{\hat{S}_w}$ (ft)	λ_t, (1/cp)
0.722	0.8310	0.1729	1.0000	1000.0	0.5415
0.732	0.8542	0.1379	0.7976	797.6	0.5713
0.743	0.8796	0.1045	0.6044	604.4	0.6049
0.753	0.9023	0.0782	0.4523	452.3	0.6360
0.764	0.9282	0.0532	0.3077	307.7	0.6725
0.774	0.9513	0.0335	0.1938	193.8	0.7061
0.785	0.9769	0.0147	0.0850	85.0	0.7444
0.795	1.0000	0.0000	0	0	0.7800

CURRICULUM VITAE

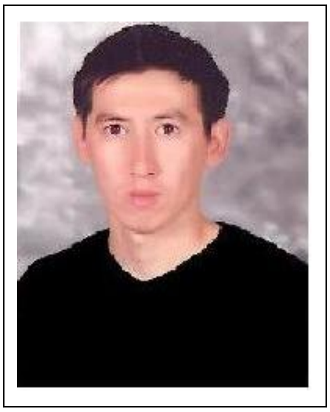

Candidate's full name: Nurbol Zharylkapov

Place and date of birth: Kazakhstan, 19 September 1981

Permanent Address: Kazakhstan, Taraz city, Telecentre 9/42

E-mail Address: nurbol19@gmail.com

Universities and
Colleges attended:

2006-2010 - Istanbul Technical University, M.S., Department of Petroleum and Natural Gas Engineering.

1998-2003 - Taraz State University, B.S., Department of Petroleum and Natural Gas Engineering.